Spring 1977

Precise Frequency Control of the Voltage Controlled Oscillator Using Finite Digital Word Lengths

Timothy Peter Hulick
Old Dominion University

PRECISE FREQUENCY CONTROL OF THE VOLTAGE CONTROLLED OSCILLATOR USING FINITE DIGITAL WORD LENGTHS

by

Timothy Peter Hulick
B.S.June 1964,United States Naval Academy
S.M.Nuclear Engineering June 1969,
Massachusetts Institute of Technology
Naval Engineer June 1969,
Massachusetts Institute of Technology

A Dissertation Submitted to the Faculty of
Old Dominion University in Partial Fulfillment of the
Requirements for the Degree of

DOCTOR OF PHILOSOPHY

ENGINEERING

OLD DOMINION UNIVERSITY
May, 1977

Approved by:

[redacted]
William D. Stanley (Director)

Preston B. Johnson

Murali R. Varanasi

Roland R. Mielke

Billy J. Gulpin

DEDICATION

This dissertation is dedicated to my late father who introduced the wonderment of "wireless" to me at a very early age and who instilled my desire to seek education to the fullest of my capacity.

This dissertation is also dedicated to my beloved sister, Patricia, who deceased shortly before completion of this work.

ABSTRACT

PRECISE FREQUENCY CONTROL OF THE
VOLTAGE CONTROLLED OSCILLATOR
USING FINITE DIGITAL WORD LENGTHS

Timothy Peter Hulick
Old Dominion University, 1977
Director:Dr.William D.Stanley

For an oscillator that is periodically swept in frequency between some upper and lower bound, the output amplitude may easily be made constant and therefore known with a high degree of certainty. The instantaneous frequency exists only at a point in time and therefore possesses a zero probability of existing at any point. This thesis deals with the development of a method for interchanging the probability density functions of amplitude and frequency so that the latter becomes known with certainty while the former is known only to the extent that it is within a certain range.

The method developed makes practical the use of the fast tuned voltage controlled oscillator as the local oscillator in a frequency scanning superheterodyne receiver. Exact frequency is expressed by a digital word of finite bit length that, in actuality, expresses the value of a quantized amplitude variable whose quantized

value represents a precise frequency. Because of the interrelationship of amplitude, frequency, and time through the Fourier Transform, functions of these variables are also interrelated suggesting the possibility that the original certainty of amplitude information may be traded with the original uncertainty of frequency information. The success of the method presented makes use of the precise knowledge of the frequencies of the sidebands generated by the angle modulation process rather than make direct use of the instantaneous frequency.

After mathematical development, a design example addresses the actual frequency range in the microwave region where the scanning superheterodyne receiver finds military application. To demonstrate the concept of precise frequency control with words of finite length, a practical frequency model is designed and constructed by scaling megahertz to hertz. Extensive use is made of monolithic waveform generators, balanced mixers, and operational amplifiers used as active filters and time domain summers. All assemblies within the model have practical microwave counterparts.

Time and frequency domain waveforms are observed at virtually every major point of the model corresponding to the functional block interfaces and are compared with the mathematical predictions. The ultimate goal of precise

frequency selection as a function of an imprecise independent variable is also obtained with the aid of a spectrum analyzer and dual trace oscilloscope.

The causes of less than optimum signal level separation of adjacent discrete frequencies are analyzed in a qualitative manner. Reasons for the ineffectiveness of a quantitative critique are also presented. Experimental results, however, are demonstrated proof of the feasibility of the concept of exchanging probability density functions of related variables and that refinement is the only ingredient missing to render the fast scan VCO a useful local oscillator.

ACKNOWLEDGEMENTS

Throughout the pursuit of this dissertation, assistance came in many forms ranging from casual conversation to equipment loans. Foremost in deserving recognition is my sponsor Mr. Eugene Newman of the Electronic Warfare Department, Naval Electronic Engineering Office, Norfolk, who recognized the microwave voltage controlled oscillator as a powerful innovation in the field of Electronic Warfare. His encouragement to "find a use" for the VCO led to this work. I am also indebted to him for his financial sponsorship and loan of equipment in carrying out practical experiments.

I wish to express my appreciation to Mr. Ed Dougherty of the Naval Electronic Engineering Office, Norfolk, for the lesson provided in learning to use specialized equipment such as the spectrum analyzer and camera. All display photographs are a result of his patience and knowledge.

Dr. Stanley Alterman of the Kuras-Alterman Corporation deserves recognition for our casual conversation that made me aware of certain pitfalls in this pursuit.

Thanks go to my friend, Mr. Gay E. Milius, Jr. for the loan of his personal photographic equipment.

Most deserving of thanks are the members of my committee who reviewed and coached my progress for nearly

two years. Their participation is most appreciated.

A kind lady known to me only as "Christine" at the MIT Hayden Mathematics Library had saved me the time and expense of a trip to MIT by locating hard to find reference material and reading information to me by telephone. Her willingness to spend her own time on more than one occasion is very much appreciated.

Typing plain text mixed with a large amount of mathematical symbology deserves an award for precision, patience, and endurance. My sincere thanks to Mrs. Virginia Goetz for her patience with my handwritten undecypherables and the endurance and the precision necessary for successfully putting this work on paper.

Mostly I appreciate the caring and patience provided to me by my wife and children who often wondered if I would ever leave my workshop. Their ability to recognize the difference between my mental absence from the family and yet my devotion to them allowed the expansion of the day (and night) into more hours than previously thought possible.

TABLE OF CONTENTS

LIST OF TABLES

LIST OF FIGURES

LIST OF SYMBOLS

Variables and Constants

A - amplitude

a - general function

B - bandwidth

D - constant of proportionality

E - constant of proportionality

e - composite time domain signal voltage

f - frequency

G - gain

J - Bessel function of the first kind

k - inverse amplitude modulation index, an integer

ℓ - tolerable worst case adjacent channel amplitude separation (low side), summation index

M - amplitude of the modulation on m

m - amplitude modulation index

N - noise power

n - sideband number, an integer if noted otherwise

p - harmonic number, an integer

r - number of bits

S - quantized signal power

t - time

u - tolerable worst case adjacent channel amplitude separation (high side)

$\hat{V}$ - a constant representing VCO output level

v - voltage random variable

x - a variable

y - a variable

β - angle modulation index

δ - dirac delta

ε - a quantity expressing the relative dependence of $e_1 + e_2$ on m

λ - amplitude clipping level

τ - pulse duration

ω - radial frequency

Subscripts

c - refers to channel center, carrier

k - an integer

LSB - lower sideband

ℓ - refers to low frequency side or limit

m - modulation

n - sideband number, an integer

p - an integer referring to harmonic number

q - refers to quantization

r - range

s - refers to scan modulation

USB - upper sideband

u - refers to high frequency side or limit

β - refers to a number identical to the angle modulation index

$_0$ - refers to the time domain composite of $_1$ and $_2$, order of Bessel function, output

$_1$ - refers to the channel not associated with frequency shifting, order of Bessel function

$_2$ - refers to the channel associated with frequency shifting, order of Bessel function

LIST OF TERMS

Basic VCO - refers to the voltage controlled oscillator unit itself.

Ultimate or Fast Scan VCO - refers to the local oscillator system with all filters, summers, amplifiers and limiters including the basic VCO.

CHAPTER I

THE VOLTAGE CONTROLLED OSCILLATOR

1-1 Background

A radio frequency sinusoidal oscillator that may be controlled in frequency by a voltage has been a practical device for many years. In fact, since the earliest days of radio voice communication, the reactance tube modulator represented the common means in achieving frequency control by a voltage derived from a voice signal (refs. 1,2). Although an oscillator controlled in this fashion is a "voltage controlled oscillator," it was not thought of as such until other applications were employed. The phase locked loop is perhaps the earliest design that makes mention of such a device as a voltage controlled oscillator (VCO). The phase locked loop (PLL) is a negative feedback device whereby the error signal (voltage) is derived from the phase difference of a stable frequency standard and a non standard. The control voltage moves the frequency of oscillations in the correct direction to drive the phase error to zero (ref.3). The result is that an otherwise frequency unstable variable frequency oscillator may be made nearly as stable as the standard. Even the intrigue of the PLL was shelved for many years because of the extensive list of individual components necessary to construct the circuit. Cost and size simply limited the practical usefulness of the PLL.

During the evolvement of the integrated circuit, it became practical to concentrate the PLL circuit into a single inexpensive package, e.g. Signetics 560, 561 and Fairchild NE563. Since this rebirth of the PLL with the VCO, the combination device has found universal application in VHF FM communications equipment. In voice transmitters the pair form the frequency synthesizer or carrier generator-modulator, while in the receiver they make up the FM demodulator (ref. 4). Also the PLL with the VCO used as a very stable first conversion oscillator in a communications receiver and the practical circuitry illustrated has been designed by Robbins (ref. 5).

The appeal of the VCO was farther enhanced by the introduction of the variable capacitance diode. This solid state device eliminates the need for the reactance tube and associated circuitry allowing a relatively significant reduction in cost, size and increased frequency limit of the VCO. This device known most commonly as a varactor makes use of the variation of PN junction capacitance with reverse bias voltage. When used as the capacitive element in a resonant network, it becomes possible to voltage control an oscillator (ref. 6). Currently, varactors and other solid state devices are useful well into H, I and even J band (ref. 7). Their recent application to microwave frequencies and nanosecond

response to step changes in voltage and therefore frequency have served to motivate this thesis.

1-2 Current State-of-the-Art of Voltage Controlled Oscillators

Microwave voltage controlled oscillators have become particularly important in recent years because of their extremely fast response to changes in tuning voltage. RCA reports instantaneous frequency "settle-on" times to within three MHz to be as low as ten ns for a step change from eight to twelve GHz (ref.8). Characteristic of the VCO is its ability to simultaneously achieve relatively high power output, large control input bandwidth and consequently high tuning speed. Typically, its power output ranges from a minimum of 50 mw over octave bandwidths from 0.25 to 8 GHz and 20 mw over gigahertz segments from 8 to 18 GHz. Watkins-Johnson Company reports that their VCO's are able to sweep a full frequency range in less than ten ns also (ref.9).

A major problem observed by the two manufacturers is post tuning drift of the VCO, i.e. the frequency drift of the VCO long after frequency settle-on. The drift has been associated primarily with junction heating of the varactor and power supply regulation when confronted with abrupt changes in current drain. These are problems currently under investigation by both companies mentioned. It

remains that if these limitations are brought to within acceptable limits, advantage may be taken of its rapid tuning capability in many applications.

The settle-on time is a function of the tuning voltage input time constant of the VCO. The driven element is the capacitive varactor. This element is equivalently connected in series with some resistance that results in a time constant that exponentially controls the voltage across the diode. If the VCO is to be step tuned to an accuracy of one MHz for a two GHz change in frequency (0.05%), a duration equal to about eight time constants is needed for the bias voltage across the capacitor to change to the proper value, i.e. exp (-8) $\doteq$ 0.05%. From this computation, the tuning voltage at the control voltage input port could theoretically be caused to rise instantaneously. The corresponding instantaneous frequency output of the VCO would follow and be settled within 0.05% in eight time constants or ten ns. This is an oversimplification, however, because the vacator capacitance is a function of applied voltage and as a result, the driving point impedance and time constant are functions of time also.

CHAPTER II

SWEPT VOLTAGE CONTROLLED OSCILLATORS

2-1 Statement of the Problem

Given that the voltage controlled microwave oscillator is capable of step changes in instantaneous frequency with "settle-on" time as low as ten ns, a natural application of the device is as the local oscillator in a fast frequency scan superheterodyne search receiver. Although the specific requirement for such a receiver is security classified military information, it is sufficient to say that there is a need for super fast frequency scanning microwave receivers capable of 100% detection of a single short pulse emission from an unknown RF source at an unknown carrier frequency within a specified band. It must be indicated that this requirement is not the only one to be met for 100% detection probability. Receive and transmit beams must point at one another and the effective radiated power and receiver sensitivity must be such to permit detection. Hatcher provides a detailed analysis of intercept probability.[1] If the VCO can follow a tuning control voltage across the full frequency range and not lag by more than ten ns, then it may be tuned at a rate not to exceed one sweep in ten ns. This corresponds to a sweep waveform bandlimited to no less than 100 MHz. For sinusoidal modulation, the upper

---

[1]B. R. Hatcher, "Intercept Probability and Intercept Time," Electronic Warfare (March/April 1976), 95-103.

frequency limit becomes 100 MHz. The application of the VCO in a fast scan superheterodyne receiver from this point on is considered the focal point of attention.

The problem of frequency correspondence with time as the VCO is swept is a major problem in rendering the VCO useful in the superhet receiver application. If 1) the receiver is searching a frequency band in the microwave region that is $f_u - f_\ell$ wide, 2) the receiver bandwidth is B, and 3) the shortest single pulse that must be intercepted with 100% detection probability is τ, then the sinusoidal rate at which the VCO must be swept becomes $f_m = 1/\tau$ and the frequency deviation is $\Delta f = \frac{1}{2}(f_u - f_\ell - B)$. If, for example, the receiver is expected to intercept a single pulse as narrow as 0.10 μs somewhere in any frequency range 1600 MHz wide and the bandwidth of the receiver is 4 MHz then

$$f_m = \frac{1}{(.1)(10)^{-6}} = 10 \text{ MHz} \qquad (1)$$

$$\Delta f = \frac{1600-4}{2} \quad 800 \text{ MHz} \qquad (2)$$

This corresponds to an angle modulation index $\beta = 800/10 = 80$. In search systems that are not automated, the linearized VCO driving voltage is also used as the horizontal time base on a panoramic display so that there is an analog correlation between the instantaneous center

of channel frequency to which the receiver is tuned and the instantaneous horizontal position of the panoramic trace. Generally, no major obstacle is presented to this type of frequency determination. In more modern systems that make use of digital signal processing, however, at some point the instantaneous center of bandwidth frequency must be digitized into a binary code of finite bits. Tuning is continuous requiring an infinite number of bits to precisely express the instantaneous frequency of the VCO. This implies an infinite bandwidth to contain the information. In practice, of course, this is not possible nor is it actually required since the receiver bandwidth is not zero. The number of VCO frequencies that must be known is simply $(f_u-f_\ell)/B$ and the number of binary bits necessary to express this number may be derived from

$$2^r = \frac{f_u-f_\ell}{B} = \frac{2\Delta f+B}{B} \simeq \frac{2\Delta f}{B} \tag{3}$$

In addition, r need not be astronomical since for the realistic example already cited

$$r = \log_2 \left(\frac{2\Delta f}{B}\right) \tag{4}$$

which is well within the capacity limits of modern computing systems. Knowing when the instantaneous frequency of the VCO is actually at the digitized frequency is a far greater problem to overcome since tuning at the modulation

rate is assumed continuous and successive bandwidth centers are very close together in time. In fact, if the sweep is linear, the time duration for the VCO to change instantaneous frequency from one bandwidth center to the next successive one is

$$t_{1-2} = \frac{B}{2\Delta f} \cdot \frac{1}{2f_m} = \frac{B}{4f_m \Delta f} \tag{5}$$

$$t_{1-2} = \frac{4}{4(10)(800)} = 0.125 \text{ ns} \tag{6}$$

If it is acceptable to know the precise VCO instantaneous frequency within 10% of receive channel bandwidth, then it must be known within ±5% when the instantaneous frequency passes through the channel center. This would require 0.0125 nanosecond timing synchronization between the instantaneous frequency and the execution time of the binary code to express the r bit frequency word. Quantization, encoding, transmission, decoding and general signal processing must, therefore, be accomplished in incredibly short lengths of time dictated by the range of tuning, receiver bandwidth and tuning rate. These values are fixed according to the specifications imposed on the receiver. It is important to realize, however, that the r bit frequency information can only express the value of a quantized point frequency that in reality must be a range of frequencies of the VCO as it is scanned through

the point. The quantization noise associated with this uncertainty may be determined.

For a binary encoding system with a relatively small quantum gap compared to the full tuning voltage range, i.e. r large, it may be said that the probability density function of the unquantized voltage is flat. Furthermore, for 2^r quantization levels, there are 2^r-1 quantization gaps. For a VCO subject to a range of control voltage v_r, the input voltage to the VCO linearizer could be $-\frac{1}{2}v_r$ to $+\frac{1}{2}v_r$. The voltage quantization gap is

$$\Delta v = \frac{\frac{1}{2}v_r - (-\frac{1}{2}v_r)}{2^r-1} = \frac{v_r}{2^r-1} \tag{7}$$

Assuming a uniform probability density function of the voltage, the noise power N_q due to quantization is

$$N_q = \int_{-\frac{1}{2}(\Delta v)}^{\frac{1}{2}(\Delta v)} \frac{v^2}{(\Delta v)}\, dv = \frac{(\Delta v)^2}{12} \tag{8}$$

To find the quantized signal power, it is necessary to find the mean square value of the quantized signal. The quantized signal can assume r discrete values so that in a bipolar binary encoding system, 2^r characters are necessary to express all quantized levels. If these 2^r discrete words are considered to be equiprobable, the signal may be expected to assume any of the 2^r

combinations of bit configurations. Since the voltage range may be symmetrically placed below and above zero volts with $2^r/2 = 2^{r-1}$ combinations on each side, the equiprobable voltage range becomes $-(\Delta v)2^{r-1} < v < (\Delta v)2^{r-1}$. The quantized signal power $\overline{S^2(t)}$ is

$$\overline{S^2(t)} = \int_{-(\Delta v)2^{r-1}}^{(\Delta v)2^{r-1}} \frac{v^2}{(\Delta v)2^r}\, dv \tag{9}$$

$$\overline{S^2(t)} = (\Delta v)^2 \frac{2^{2r}}{12} \tag{10}$$

From (8) and (10) the signal to quantization noise power ratio is found to be

$$\frac{S}{N_q} = 2^{2r} \tag{11}$$

and the voltage signal to quantization noise ratio is

$$\left(\frac{S}{N_q}\right)_{vr} = 2^r \tag{12}$$

The result shown in (12) is not too startling since in effect the system cited is a pulse code modulation system and for PCM systems in general, the voltage signal to quantization noise ratio increases exponentially with bandwidth (ref.10). For a given length of time, r is

directly proportional to bandwidth so that (12) may be interpreted as

$$\left(\frac{S}{N_q}\right)_{vr} = 2^{EB} \tag{13}$$

where E is a constant of proportionality

For an oscillator that is sinusoidally swept in frequency over a range from $\omega_c-\Delta\omega$ to $\omega_c+\Delta\omega$ at modulation rate ω_m, and modulation index $\beta=\Delta\omega/\omega_m$, the amplitude of the instantaneous frequency remains constant. Expressed mathematically

$$v(t) = A \cos (\omega_c t + \beta \sin \omega_m t) \tag{14}$$

for frequency modulation. The value of A may be assigned and known with certainty regardless of frequency and time. In addition if $\omega_m \longrightarrow 0$ or $\beta \longrightarrow \infty$, (14) reduces to simply a moving carrier. Let

$$\theta = \omega_c t + \beta \sin \omega_m t \tag{15}$$

and the instantaneous frequency ω_i becomes

$$\omega_i = \frac{d\theta}{dt} = \omega_c + \Delta\omega \cos \omega_m t \tag{16}$$

Finding the limit

$$\lim_{\omega_m \longrightarrow 0} v(t) = A \lim_{\omega_m \longrightarrow 0} \cos \left(\omega_c t + \frac{\Delta\omega}{\omega_m} \sin \omega_m t\right) \tag{17}$$

and

$$v(t) \simeq A \lim_{\omega_m \to 0} \cos\left(\omega_c t + t\Delta\omega \frac{\sin \omega_m t}{\omega_m t}\right) = A \cos(\omega_c + \Delta\omega)t \quad (18)$$

For the linearized VCO, $\omega_i = Dv$ where D is some constant of proportionality. This relationship neglects any bias, but indicates the equivalency of v and ω_i.

For any configuration of r bits representing the VCO frequency control driving voltage at any quantized voltage level v, the probability density function that the VCO is on a frequency corresponding to $v_c - \frac{\Delta v}{2} < v < v_c + \frac{\Delta v}{2}$ (in other words, anywhere within $\pm \frac{\Delta v}{2}$ from v_c) is shown in Figure 2-1.

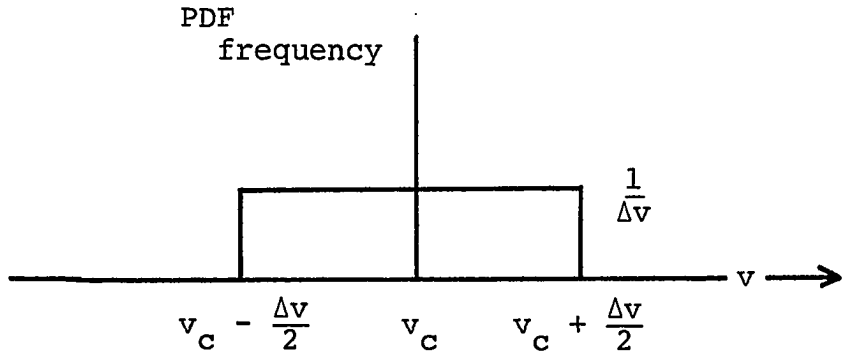

Fig. 2-1

Probability Density Function of instantaneous frequency as a function of quantized control voltage.

A flat probability density function is assumed even though v is sinusoidal since r > > 1 and the gap represents only a very small portion of the full range v_r. Also the flat distribution represents the worst possible case for certainty of information since the occurrence of each voltage (or frequency) is equiprobable.

Because VCO output signal amplitude was shown to be constant over the range of v within a quantization gap for $\beta > > 1$, it is certain that the amplitude value will be A. The probability density function of the instantaneous frequency amplitude is therefore an impulse of unity area at v_c as shown in Figure 2-2.

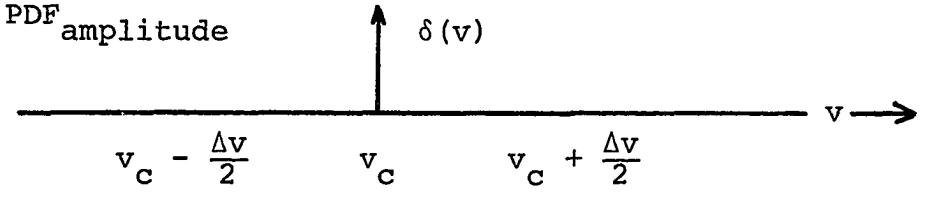

Fig. 2-2

Probability Density Function of VCO output amplitude as a function of control voltage within a quantization gap.

All possibilities are exhausted since

$$\int_{v_c - \frac{\Delta v}{2}}^{v_c + \frac{\Delta v}{2}} \delta(v)\,dv = 1 \qquad (19)$$

It is apparent that the amplitude of the signal may be known without ambiguity since it is not quantized. It is also apparent that the instantaneous frequency is not known without ambiguity since it is quantized to r bits.

In the most general sense, the Fourier transform F(y) of a function of a real variable f(x) is defined by the integral

$$F(y) = \int_{-\infty}^{\infty} f(x)\ e^{-j2\pi xy} dx \tag{20}$$

provided this integral exists for every real value of x. A sufficient (but not necessary) existence condition is that f(x) be absolutely integrable or that

$$\int_{-\infty}^{\infty} |f(x)| dx < \infty \tag{21}$$

The inverse is also true. Again, in the most general sense

$$f(x) = \int_{-\infty}^{\infty} F(y)\ e^{j2\pi xy} dy \tag{22}$$

where it is assumed that, at points of discontinuity of the integral (if any), the function f(x) is given the value $f(x) = [f(x^+) + f(x^-)]/2$ (ref.11). It must be mentioned that although x is real, f(x) may be complex as may be F(y). In electrical engineering x is normally taken to be time

possible to analyze a time domain waveform from the aspect of frequency or the frequency spectrum from the aspect of time. Figure 2-3 indicates the three dimensional amplitude-frequency-time relationship as imagined in three dimensional space (ref.12).

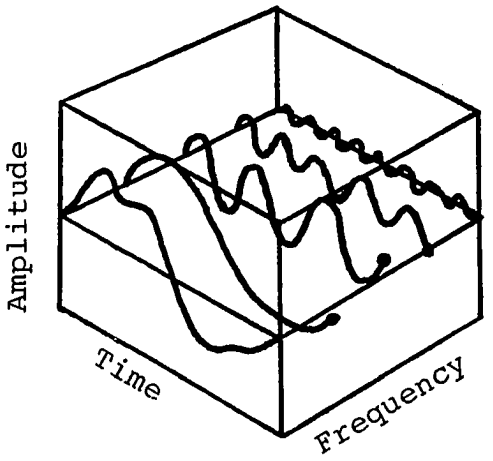

Fig. 2-3

Amplitude-frequency-time cube

If the cube of Fig. 2-3 is mentally oriented for two dimensional viewing so that the frequency axis is a point, knowledge of frequency is non-existent since all harmonic frequencies are indistinguishably absorbed into the arbitrary waveform which is their point to point amplitude sum. Through (20) a rotation of the cube takes place (clockwise looking down) so that the time axis becomes a point while the frequency axis becomes visible. Since the

choice of real world variables for x and y in (20) and (22) is arbitrary except for the constraint in (21), it should be possible to define a transform pair like (20) and (22) between any two of three interdependent variables. In other words, there should exist a transform pair to allow two way transformation not only between time and frequency, but time and amplitude, and frequency and amplitude and from a physical standpoint observable by proper cube rotation.

2-2 Amplitude-Frequency-Time Trade-offs

In communications systems design, trade-offs are frequently performed between time and frequency. Narrow bandwidth implies a long information transmission time while a wide bandwidth implies a short "equivalent information" transmission time. The possibility of frequency-time trade-off is well known and easily analyzed through the familiar Fourier Transform (20). Likewise, functions of these two variables may also be traded to meet the particular communication system's needs. It is seldom that any trade-off of time or frequency is made with amplitude, the third variable in the three interdependent variable system of Figure 2-3. On the assumption that the transform pair exists between frequency and amplitude, it should be possible to trade functions of these two variables for the purpose of sacrificing something about one to enhance something else about the other. More specifically, it may

be possible to trade the worst case uncertainty of frequency information shown in Figure 2-1 with the certainty of amplitude information shown in Figure 2-2 for the purpose of enhancing frequency knowledge at the expense of amplitude knowledge. The quantized variable would then represent some amplitude variable and would be worst case ambiguous while the unquantized variable would represent frequency and would be essentially certain. If the trade-off is physically realizable, it would be possible to express VCO frequency with certainty (to the extent that the approximation of (18) is exact) at the expense of loss of precise signal amplitude information at that frequency. Certainty of frequency would exist within any $v_c - \frac{\Delta v}{2} < v < v_c + \frac{\Delta v}{2}$. The actual value of the frequency is determined by the exact numerical value assigned to v_c and not the uncertain range of v surrounding it. (It should also be mentioned that precise amplitude information is relatively unimportant since it only affects receiver sensitivity in the first mixer of the receiver. It is assumed that minimum acceptable sensitivity is maintained according to receiver specification and that random excess sensitivity due to VCO amplitude uncertainty simply exceeds the requirement).

The following parts of this thesis deal with the search of a solution and design of a system that permits the trading of the frequency probability density distribution with that of the VCO signal amplitude.

CHAPTER III

MATHEMATICAL FORMULATION

3-1 The Fast Scan Superheterodyne Receiver Local Oscillator - Analysis of a Solution

When a cosinusoidal carrier is sinusoidally angle modulated with modulation index β and simultaneously cosinusoidally amplitude modulated with modulation index m and the frequencies of modulation are the same, the instantaneous signal is completely described by

$$v(t) = (1-m \cos \omega_m t) \left(\cos (\omega_c t + \beta \sin \omega_m t)\right) \qquad (23)$$

(ref.13).

Algebraic and trigonometric manipulation provides

$$\begin{aligned} v(t) = {} & J_0(\beta)\cos \omega_c t \\ & -J_1(\beta)\cos(\omega_c - \omega_m)t + J_1(\beta)\cos(\omega_c + \omega_m)t \\ & +J_2(\beta)\cos(\omega_c - 2\omega_m)t + J_2(\beta)\cos(\omega_c + 2\omega_m)t \\ & -J_3(\beta)\cos(\omega_c - 3\omega_m)t + J_3(\beta)\cos(\omega_c + 3\omega_m)t \\ & +\ldots \qquad\qquad +\ldots \\ & -\frac{m}{2}\left(J_0(\beta) + J_2(\beta)\right)\cos(\omega_c - \omega_m)t \\ & -\frac{m}{2}\left(J_0(\beta) + J_2(\beta)\right)\cos(\omega_c + \omega_m)t \\ & +\frac{m}{2}\left(J_1(\beta) + J_3(\beta)\right)\cos(\omega_c - 2\omega_m)t \\ & -\frac{m}{2}\left(J_1(\beta) + J_3(\beta)\right)\cos(\omega_c + 2\omega_m)t \\ & -\ldots \end{aligned} \qquad (24)$$

Combining terms of common frequency provides

$$\begin{aligned} v(t) = J_0(\beta)\cos\omega_c t &- \left(\frac{m}{2}\{J_0(\beta)+ J_2(\beta)\}+ J_1(\beta)\right)\cos(\omega_c - \omega_m)t \\ &- \left(\frac{m}{2}\{J_0(\beta)+ J_2(\beta)\}- J_1(\beta)\right)\cos(\omega_c + \omega_m)t \\ &+ \left(\frac{m}{2}\{J_1(\beta)+ J_3(\beta)\}+ J_2(\beta)\right)\cos(\omega_c - 2\omega_m)t \\ &- \left(\frac{m}{2}\{J_1(\beta)+ J_3(\beta)\}- J_2(\beta)\right)\cos(\omega_c + 2\omega_m)t \\ &- \left(\frac{m}{2}\{J_2(\beta)+ J_4(\beta)\}+ J_3(\beta)\right)\cos(\omega_c - 3\omega_m)t \\ &- \left(\frac{m}{2}\{J_2(\beta)+ J_4(\beta)\}- J_3(\beta)\right)\cos(\omega_c + 3\omega_m)t \\ &+ \left(\frac{m}{2}\{J_3(\beta)+ J_5(\beta)\}+ J_4(\beta)\right)\cos(\omega_c - 4\omega_m)t \\ &- \left(\frac{m}{2}\{J_3(\beta)+ J_5(\beta)\}- J_4(\beta)\right)\cos(\omega_c + 4\omega_m)t \\ &- \ldots \end{aligned} \tag{25}$$

In general any upper sideband component may be expressed by

$$\begin{aligned} v_{n(USB)}(t) = &-\left(\frac{m}{2}\{J_{n-1}(\beta)+ J_{n+1}(\beta)\}- J_n(\beta)\right) \\ &\times \cos(\omega_c + n\omega_m)t \end{aligned} \tag{26}$$

Now suppose that amplitude modulation is applied in the form of

$$v(t) = (1 + m\cos\omega_m t)\left(\cos(\omega_c t + \beta\sin\omega_m t\right) \tag{27}$$

instead of the form of (23). Algebraic and trigonometric manipulation would provide

$$
\begin{aligned}
v(t) = \; & J_0(\beta)\cos\omega_c t - J_1(\beta)\cos(\omega_c - \omega_m)t + J_1(\beta)\cos(\omega_c + \omega_m)t \\
& + J_2(\beta)\cos(\omega_c - 2\omega_m)t + J_2(\beta)\cos(\omega_c + 2\omega_m)t \\
& - J_3(\beta)\cos(\omega_c - 3\omega_m)t + J_3(\beta)\cos(\omega_c + 3\omega_m)t \\
& + J_4(\beta)\cos(\omega_c - 4\omega_m)t + J_4(\beta)\cos(\omega_c + 4\omega_m)t \\
& - \ldots \qquad\qquad + \ldots \qquad\qquad + \\
& + \frac{m}{2}\left(J_0(\beta) + J_2(\beta)\right)\cos(\omega_c - \omega_m)t \\
& + \frac{m}{2}\left(J_0(\beta) + J_2(\beta)\right)\cos(\omega_c + \omega_m)t \\
& - \frac{m}{2}\left(J_1(\beta) + J_3(\beta)\right)\cos(\omega_c - 2\omega_m)t \\
& + \frac{m}{2}\left(J_1(\beta) + J_3(\beta)\right)\cos(\omega_c + 2\omega_m)t \\
& + \frac{m}{2}\left(J_2(\beta) + J_4(\beta)\right)\cos(\omega_c - 3\omega_m)t \\
& + \frac{m}{2}\left(J_2(\beta) + J_4(\beta)\right)\cos(\omega_c + 3\omega_m)t \\
& - \frac{m}{2}\left(J_3(\beta) + J_5(\beta)\right)\cos(\omega_c - 4\omega_m)t \\
& + \frac{m}{2}\left(J_3(\beta) + J_5(\beta)\right)\cos(\omega_c + 4\omega_m)t + \ldots \qquad (28)
\end{aligned}
$$

In general, any lower sideband component may be expressed by

$$
\begin{aligned}
& v_{n(LSB)}(t) = -(-1)^n\left(\frac{m}{2}\left\{J_{n-1}(\beta) + J_{n+1}(\beta)\right\}\right) - J_n(\beta)\Big) \\
& \times \cos(\omega_c - n\omega_m)t \qquad (29)
\end{aligned}
$$

Recalling the formal statement of the Bessel function of the first kind

$$
J_n(\beta) = \sum_{\ell=0}^{\infty} \frac{(-1)^{\ell}(\beta/2)^{n+2\ell}}{\ell!\,(\ell+n)!} \qquad (30)
$$

It follows that

$$J_{n-1}(\beta) = \sum_{\ell=0}^{\infty} \frac{(-1)^{\ell}(\beta/2)^{n+2\ell-1}}{\ell!(\ell+n-1)!} \tag{31}$$

and

$$J_{n+1}(\beta) = \sum_{\ell=0}^{\infty} \frac{(-1)^{\ell}(\beta/2)^{n+2\ell+2}}{\ell!(\ell+n+2)!} \tag{32}$$

Combining (30), (31), and (32) it may be shown that (ref. 14)

$$J_{n+1}(\beta) = \frac{2n}{\beta} J_n(\beta) - J_{n-1}(\beta) \tag{33}$$

which establishes an exact recursive relationship between successive Bessel functions of the first kind and argument β. For amplitude modulation in the form of $(1-m \cos \omega_m t)$ the amplitude of the nth upper sideband of (23) is

$$A_n = -\left(\frac{m}{2}\{J_{n-1}(\beta) + J_{n+1}(\beta)\} - J_n(\beta)\right) \tag{34}$$

For amplitude modulation in the form of $(1+m \cos \omega_m t)$ the amplitude of the nth lower sideband of (27) is

$$A_n = -(-1)^n\left(\frac{m}{2}\{J_{n-1}(\beta) + J_{n+1}(\beta)\} - J_n(\beta)\right) \tag{35}$$

In either (34) or (35) the condition for any A_n to be zero rendering the disappearance of the nth upper sideband for (34) or nth lower sideband for (35) is that

$$\frac{m}{2}\{J_{n-1}(\beta)+ J_{n+1}(\beta)\} = J_n(\beta) \tag{36}$$

or that

$$J_{n-1}(\beta)+ J_{n+1}(\beta) = \frac{2}{m} J_n(\beta) \tag{37}$$

Solving (37) equation for $J_{n+1}(\beta)$,

$$J_{n+1}(\beta) = \frac{2}{m} J_n(\beta)- J_{n-1}(\beta) \tag{38}$$

This equation is precisely the form of (33), the recursive relationship linking three successive Bessel functions of the first kind. In fact, if

$$\frac{2}{m} = \frac{2n}{\beta} \qquad \text{or if} \qquad m = \frac{\beta}{n} \tag{39}$$

the amplitude of the nth sideband becomes zero (whether upper or lower sideband depends on the form of the amplitude modulation).

Since the range of the amplitude modulation index is $0 \leq m \leq 1$, a zero amplitude condition can only occur for $n \geq \beta$. Stated another way, only the βth sideband and beyond may have a zero amplitude and never more than one sideband may have a zero amplitude for any value of m.

With the notion that the frequencies of the sidebands generated depend only on the VCO carrier and modulation frequencies, a significant enhancement of frequency knowledge may be obtained if, selectively, one sideband is used as the local oscillator signal and not the instantaneous frequency of the VCO. It has been shown that for $n > \beta$ it is possible to suppress one sideband while maintaining all others. If the inverse is possible, the VCO could function as a local oscillator whose frequency changes discretely from one sideband to another while all others are suppressed. To continue this development, if the amplitude of the nth sideband is zero by the equality of (33), then the amplitude of any other kth sideband at β or beyond is governed by

$$m = \frac{\beta}{k} \tag{40}$$

Substituting (40) into (34), it becomes possible to describe the amplitude of the nth upper sideband (whether it is zero or not) for any $m = \frac{\beta}{k}$.

$$A(k,n) = -\left(\frac{\beta}{2k}\{J_{n-1}(\beta) + J_{n+1}(\beta)\} - J_n(\beta)\right) \tag{41}$$

From (26) and (40), the time function is described by

$$v_{n(USB)}(k,t) = -\left(\frac{\beta}{2k}\{J_{n-1}(\beta) + J_{n+1}(\beta)\} - J_n(\beta)\right) \times \cos(\omega_c + n\omega_m)t \tag{42}$$

where amplitude modulation is of the form $(1-m \cos \omega_m t)$. For the lower sideband case and from (29) and (40) the time function is described by

$$v_{n(LSB)}(k,t) = -(-1)^n\left(\frac{\beta}{2k}\{J_{n-1}(\beta) + J_{n+1}(\beta)\} - J_n(\beta)\right) \times \cos\ (\omega_c - n\omega_m)t \tag{43}$$

where amplitude modulation is of the form $(1 + m \cos \omega_m t)$. For both (42) and (43), $k = \beta/m$, $k \geq \beta$, and $0 \leq m \leq 1$. The amplitude coefficient becomes zero for $k = n$. Equation (42) may be interpreted in two ways:

(1) The instantaneous time domain expression for any one upper sideband at $(\omega_c + n\omega_m)$ may be found as a function of the continuous variable k; or

(2) The instantaneous time domain expression for any upper sideband at $(\omega_c + n\omega_m)$ may be found for some fixed k.

In the first case, n is a fixed integer ($n \geq \beta$) and k is a continuous variable ($k \geq \beta$) while in the second case k is a constant ($k \geq \beta$) and n is a discrete variable ($n \geq \beta$). Equation (42) represents the first case while the second case is represented by

$$v_{k(USB)}(n,t) = -\left(\frac{\beta}{2k}\{J_{n-1}(\beta) + J_{n+1}(\beta)\} - J_n(\beta)\right) \times \cos(\omega_c + n\omega_m)t \tag{44}$$

Now for $(1 + m \cos \omega_m t)$ amplitude modulation, (43) may similarly be interpreted to be a function of n or k so that

$$v_{n(LSB)}(k,t) = -(-1)^n \frac{\beta}{2k}\{J_{n-1}(\beta) + J_{n+1}(\beta)\} - J_n(\beta)\Big) \times \cos(\omega_c - n\omega_m)t \tag{45}$$

where n = constant

k = continuous variable

or

$$v_{k(LSB)}(n,t) = -(-1)^n\left[\frac{\beta}{2k}\{J_{n-1}(\beta)+ J_{n+1}(\beta)\}- J_n(\beta)\right] \times \cos(\omega_c - n\omega_m)t \qquad (46)$$

Because the forms of the time domain expressions for the upper sideband case ((42) for amplitude modulation of the form (1 - m cos $\omega_m t$)) is identical to the form of the time domain expression for the lower sideband case (43) for amplitude modulation of the form (1 + m cos $\omega_m t$), the upper sideband case will be temporarily set aside. Subsequent discussion will pertain specifically to amplitude modulation of the form (1 + m cos $\omega_m t$) which contains the $-(-1)^n$ factor.

It is helpful to look at values of the amplitude coefficients of several nth lower sidebands. Table 3-1 indicates the behavior of the amplitude as a function of the inverse amplitude modulation index k, for the example case where $\beta = 80$. If k is some integer greater than or equal to 80, then some nth lower sideband will have zero amplitude. For non-integer values of k, all lower sideband amplitudes are non-zero. Table 3-1 should be read horizontally if n is considered the variable and k fixed. It should be read vertically if the sideband amplitude of any one sideband is desired for variable k and n fixed.

Figure 3-1 illustrates the general trend of the results of Table 3-1 read vertically, i.e. fixed n (odd) and variable k.

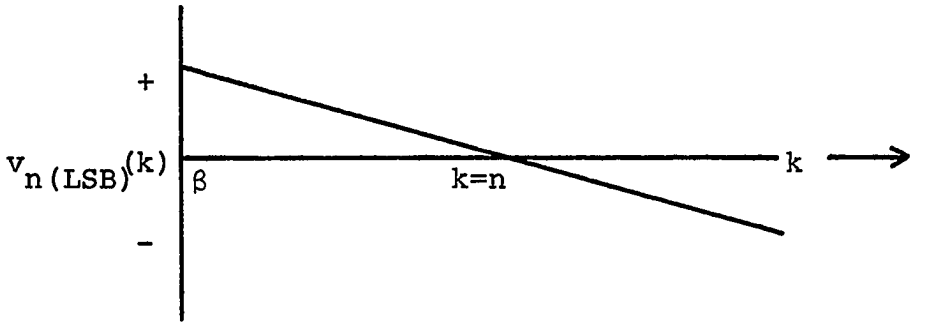

Fig. 3-1

Amplitude of nth frequency component $(\omega_c - n\omega_m)$ versus inverse amplitude modulation index, k (n constant and odd).

Figure 3-2 is the same representation as Figure 3-1, but with n even.

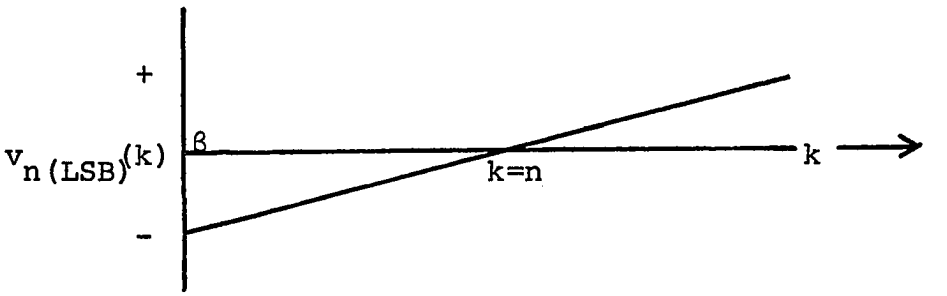

Fig. 3-2

Amplitude of nth frequency component $(\omega_c - n\omega_m)$ versus inverse amplitude modulation index, k (n constant and even).

SIDEBAND AMPLITUDE VALUES FOR $\beta = 80$, $k \geq \beta$, $0 \leq m \leq 1.0000$

		n										
m	k	80	81	82	83	84	85	86	87	88	89	90
1.0000	80	0.000000	0.001024	-0.001552	0.001702	-0.001604	0.001374	-0.001098	0.000829	-0.000598	0.000415	-0.000277
0.9876	81	0.001287	0.000000	-0.000766	0.001121	-0.001188	0.001085	-0.000903	0.000702	-0.000517	0.000364	-0.000246
0.9756	82	0.002532	-0.000999	0.000000	0.000553	-0.000782	0.000804	-0.000714	0.000578	-0.000438	0.000314	-0.000216
0.9638	83	0.003757	-0.001974	0.000748	0.000000	-0.000386	0.000529	-0.000529	0.000457	-0.000360	0.000266	-0.000187
0.9523	84	0.004951	-0.002926	0.001478	-0.000540	0.000000	0.000261	-0.000348	0.000338	-0.000285	0.000219	-0.000158
0.9411	85	0.006114	-0.003855	0.002192	-0.001068	0.000377	0.000000	-0.000172	0.000223	-0.000211	0.000173	-0.000130
0.9302	86	0.007245	-0.004763	0.002889	-0.001583	0.000746	-0.000255	0.000000	0.000110	-0.000139	0.000128	-0.000103
0.9195	87	0.008356	-0.005650	0.003560	-0.002087	0.001106	-0.000505	0.000168	0.000000	-0.000068	0.000084	-0.000076
0.9090	88	0.009446	-0.006517	0.004232	-0.002579	0.001458	-0.000749	0.000332	-0.000107	0.000000	0.000041	-0.000050
0.8988	89	0.010505	-0.007365	0.004885	-0.003060	0.001802	-0.000988	0.000493	-0.000213	0.000067	0.000000	-0.000024
0.8888	90	0.011543	-0.008193	0.005521	-0.003531	0.002139	-0.001221	0.000650	-0.000316	0.000133	-0.000040	0.000000

TABLE 3-1

If Table 3-1 is read horizontally so that k is a constant, but not necessarily an integer, $v_{k(LSB)}(n)$ may be plotted and results in a discrete amplitude impulse at each sideband frequency. If say k = 85, then Figure 3-3 illustrates the amplitude trend of the n sidebands as a function of n.

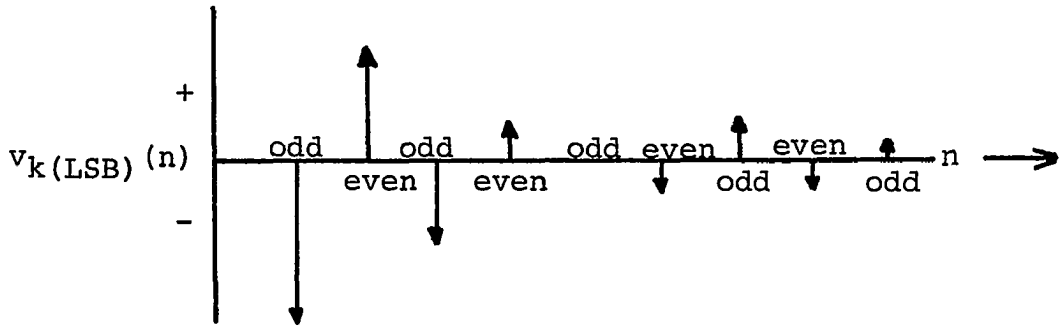

Fig.3-3

n frequency component amplitudes $(\omega_c - n\omega_m)$ versus n for a fixed integer value of k.

Observations from Table 3-1 and Figures 3-1, 3-2, and 3-3 are:

1. A zero amplitude lower sideband at $(\omega_c - n\omega_m)$ with $n \geq \beta$ can only occur if k is an integer. However, k is a continuous variable since $m = \beta/k$ and the only restriction here is that $0 \leq m \leq 1$.

2. For any odd numbered lower sideband n, with $n \geq \beta$, the amplitude of the sideband decreases with increasing k.

3. For a constant $k \leq n$ all odd numbered lower sideband $(\omega_c - n\omega_m)$ amplitudes are negative and all even numbered lower sideband amplitudes are positive. For $k \geq n$ all odd numbered lower sidebands are negative.

Since the inverse of single sideband suppression is desired, it is anticipated that some system of sideband cancellation is possible so that one is remaining while all others are cancelled. No attention is given to any sidebands other than $(\omega_c - n\omega_m)$ with $n \geq \beta$ since amplitude cancellation is not possible for other sidebands due to the natural restrictions on m. For those sidebands $(\omega_c - n\omega_m)$ with $n < \beta$, it is required that $m > 1$. Similarly, if (42) were being developed in parallel fashion, the condition where $n < \beta$ would also require that $m > 1$. In either case this condition represents saturation of a device when a physical realization is considered and is therefore not permitted.

The cancellation of a single sideband component for a particular value of $m = \frac{\beta}{k}$ is precisely the opposite of the condition that is desired. To reiterate, a single frequency component having the appearance of discrete rapid frequency change with the probability density distribution of Figure 2-1 is necessary in order to precisely describe the VCO frequency output as a function of some quantized amplitude variable. Precise receiving frequency information will then be available when the VCO is used as the local oscillator in the first mixer of a fast frequency scan superheterodyne receiver.

3-2 Observations and Derived Conclusions of Bessel Function Behavior

Observations of the behavior of the Bessel function of the first kind and the interrelationships of the Bessel functions of different orders (same argument) as they appear in the form of (43) will lead to certain conclusions governing the behavior of sideband amplitudes. These conclusions will provide guidance and indicate methods of approach to achieve the inverse of the sideband amplitude relationship already known possible by application of (43).

General observations on the behavior of $J_n(\beta)$ for $\beta >> 1$.

1. For all $n > \beta$, $J_n(\beta)$ is always greater than zero, but monotonically decreases as n increases.
2. $J_n(\beta)$ is approximately constant for $n - \beta$ = constant.
3. $J_\beta(\beta) \simeq 0.1$ or 20 dB down from the greatest possible value of any $J_n(\beta)$.
4. $J_{\beta+10}(\beta)$ is 34 dB down from $J_\beta(\beta)$ so that $\beta \leq n \leq (\beta+10)$ is considered the useful range of $J_n(\beta)$ for $n \geq \beta$.

The system derivation may be somewhat generalized because of these observations even though a specific example ($\beta = 80$) is cited. Generality is not lost due to numerical specifications.

Substituting (40) into (43) and rewriting to reflect the dependence of v_n on m

$$v_{n(LSB)}(m,t) = -(-1)^n\left(\frac{m}{2}\{J_{n-1}(\beta)+ J_{n+1}(\beta)\}- J_n(\beta)\right) \times \cos(\omega_c - n\omega_m)t \qquad (47)$$

If m is considered to be a weak function of t, i.e. any periodic frequency associated with m is much less than $\omega_c-(\beta+10)\omega_m$, then m may be considered independent of t. This assumption eases analysis of (47) and is accepted as realistic from the standpoint of receiver implementation. If $v_{n(LSB)}(m,t)$ is recognized to be the time function of any nth lower sideband, then it follows that the composite time domain signal e(m,t) becomes

$$e(m,t) = \sum_{n=\beta}^{\beta+10} (-1)^n\left(\frac{m}{2}\{J_{n-1}(\beta)+ J_{n+1}(\beta)\}- J_n(\beta)\right) \times \cos(\omega_c - n\omega_m)t \qquad (48)$$

In addition, if a second composite signal is derived from e(m,t) through frequency heterodyning down by ω_m in say a double balanced mixer and ignoring intermodulation distortion and any other peculiarities due to actual devices, e(m,t) is relabled $e_1(m,t)$ and $e_2(m,t)$ becomes the frequency shifted signal.

$$e_1(m,t) = -\sum_{n=\beta}^{\beta+10} (-1)^n \left[\frac{m}{2}\{J_{n-1}(\beta) + J_{n+1}(\beta)\} - J_n(\beta)\right] \times \cos(\omega_c - n\omega_m)t \qquad (49)$$

$$e_2(m,t) = -\sum_{n=\beta}^{\beta+10} (-1)^n \left[\frac{m}{2}\{J_{n-1}(\beta) + J_{n+1}(\beta)\} - J_n(\beta)\right] \times \cos(\omega_c - (n+1)\omega_m)t \qquad (50)$$

By substituting n for n+1 in (50), while maintaining the same frequency range of interest, $e_2(m,t)$ becomes

$$e_2(m,t) = \sum_{n=\beta}^{\beta+10} (-1)^n \left[\frac{m}{2}\{J_{n-2}(\beta) + J_n(\beta)\} - J_{n-1}(\beta)\right] \times \cos(\omega_c - n\omega_m)t \qquad (51)$$

3-3 Analysis of an Unsuccessful Approach

The sideband component amplitudes of (49) and (51) are of opposite sign for the same n so that if the signals are summed in the time domain, some degree of amplitude cancellation may be expected at all sideband frequencies. Perhaps amplitude enhancement at the frequency that has zero amplitude in either one of the two signals may be expected because an amplitude will be added to zero and not one of near equal, but opposite sign.

Table 3-1 is read horizontally for m =0.9756 to produce $e_1(m,t)$ points in Figure 3-4. The e_2 points are derived from the e_1 points. $\beta = 80$ and $80 \leq n \leq 90$.

RELATIVE
SIDEBAND AMPLITUDE
vs
SIDEBAND NUMBER

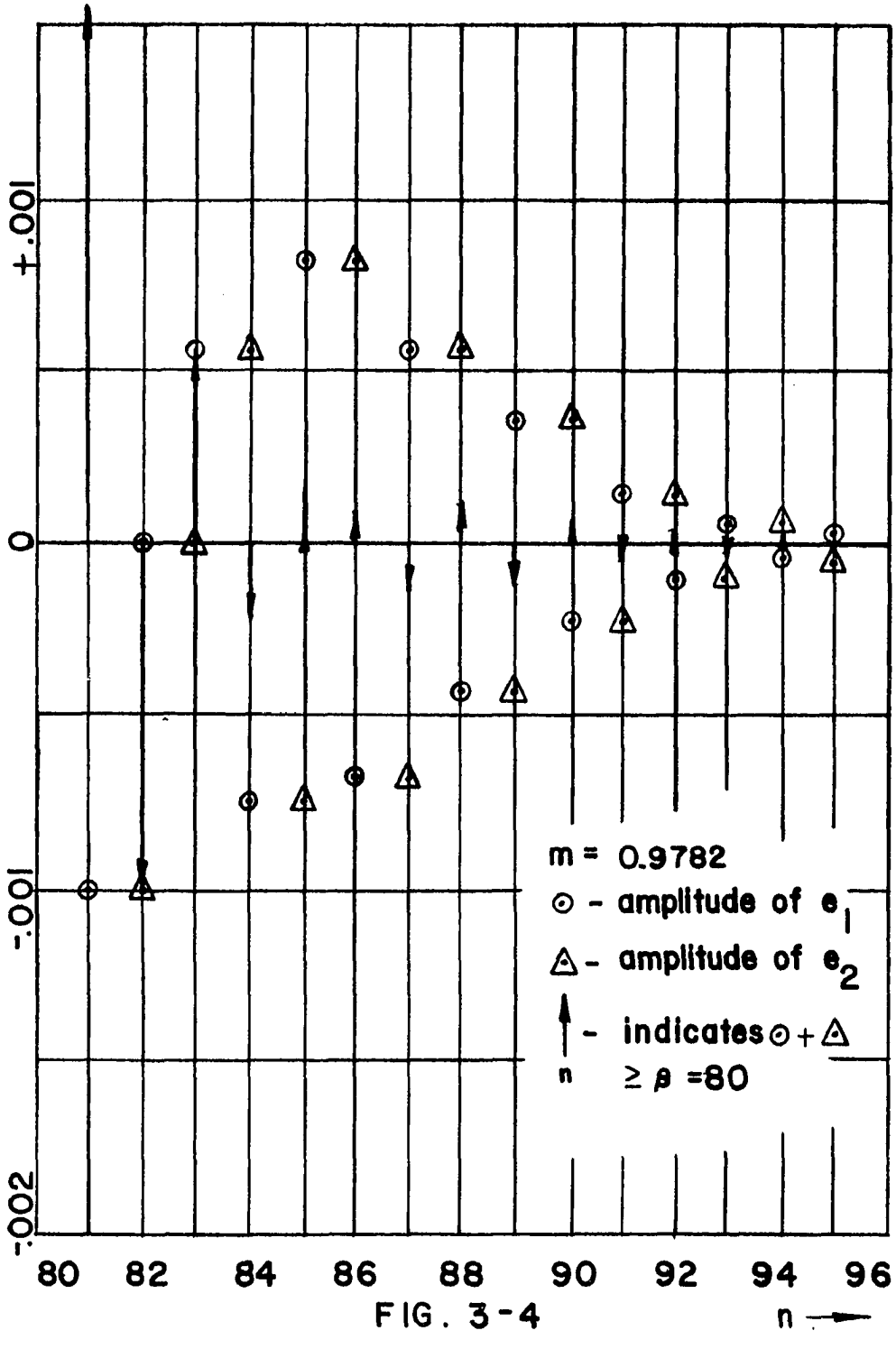

FIG. 3-4

By performing $e_1 + e_2$ significant amplitude cancellation is possible for those sidebands lower in frequency than the zero amplitude sideband of either signal. This is indicated by the impulse arrow lengths in Figure 3-4. The zero amplitude sideband for e_1 occurs at n = 82 and at n = 83 for e_2 for the value of m specified. Even though the zero amplitude frequency of both signals is enhanced by the resultant amplitude existing by virtue of the opposite signal, the amplitude cancellation above the zero amplitude crossover frequencies is so poor that by comparison it is as if the higher frequencies are enhanced. Figures 3-5 and 3-6 support this argument for smaller values of m. In addition, if $e_1 + e_2$ were not a strong function of m, either composite signal could be properly scaled and/or shaped by an appropriate filter so that non-zero amplitudes could be better matched in magnitude to provide better cancellation. Even though e_1 and e_2 are strong functions of m, a matter of judgment is needed to determine the relative dependence of their sum on m. Considering any single frequency component, let

$$a_n(m) = \frac{m}{2}\left(J_{n-1}(\beta) + J_{n+1}(\beta)\right) - J_n(\beta) - \frac{m}{2} \times \left(J_{n-2}(\beta) + J_n(\beta)\right) \quad , \; n = \text{constant} \qquad (52)$$

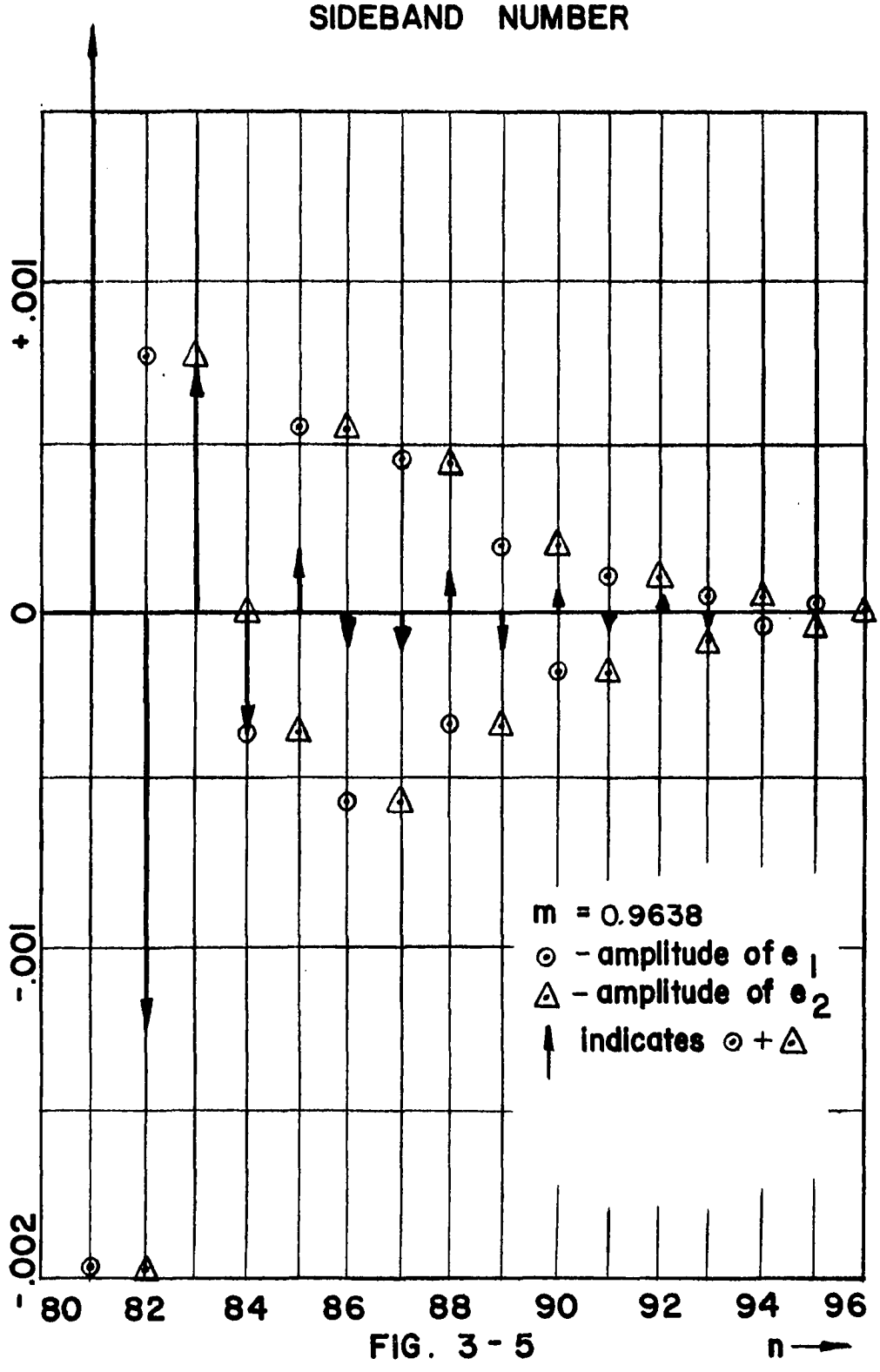

FIG. 3 - 5

RELATIVE
SIDEBAND AMPLITUDE
vs
SIDEBAND NUMBER

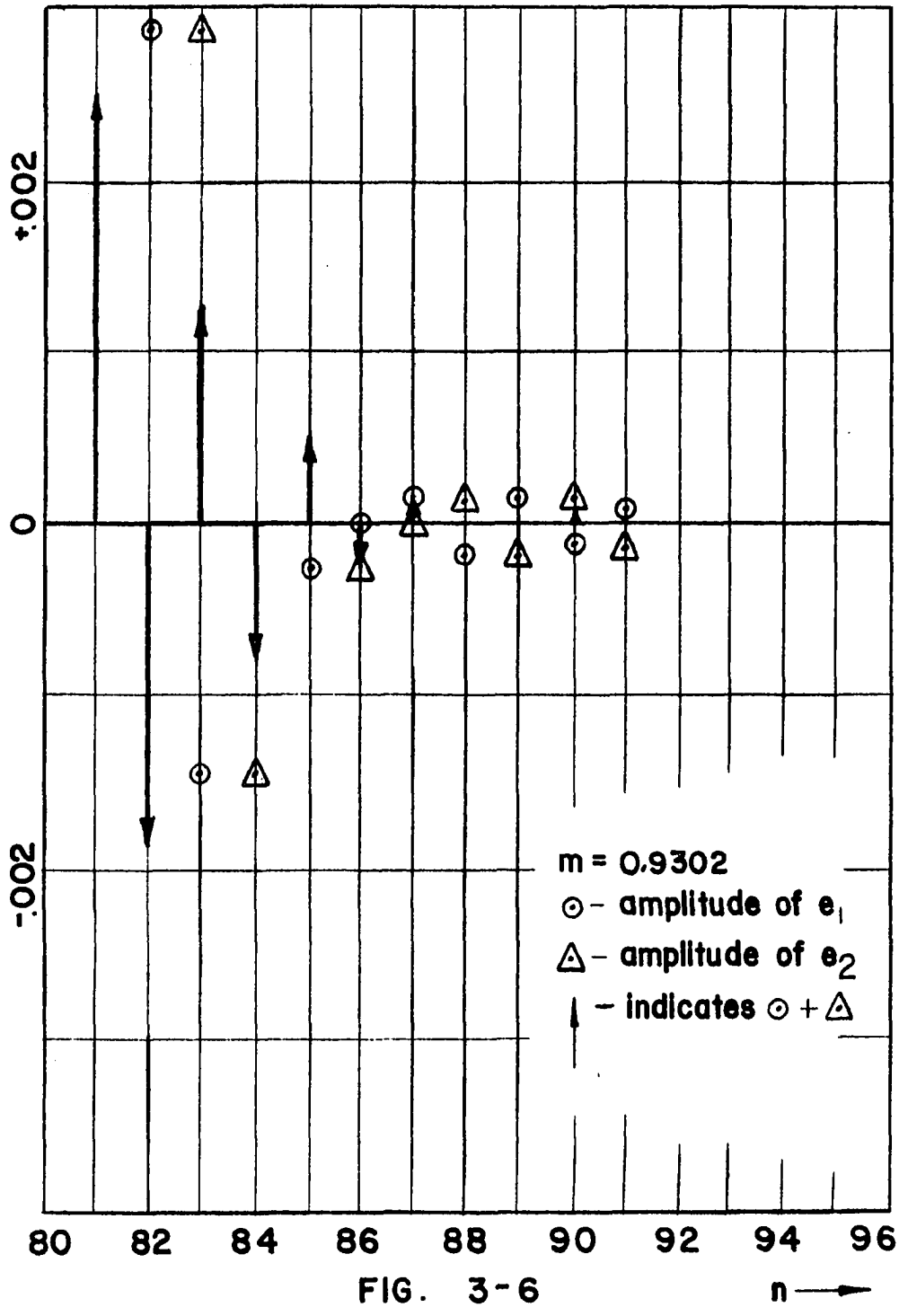

FIG. 3-6

If this sum is relatively constant, it would be possible to describe a passband gain (or attenuation) of a filter at $\omega = \omega_c - n\omega_m$ for each n that would provide the proper output signal level for unwanted sideband cancellation that would hold for all absolute levels. For $a_n(m)$ to be constant, $da_n(m)/dm = 0$.

$$\frac{da_n(m)}{dm} = \frac{1}{2}\left(J_{n-1}(\beta) + J_{n+1}(\beta)\right) - \frac{1}{2}\left(J_{n-2}(\beta) + J_n(\beta)\right) = 0 \quad (53)$$

or

$$J_{n-1}(\beta) + J_{n+1}(\beta) = J_{n-2}(\beta) + J_n(\beta) \quad (54)$$

If $J_{n-1}(\beta) + J_{n+1}(\beta) - J_{n-2}(\beta) - J_n(\beta) \simeq 0$ compared to $J_{n-1}(\beta) + J_{n+1}(\beta)$ or $J_{n-2}(\beta) + J_n(\beta)$, the functional dependence of $e_1 + e_2$ on m is weak. Let

$$\varepsilon = J_{n-1}(\beta) + J_{n+1}(\beta) - J_{n-2}(\beta) - J_n(\beta) \quad (55)$$

to indicate this dependence. Table 3-2 lists ε and $J_{n-1}(\beta) + J_{n+1}(\beta)$ for $\beta = 80$ and $80 \leq n \leq 90$.

TABLE 3-2.--Relative sideband amplitude dependence indicator ε and $J_{n+1}(\beta)+J_{n-1}(\beta)$ for $80 \leq n \leq 90$

n	ε	$J_{n+1}(\beta)+J_{n-1}(\beta)$
80	-0.0406	0.2076
81	-0.0417	0.1659
82	-0.0386	0.1273
83	-0.0331	0.0942
84	-0.0268	0.0674
85	-0.0207	0.0467
86	-0.0153	0.0315
87	-0.0108	0.0206
88	-0.0075	0.0132
89	-0.0049	0.0082
90	-0.0032	0.0049

From Table 3-2 it is evident that the magnitude of ε is not small with respect to the magnitude of one of the Bessel function sums that it was derived from except for n near β. The sum of e_1 and e_2 at individual frequencies is therefore a strong function of m. Further observance of Table 3-2 shows that a non-linear relationship exists between ε and $J_{n+1}(\beta)+J_{n-1}(\beta)$ indicating that the functional dependence of $e_1 + e_2$ on m is at least quadratic if not higher order. It is concluded that any filter operating on $e_1 + e_2$ must have a frequency point to frequency point gain (or attenuation) that is dependent on m in a more than trivial fashion if those frequency components at the zero amplitude frequencies are to be attenuated. The frequency component amplitudes are very non-linear with m in the vicinity of the sideband to be enhanced.

In addition, the functional dependence of e_1 or e_2 on m is very strong so that a filter that might be used to adjust the sideband amplitudes of either signal to enhance cancellation in $e_1 + e_2$ would also require passband characteristics changing with m. Filters whose passband characteristics are a function of m are considered impractical. Most of this approach is abandoned, but realistic portions are retained for further possible application.

3-4 Analysis of a Successful Approach

If the signals of (49) and (51) are passed through separate parallel banks of bandpass filters, one filter in each bank for each lower sideband of interest, and then hard limited, it becomes possible to equalize the amplitudes of the fundamental components at the corresponding frequency limiter outputs. Harmonic frequency components of the limiter outputs would be at $\omega_p = p(\omega_c - n\omega_m)$, $p = 2,3,4,\ldots,$ and they may be filtered out in follow-on circuitry since they are p octaves distant. Considering a single frequency component from (49) it is expressible in the form of (27).

A limiter output[2] (after bandpass filtering) becomes

$$v_{n_1(LSB)}(m,t) = -(-1)^n\left(\frac{m}{2}\{J_{n-1}(\beta)+ J_{n+1}(\beta)\}- J_n(\beta)\right) X \cos(\omega_c - n\omega_m)t \quad (56)$$

Again m is not considered to be a function of t since it is still maintained that any frequency associated with m is much less than $\omega = \omega_c - n\omega_m$. For n odd, $v_{n_1(LSB)}$ becomes

$$v_{n_1(LSB)}(m,t) = \left(\frac{m}{2}\{J_{n-1}(\beta)+ J_{n+1}(\beta)\}- J_n(\beta)\right) X \cos[(\omega_c - n\omega_m)t + \phi] \quad (57)$$

By amplifying by G and considering a constant $\hat{V}$, associated with the actual output level of the VCO, and amplitude limiting, the fundamental amplitude at $\omega = \omega_c - n\omega_m$ is derived from

$$A_{n_1} = \frac{G\hat{V}}{\pi}\int_{-\pi}^{\pi} v_{n_1(LSB)}(m,t)\ \text{clipped}\left(\cos[(\omega_c - n\omega_m)t + \phi] X\ d\{(\omega_c - n\omega_m)t\}\right) \quad (58)$$

---

[2]Although the bandpass filter introduces a phase shift to the signal, the frequency shifted signal will be similarly clipped and filtered and then summed with (56). The phase difference between these two signals is zero, therefore, their individual phase shifts are arbitrarily set equal to zero. The worst possible case is that the phase difference between the two signals is some non-zero constant.

If by the amplitude modulation process, the angle modulated signal is multiplied by $(1 + m \cos \omega_m t)$ and $m = m(t) = M \cos \omega_s t$, then the amplitude modulation process becomes a multiplication of the angle modulated signal by $(1 + M \cos \omega_s t \cos \omega_m t)$. If however, $\omega_s << \omega_m$, that is, the rate of change of amplitude modulation index is small compared to the modulation frequency then it is maintained that m is not a function of time and the Fourier requirement that a sinusoidal signal must exist from $-\infty < t < \infty$ to be truly an impulse in the frequency domain is approximated. It is therefore considered that the rate of change of amplitude modulation is much lower than the amplitude modulation frequency or than $m \neq m(t)$.

Figure 3-7 is a pictorial of any $\omega_c - n\omega_m$ waveform with clipping applied at points symmetrically placed before and after the zero crossovers. The angular displacement of the clipping points from the zero crossover points is $\pm\theta$.

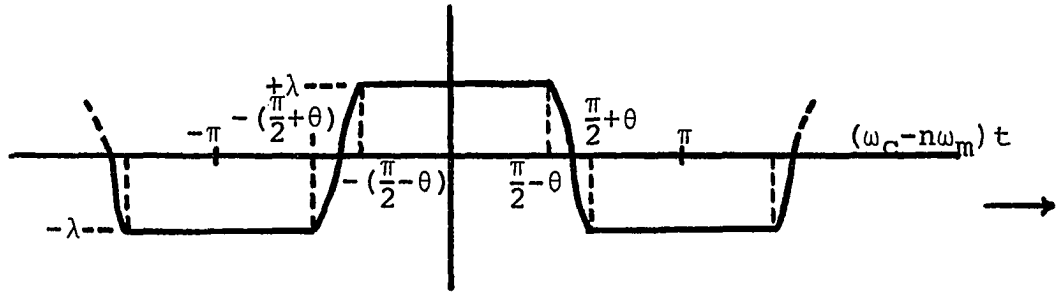

Fig. 3-7

Amplitude-limiter output versus time

Clipping the cosine function of (58) at $\pm\lambda$

$$A_n = (-1)^n \left[\frac{-\lambda}{\pi} \int_{-\pi}^{-(\frac{\pi}{2}+\theta)} \cos(\omega_c - n\omega_m)t\, d\left((\omega_c - n\omega_m)t\right) + \right.$$

$$\int_{-(\frac{\pi}{2}+\theta)}^{-(\frac{\pi}{2}-\theta)} \frac{G\hat{V}}{\pi} \left(\frac{m}{2}\{J_{n-1}(\beta) + J_{n+1}(\beta)\} - J_n(\beta)\right)\cos^2(\omega_c - n\omega_m)t$$

$$\times\, d\left((\omega_c - n\omega_m)t\right) +$$

$$\int_{-(\frac{\pi}{2}-\theta)}^{\frac{\pi}{2}-\theta} \frac{\lambda}{\pi} \cos(\omega_c - n\omega_m)t\, d\left((\omega_c - n\omega_m)t\right) +$$

$$\int_{\frac{\pi}{2}-\theta}^{\frac{\pi}{2}+\theta} \frac{G\hat{V}}{\pi} \left(\frac{m}{2}\{J_{n-1}(\beta) + J_{n+1}(\beta)\} - J_n(\beta)\right)\cos^2(\omega_c - n\omega_m)t$$

$$\times\, d\left((\omega_c - n\omega_m)t\right) -$$

$$\left. \int_{\frac{\pi}{2}+\theta}^{\pi} \frac{\lambda}{\pi} \cos(\omega_c - n\omega_m)t\, d\left((\omega_c - n\omega_m)t\right) \right] \qquad (59)$$

After integration and evaluation at the limits

$$A_{n_1} = (-1)^n \frac{3\lambda}{\pi} \cos\theta + \frac{2G\hat{V}}{\pi}\left(\frac{m}{2}\{J_{n-1}(\beta) + J_{n+1}(\beta)\} - J_n(\beta)\right) \tag{60}$$

Independent of (60), (61) is derived from Figure 3-7 and the form of (57).

$$\lambda = G\hat{V}\left(\frac{m}{2}\{J_{n-1}(\beta) + J_{n+1}(\beta) - J_n(\beta)\right) \times \cos\left(\frac{\pi}{2} - \theta\right) = \sin\theta \tag{61}$$

Solving for sin θ in terms of m

$$\sin\theta = \frac{\lambda}{G\hat{V}\left(\frac{m}{2}\{J_{n-1}(\beta) + J_{n+1}(\beta)\} - J_n(\beta)\right)} \tag{62}$$

$$0 \leq \theta \leq \frac{\pi}{2}$$

Applying the Pythagorean Theorem

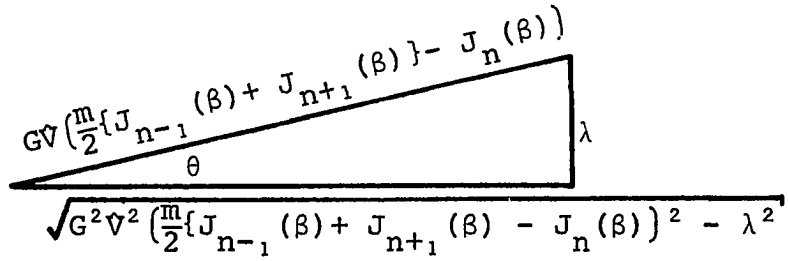

Fig. 3-8

The Pythagorean Theorem allows (60) to be expressed in fewer variables

and rewriting (60) as a function of m alone

$$A_{n_1} = (-1)^n \left\{ \frac{3\lambda}{\pi} \left[\frac{\sqrt{G^2\hat{V}^2 \left(\frac{m}{2}\{J_{n-1}(\beta) + J_{n+1}(\beta)\} - J_n(\beta)\right)^2 - \lambda^2}}{G\hat{V}\left(\frac{m}{2}\{J_{n-1}(\beta) + J_{n+1}(\beta)\} - J_n(\beta)\right)} \right] + \right.$$

$$\frac{2G\hat{V}}{\pi}\left(\frac{m}{2}\{J_{n-1}(\beta) + J_{n+1}(\beta)\} - J_n(\beta)\right) \sin^{-1}$$

$$\left. \left| \frac{\lambda}{G\hat{V}\left(\frac{m}{2}\{J_{n-1}(\beta) + J_{n+1}(\beta)\} - J_n(\beta)\right)} \right| \right\} \qquad (63)$$

Rewriting once again in terms of the $G\hat{V}/\lambda$ ratio

$$A_{n_1} = (-1)^n \left\{ \frac{3\lambda \sqrt{\left(\frac{G\hat{V}}{\lambda}\right)^2 \left(\frac{m}{2}\{J_{n-1}(\beta) + J_{n+1}(\beta)\} - J_n(\beta)\right)^2 - 1}}{\pi\left(\frac{G\hat{V}}{\lambda}\right)\left(\frac{m}{2}\{J_{n-1}(\beta) + J_{n+1}(\beta)\} - J_n(\beta)\right)} + \right.$$

$$\frac{2G\hat{V}}{\pi}\left(\frac{m}{2}\{J_{n-1}(\beta) + J_{n+1}(\beta)\} - J_n(\beta)\right) \sin^{-1}$$

$$\left. \left| \frac{1}{\left(\frac{G\hat{V}}{\lambda}\right)\left(\frac{m}{2}\{J_{n-1}(\beta) + J_{n+1}(\beta)\} - J_n(\beta)\right)} \right| \right\} \qquad (64)$$

for

$$\left(\frac{G\hat{V}}{\lambda}\right)\left(\frac{m}{2}\{J_{n-1}(\beta) + J_{n+1}(\beta)\} - J_n(\beta)\right) \geq 1$$

It must be realized that (64) is correct only if amplitude limiting actually takes place. If the limiter input signal is not great enough to cause clipping, then the quantity under the radical becomes negative and the arc-sine argument becomes greater than one. Under this condition, (58) is rewritten as (65) for no amplitude limiting.

$$A_{n_1} = -(-1)^n G\hat{V}\left(\frac{m}{2}\{J_{n-1}(\beta) + J_{n+1}(\beta)\} - J_n(\beta)\right) \tag{65}$$

for

$$\frac{G\hat{V}}{\lambda}\left(\frac{m}{2}\{J_{n-1}(\beta) + J_{n+1}(\beta)\} - J_n(\beta)\right) < 1$$

A_{n_2} is plotted against m for n even in Figure 3-9. An example for n odd is plotted in Figure 3-10. For the case when clipping occurs, the amplitude of the nth component of the frequency shifted signal of (51) is written as (66).

$$A_{n_2} = (-1)^n \left\{ \frac{3\lambda \sqrt{\left(\frac{G\hat{V}}{\lambda}\right)^2 \left(\frac{m}{2}\{J_{n-2}(\beta) + J_n(\beta)\} - J_{n-1}(\beta)\right)^2 - 1}}{\pi\left(\frac{G\hat{V}}{\lambda}\right)\left(\frac{m}{2}\{J_{n-2}(\beta) + J_n(\beta)\} - J_{n-1}(\beta)\right)} + \right.$$

$$\left. \frac{2G\hat{V}}{\pi}\left(\frac{m}{2}\{J_{n-2}(\beta) + J_n(\beta)\} - J_{n-1}(\beta)\right) \sin^{-1} \left| \frac{1}{\left(\frac{GV}{\lambda}\right)\left(\frac{m}{2}\{J_{n-2}(\beta) + J_n(\beta)\} - J_{n-1}(\beta)\right)} \right| \right\} \tag{66}$$

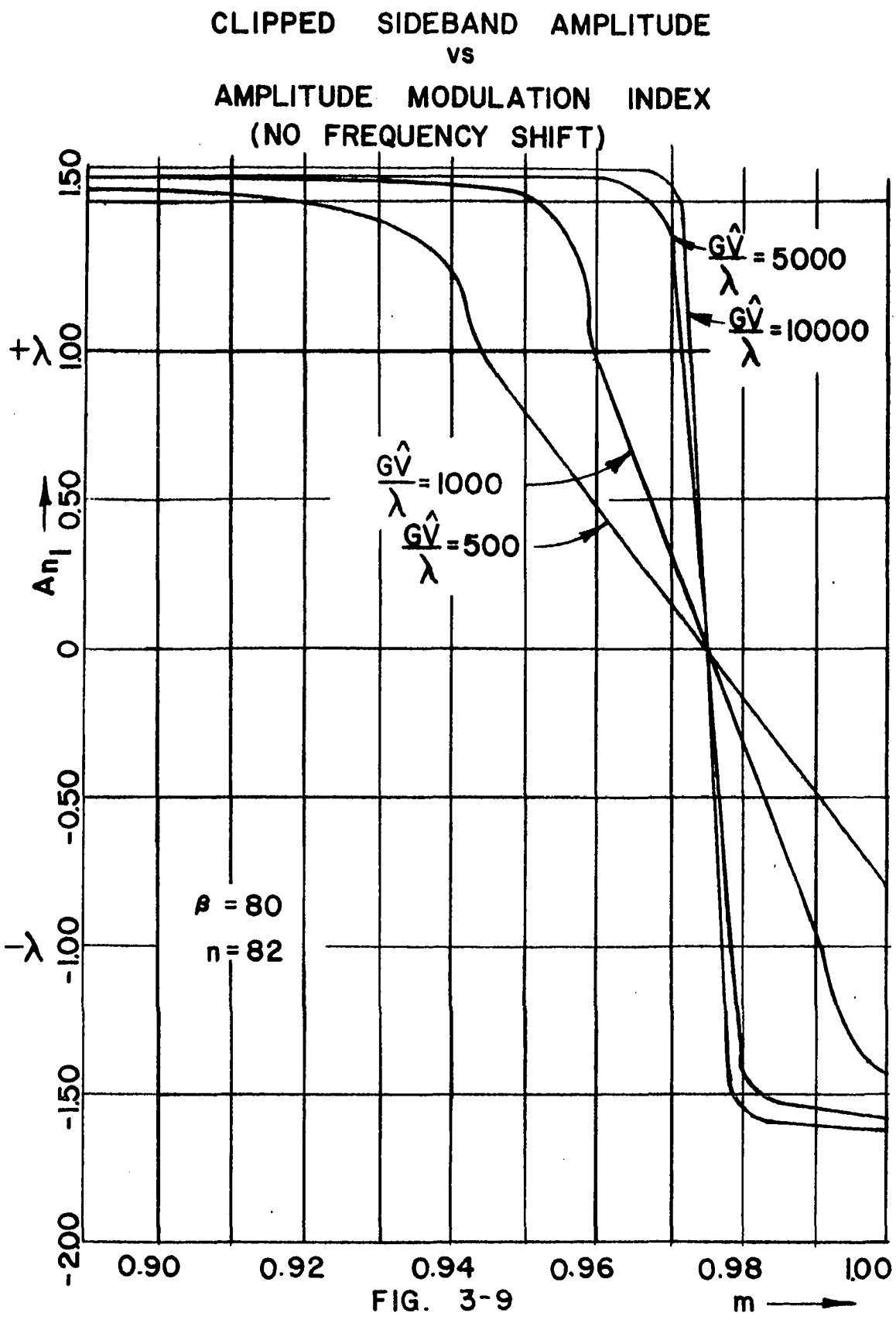

FIG. 3-9

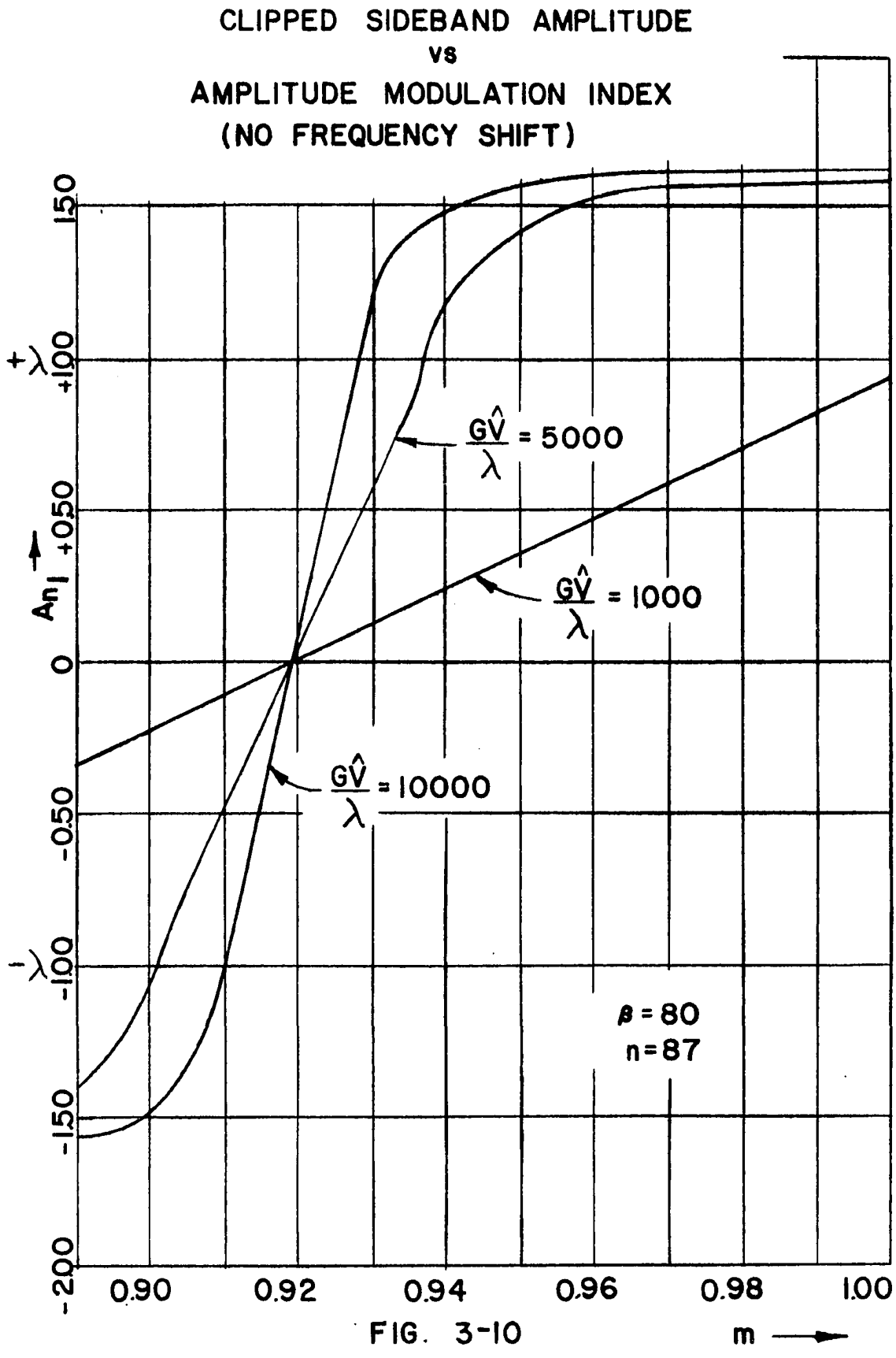

FIG. 3-10

for

$$\left(\frac{GV}{\lambda}\right)\left(\frac{m}{2}\{J_{n-2}(\beta)+ J_n(\beta)\}- J_{n-1}(\beta)\right) \geq 1$$

For the non-occurrence of clipping, the frequency shifted component amplitude is

$$A_{n_2}= (-1)^n G\hat{V}\left(\frac{m}{2}\{J_{n-2}(\beta)+ J_n(\beta)\}- J_{n-1}(\beta)\right) \qquad (67)$$

for

$$\left(\frac{G\hat{V}}{\lambda}\right)\left(\frac{m}{2}\{J_{n-2}(\beta)+ J_n(\beta)\}- J_{n-1}(\beta)\right) < 1$$

A_{n_2} is plotted against m for n even in Figure 3-11. An example for n odd is plotted in Figure 3-12. Other constants and circumstances stated for Figures 3-9 and 3-10 remain the same for A_{n_2} and Figures 3-11 and 3-12.

If the amplitude plots of Figures 3-9 and 3-11 are added, the resultant amplitude is shown in Figure 3-13 as a function of the amplitude modulation index. If the amplitude plots of Figures 3-10 and 3-12 are added, the resultant amplitude appears in Figure 3-14. Figure 3-13 is typical for n even and Figure 3-14 is typical for n odd. In both example cases the resultant amplitude of an nth lower sideband component where $n \geq \beta$ peaks for only one

CLIPPED SIDEBAND AMPLITUDE
vs
AMPLITUDE MODULATION INDEX
(FREQUENCY SHIFTED DOWN BY ω_m)

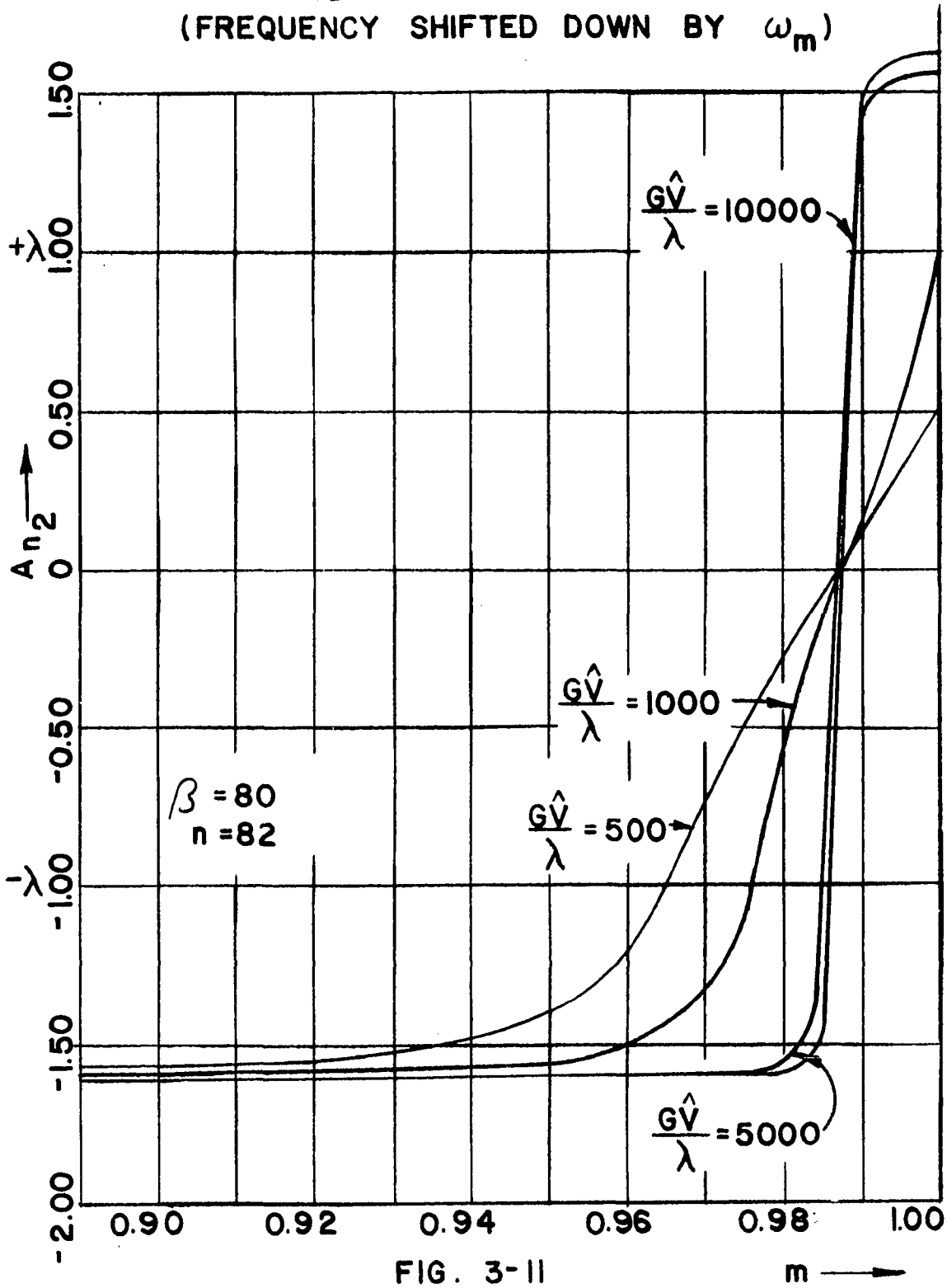

FIG. 3-11

CLIPPED SIDEBAND AMPLITUDE
vs
AMPLITUDE MODULATION INDEX
(FREQUENCY SHIFTED DOWN BY ω_m)

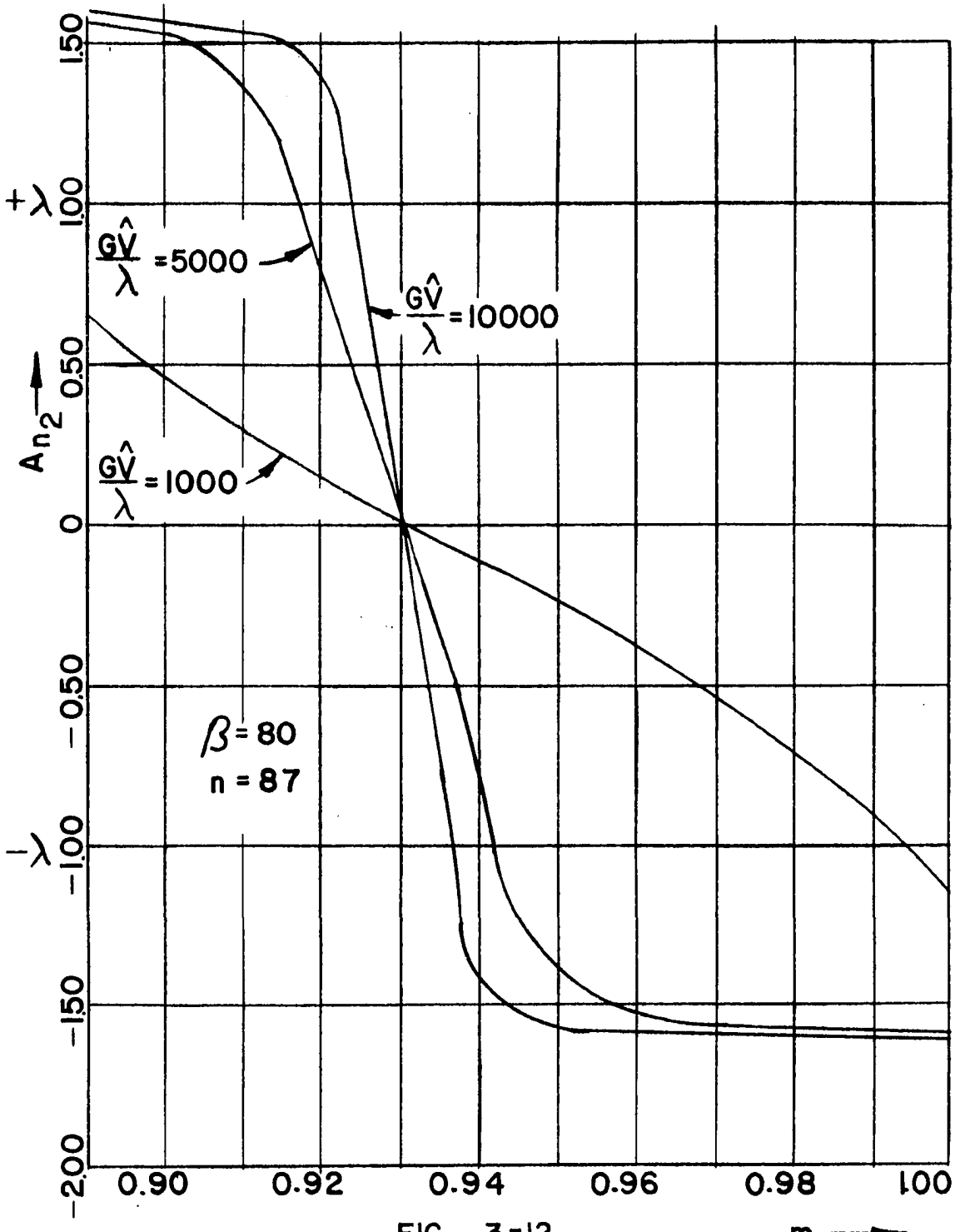

FIG. 3-12

RESULTANT SIDEBAND AMPLITUDE
vs
AMPLITUDE MODULATION INDEX

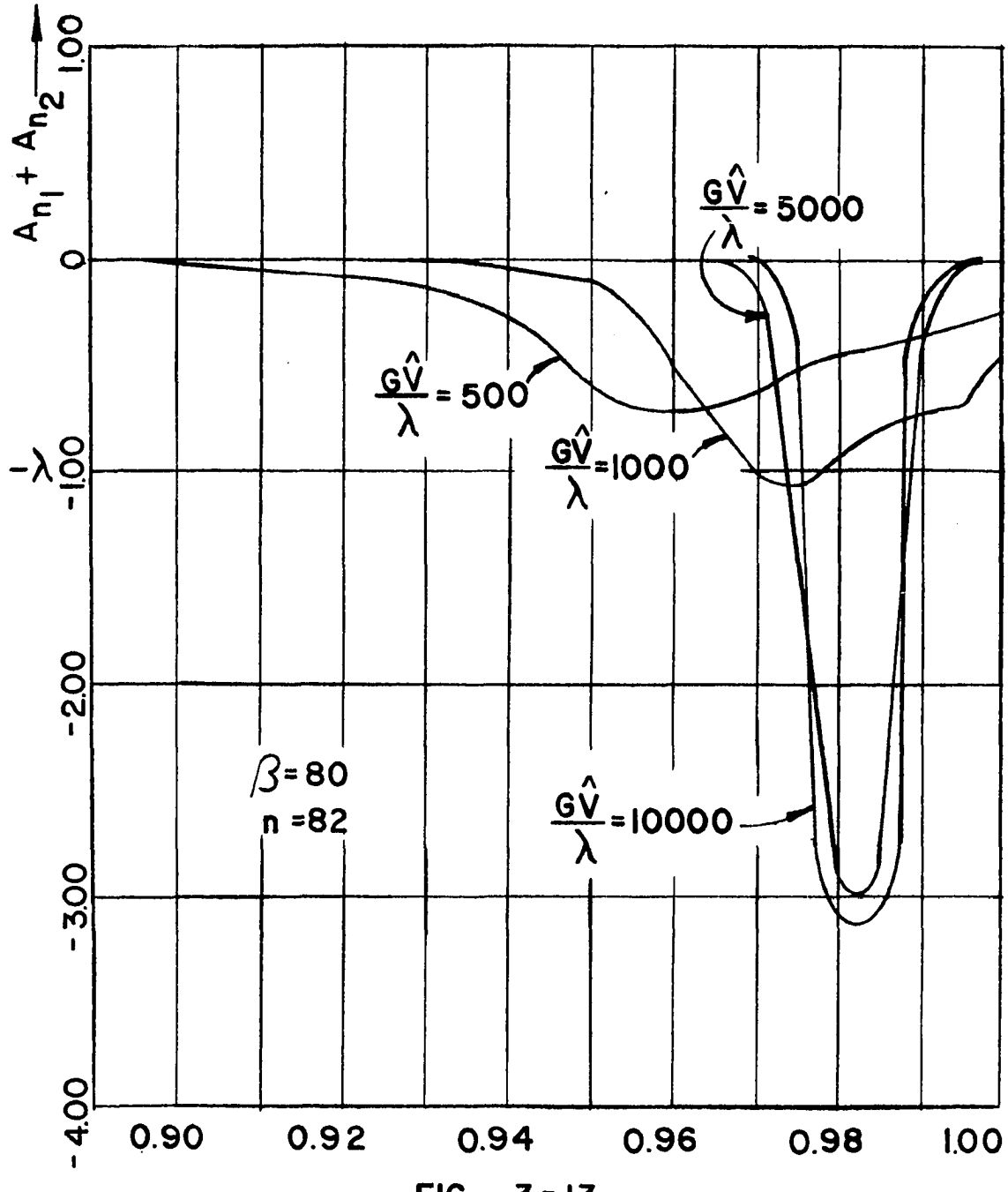

FIG. 3-13

RESULTANT SIDEBAND AMPLITUDE
vs
AMPLITUDE MODULATION INDEX

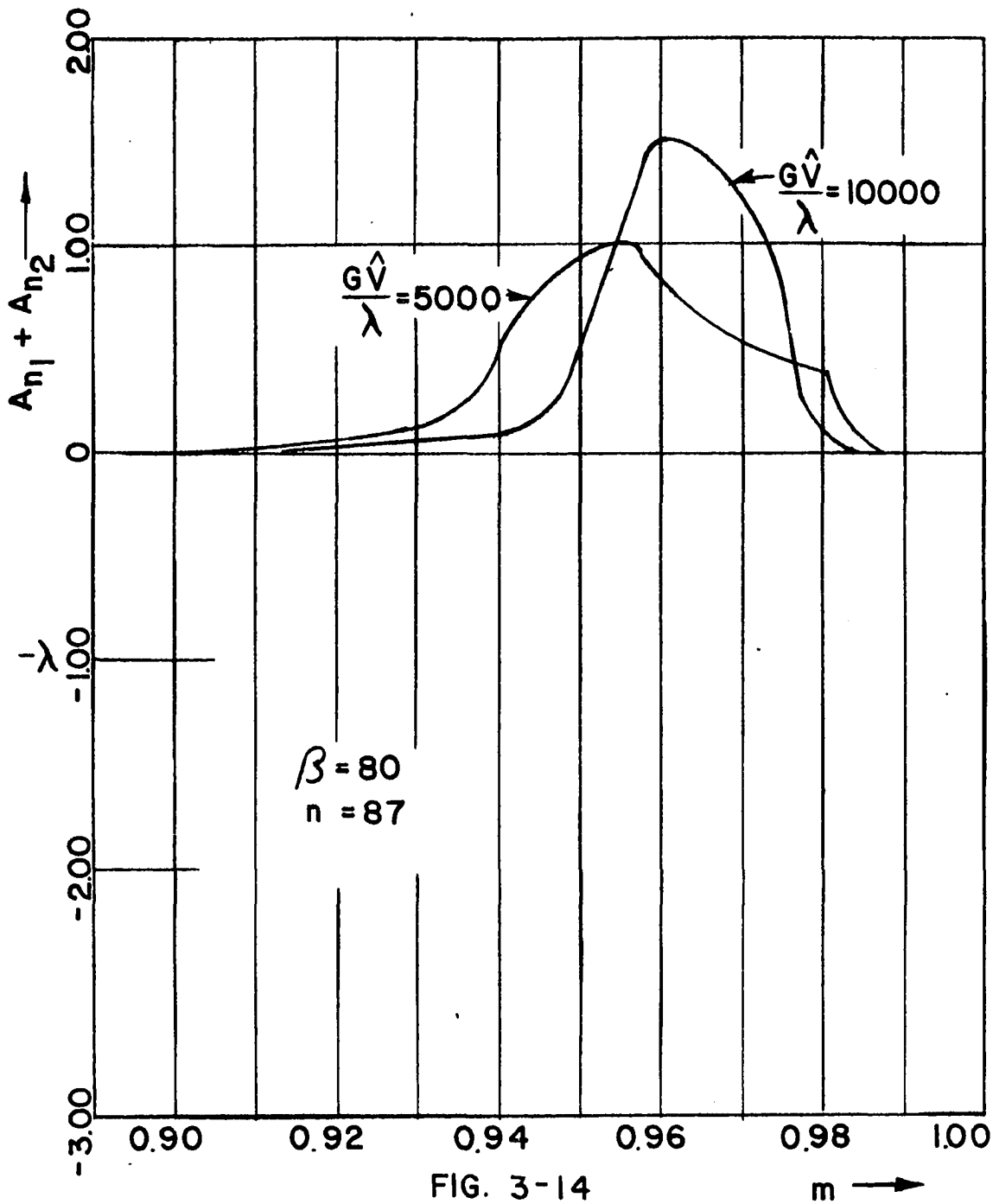

FIG. 3-14

narrow range of m and is suppressed for all other values. It should also be noticed that as n increases, the resultant amplitude curves become broader for the same value of $G\hat{V}/\lambda$. This occurs because the relative signal amplitude to limiting amplitude ratio is decreasing as n increases as a result of the monotonic decrease of the numerical value of the Bessel function $J_n(\beta)$ for $n > \beta$. The relative signal amplitude is the product of G and $\frac{m}{2}\{J_{n-1}(\beta)+ J_{n+1}(\beta)\}- J_n(\beta)$ or G and $\frac{m}{2}\{J_{n-2}(\beta)+ J_n(\beta) - J_{n-1}(\beta)$ for the non-frequency shifted or frequency shifted signal, respectively.

For relatively high values of $G\hat{V}/\lambda$ in Figure 3-13 (for n = 82) a "well shaped" resultant amplitude curve exists which peaks in amplitude at a value of m which is very nearly midway between the zero amplitude value of m in Figure 3-9 and the corresponding value in Figure 3-11. This is not the case for lower values of $G\hat{V}/\lambda$ since the peak of the resultant curve tends to shift somewhat toward the lower value of m. For the sake of illustration, in Figure 3-14, the $G\hat{V}/\lambda = 10000$ curve peaks at m = 0.920. The m values for zero crossover in Figures 3-10 and 3-12 are m = 0.918 and m =0.931. The resultant amplitude peak nearly coincides with the lower of these two values rather than midway between them. Because of this noticeable shift to the left and broadening of the resultant amplitude curve for relatively low values of $G\hat{V}/\lambda$, it is concluded

that G required must be some $G_n > G_{n-1}$. Even though the resultant amplitude curves are functions of $G\hat{V}/\lambda$, the zero crossover points of the individual signals combined to make up the resultant curves are not (see Figures 3-9, 3-10, 3-11 and 3-12). The required G_n necessary for a "well shaped" resultant amplitude curve (G_n for any $n \geq \beta$) may therefore be determined relative to G_β. ($\hat{V}$ = constant).

From (65) and (67) and relative to $n = \beta$,

$$A_{\beta_1} + A_{\beta_2} = \frac{G_\beta \hat{V}}{\lambda}\left[\frac{m_{\beta_1} + m_{\beta_2}}{4}\left(J_{\beta-1}(\beta) + J_{\beta+1}(\beta)\right) - J_\beta(\beta) - \frac{m_{\beta_1} + m_{\beta_2}}{4}\left(J_{\beta-2}(\beta) + J_\beta(\beta)\right) + J_{\beta-1}(\beta)\right]$$

$$A_{n_1} + A_{n_2} = \frac{G_n \hat{V}}{\lambda}\left[\frac{m_{n_1} + m_{n_2}}{4}\left(J_{n-1}(\beta) + J_{n+1}(\beta)\right) - J_n(\beta) - \frac{m_{n_1} + m_{n_2}}{4}\left(J_{n-2}(\beta) + J_n(\beta)\right) + J_{n-1}(\beta)\right] \quad (68)$$

where

$$m_{\beta_1} = \frac{2J_\beta(\beta)}{J_{\beta-1}(\beta) + J_{n+1}(\beta)}$$

$$m_{\beta_2} = \frac{2J_{\beta-1}(\beta)}{J_{\beta-2}(\beta) + J_n(\beta)}$$

$$m_{n_1} = \frac{2J_n(\beta)}{J_{n-1}(\beta) + J_{n+1}(\beta)}$$

$$m_{n_2} = \frac{2J_{n-1}(\beta)}{J_{n-2}(\beta) + J_n(\beta)}$$

Relative to G_β, G_n is found to be

$$\frac{G_n \hat{V}}{\lambda} \simeq \frac{\frac{G_\beta \hat{V}}{\lambda}\left(\tfrac{1}{2}\left\{\frac{J_\beta}{J_{\beta-1}+J_{\beta+1}} + \frac{J_{\beta-1}}{J_{\beta-2}+J_\beta}\right\}\{-J_{\beta-2}+J_{\beta-1}-J_\beta+J_{\beta+1}\}+J_{\beta-1}-J_\beta\right)}{\tfrac{1}{2}\left\{\frac{J_n}{J_{n-1}+J_{n+1}} + \frac{J_{n-1}}{J_{n-2}+J_n}\right\}\{-J_{n-2}+J_{n-1}-J_n+J_{n+1}\}+J_{n-1}-J_n} \tag{69}$$

(The argument of J is omitted for brevity)

This rather cumbersome relationship may be reduced considerably by substitution of the following approximations:

$$J_{\beta-2}(\beta) \simeq 0.1444$$

$$J_{\beta-1}(\beta) \simeq 0.1257$$

for any $\beta >> 1$

$$J_{\beta-0}(\beta) \simeq 0.1038$$

$$J_{\beta+1}(\beta) \simeq 0.0819$$

$$\frac{G_n \hat{V}}{\lambda} \simeq \frac{G_\beta \hat{V}}{\lambda} \frac{.0015}{\frac{1}{2}\{\frac{J_n}{J_{n-1}+J_{n+1}} + \frac{J_{n-1}}{J_{n-2}+J_n}\}\{-J_{n-2}+J_{n-1}-J_n+J_{n+1}\}+J_{n-1}-J_n} \tag{70}$$

For example, if $\beta = 80$ and $n = 87$, $G_{87}\hat{V}/\lambda$ must equal $10G_{80}\hat{V}/\lambda$ in order to produce a resultant amplitude curve at $n = 87$ that has the same shape as that at $n = 80$, that is, one that peaks midway between m_1 and m_2. Summarizing, the resultant amplitude may be expressed by (64), (65), (66), (67), and (70).

$$A_0 = A_{n_1} + A_{n_2}$$

where

$$A_{n_1} = -(-1)^n \left\{ \frac{3\lambda\sqrt{\left(\frac{G_n\hat{V}}{\lambda}\right)^2\left(\frac{m}{2}\{J_{n-1}(\beta)+J_{n+1}(\beta)\}-J_n(\beta)\right)^2-1}}{\pi\left(\frac{G_n\hat{V}}{\lambda}\right)\left(\frac{m}{2}\{J_{n-1}(\beta)+J_{n+1}(\beta)\}-J_n(\beta)\right)} + \right.$$

$$\left. \frac{2G_n\hat{V}}{\lambda}\left(\frac{m}{2}\{J_{n-1}(\beta)+J_{n+1}(\beta)\}-J_n(\beta)\right)\sin^{-1}\left| \frac{1}{\frac{G_n\hat{V}}{\lambda}\left(\frac{m}{2}\{J_{n-1}(\beta)+J_{n+1}(\beta)\}-J_n(\beta)\right)} \right| \right\} \tag{71}$$

for

$$\left| \frac{G_n\hat{V}}{\lambda}\left(\frac{m}{2}\{J_{n-1}(\beta)+J_{n+1}(\beta)\}-J_n(\beta)\right) \right| \geq 1$$

or

$$A_{n_1} = -(-1)^n G_n\hat{V}\left(\frac{m}{2}\{J_{n-1}(\beta)+J_{n+1}(\beta)\}-J_n(\beta)\right) \tag{72}$$

for

$$\left| \frac{G_n\hat{V}}{\lambda}\left(\frac{m}{2}\,J_{n-1}(\beta)+J_{n+1}(\beta)\}-J_n(\beta)\right) \right| < 1$$

and

$$A_{n_2} = (-1)^n \left\{ 3\lambda \sqrt{\left(\frac{G_n \hat{V}}{\lambda}\right)^2 \left(\frac{m}{2}\{J_{n-2}(\beta)+J_n(\beta)\}-J_{n-1}(\beta)\right)^2-1} + \right.$$

$$\frac{G_n \hat{V}}{\lambda}\left(\frac{m}{2}\{J_{n-2}(\beta)+J_n(\beta)\}-J_{n-1}(\beta)\right)$$

$$\left. \frac{2G_n \hat{V}}{\lambda}\left(\frac{m}{2}\{J_{n-2}(\beta)+J_n(\beta)\}-J_{n-1}(\beta)\right) \sin^{-1} \left| \frac{1}{\frac{G_n \hat{V}}{\lambda}\left(\frac{m}{2}\{J_{n-2}(\beta)+J_n(\beta)\}-J_{n-1}(\beta)\right)} \right| \right\} \tag{73}$$

for

$$\left| \frac{G_n \hat{V}}{\lambda}\left(\frac{m}{2}\{J_{n-2}(\beta)+J_n(\beta)\}-J_{n-1}(\beta)\right) \right| \geq 1$$

or

$$A_{n_2} = (-1)^n G_n \hat{V}\left(\frac{m}{2}\{J_{n-2}(\beta)+J_n(\beta)\}-J_{n-1}(\beta)\right) \tag{74}$$

for

$$\left| \frac{G_n \hat{V}}{\lambda}\left(\frac{m}{2}\, J_{n-2}(\beta)+J_n(\beta)\}-J_{n-1}(\beta)\right) \right| < 1$$

and

$$\frac{G_n\hat{V}}{\lambda} \simeq \frac{G_\beta\hat{V}}{\lambda}\left|\frac{.0015}{\frac{1}{2}\{\frac{J_n}{J_{n-1}+J_{n+1}}+\frac{J_{n-1}}{J_{n-2}+J_n}\}\{-J_{n-2}+J_{n-1}-J_n+J_{n+1}\}+J_{n-1}-J_n}\right| \tag{75}$$

The resultant composite signal from the form of (50) or (57) becomes

$$e_0(m,G_n,t) = \sum_{n=\beta}^{\beta+10}\left(A_{n_1}(m,G_n)+A_{n_2}(m,G_n)\right)\cos(\omega_c - n\omega_m)t \tag{76}$$

To find the minimum value of $\frac{G_\beta\hat{V}}{\lambda}$ for peaking midway between m_1 and m_2 from which $\frac{G_\beta\hat{V}}{\lambda}$ may be found and therefore all other $\frac{G_n\hat{V}}{\lambda}$, reference is made to Figure 3-13. Here the minimum $\frac{G_{82}\hat{V}}{\lambda}$ is seen to be some value between 1000 and 5000. Somewhat conservative judgment dictates that the minimum value is probably near 3000. With this value, $\hat{V}$ arbitrary and $\lambda = 1$, from (70)

$$\frac{G_{82}\hat{V}}{\lambda} = 3000 \Longrightarrow \frac{G_{80}\hat{V}}{\lambda} = \frac{G_\beta\hat{V}}{\lambda} \simeq 1900 \tag{77}$$

Table 3-3 lists all minimum G_n necessary for a "well-shaped" $e_0(m,G_n,t)$ for $\beta \leq n \leq \beta+10$ and $\beta = 80$. It is expected that $G_n > G_{n-1}$ since the Bessel amplitudes monotonically decrease with increasing n (λ and $\hat{V}$ constant).

With the G_n values cited in Table 3-3, Figure 3-15 indicates all $e_0(m,G_n,t)$ as a function of m with all appropriate conditions applied. It is an example plot of all eleven lower sidebands for the example case where $\beta = 80$ using (70). Again, generality is not lost even though a specific β is cited throughout by virtue of the observations made on Bessel function behavior in Section 3-2.

TABLE 3-3.--Required Amplifier Gain values for $80 \leq n \leq 90$

n	G_n
80	1892
81	2300
82	3000
83	4060
84	5700
85	8300
86	12400
87	19000
88	30000
89	49000
90	80000

nth SIDEBAND AMPLITUDE
vs
AMPLITUDE MODULATION INDEX

$\beta = 80$

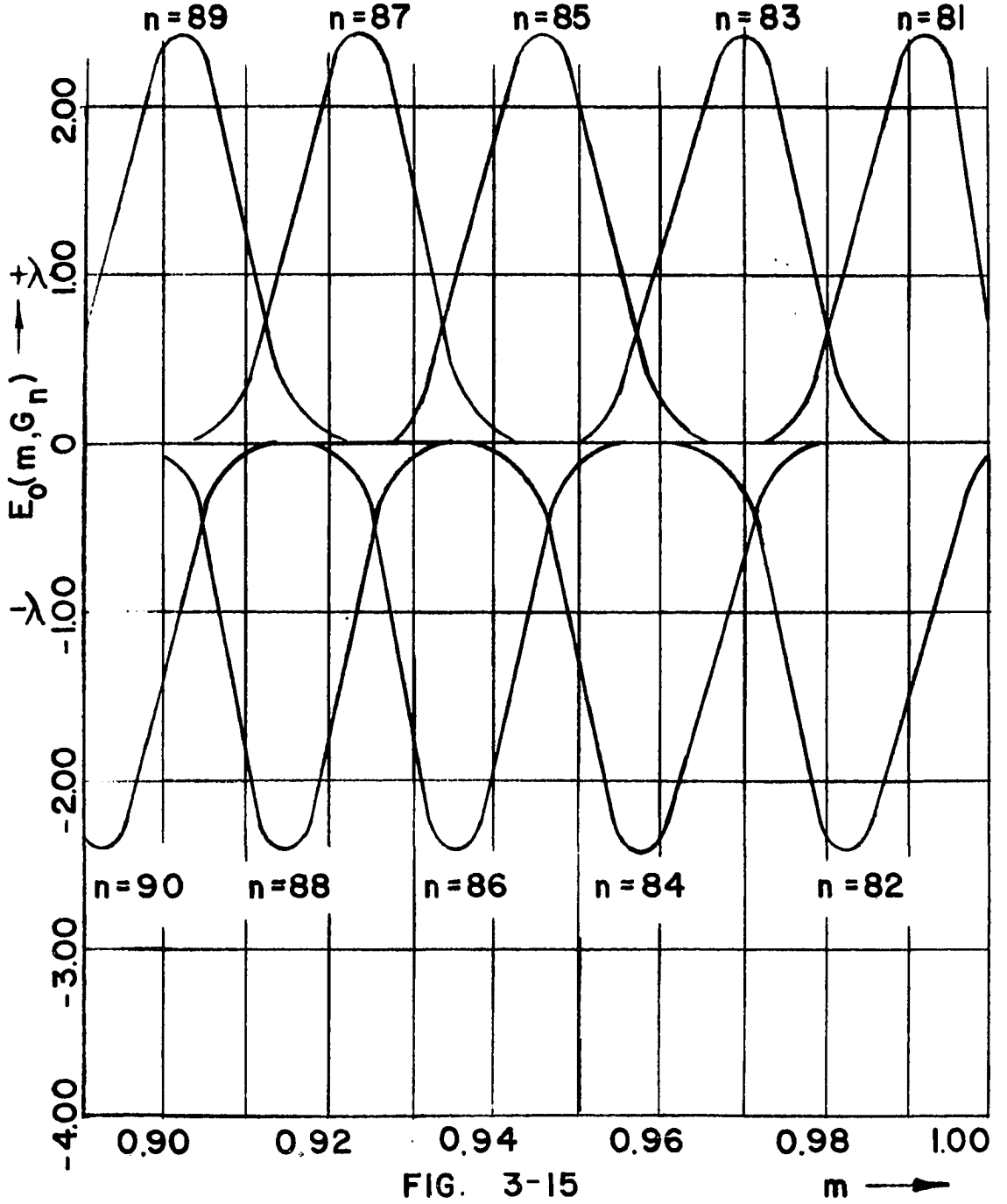

FIG. 3-15

CHAPTER IV

SYSTEM FUNCTIONAL REALIZATION

4-1 Adjacent Channel Analysis

It should be emphasized that the curves of Figure 3-15 are actually ten different amplitude curves superimposed on one coordinate system. If say m = 0.958, the amplitude of the 84th lower sideband is -2.4 voltage units. The 83rd lower sideband has an amplitude of about +0.4 voltage units while the 85th lower sideband exists with an amplitude of about +0.2 voltage units. (The (n+1)st sideband amplitude is always less than the (n-1)st for that m emphasizing the nth sideband). All other sideband amplitudes are nearly zero. For G_β = 1900 and all other minimum G_n calculated from G_β by (70), the higher frequency adjacent sideband amplitude is never more than 20 log $(\frac{2.4}{0.4})$ = 15.6 dB down from the sideband amplitude being emphasized. This sideband suppression figure may be improved by increasing G_β and correspondingly all G_n. This effect may be noticed by observing that the width of the amplitude curve shown in Figure 3-13 narrows with increased G_n. For G_β = 1900, that value of m that maximizes the nth lower sideband will also cause amplitude limiting to occur in the $A_{(n-1)1}$ and $A_{(n-1)2}$ signals added to produce the signal at the (n-1)st sideband frequency. Equation (71) and (73) apply for the emphasized and next higher frequency adjacent sideband components so that the best case voltage ratio of the two

components is known. Best case occurs for

$$m_n = \frac{\frac{\beta}{k} + \frac{\beta}{k-1}}{2} = \frac{m_{n_1} + m_{n_2}}{2}, \quad n = k,\ k \text{ is an integer} \tag{78}$$

where $\frac{\beta}{k} = m_{n_1}$

$\frac{\beta}{k-1} = m_{n_2}$

see page 55 and Table 3-1.

The value of m_n obtained from (78) will maximize the amplitude of the nth component. The value of m_n may also be obtained graphically from Figure 3-15. The amplitude of the nth component is found by the addition of (71) and (73) with $m = m_n$ or by graphical addition. The amplitude of the next higher frequency component for $m = m_n$ is also found from the addition of (71) and (73), but here n is replaced by n-1.

With these observations, the best case amplitude separation of the nth component to the (n-1)st component becomes

$$\left(\frac{A_0 n}{A_0 (n-1)}\right)_{dB} = 20 \log \left| \frac{A_{n_1} + A_{n_2}}{A_{(n-1)_1} + A_{(n-1)_2}} \right|_{m_n} \tag{79}$$

From (71) and (73) for $m = \frac{m_{n_1} + m_{n_2}}{2}$, this ratio becomes

$$\left(\frac{A_{0n}}{A_{0(n-1)}}\right)_{dB} = 20 \log \left| \frac{G_n}{G_{n-1}} \frac{\left(\frac{J_n}{J_{n-1}+J_{n+1}} + \frac{J_{n-1}}{J_{n-2}+J_n}\right)}{\left(\frac{J_n}{J_{n-1}+J_{n+1}} + \frac{J_{n-1}}{J_{n-2}+J_n}\right)} \right.$$

$$\left. \times \frac{\left(J_{n-1}+J_{n+1}-J_{n-2}-J_n\right)-2\left(J_n-J_{n-1}\right)}{\left(J_{n-2}+J_n-J_{n-3}-J_{n-1}\right)-2\left(J_{n-1}-J_{n-2}\right)} \right| \qquad (80)$$

where n = the emphasized sideband number

and is constant at 15.6dB. Constancy is maintained because the G_n to G_{n-1} ratio was chosen to precisely offset the Bessel function values associated with adjacent sideband amplitudes. Equation (70) and the consistent shape and amplitude of all curves in Figure 3-15 support this conclusion.

The best case amplitude separation is considered to be of minor concern since it may always be improved by increasing G_β and consequently the $G_n\hat{V}$ to λ ratio of each component. Practical limits must of course be considered. These limits naturally depend on the availability of amplifiers with gain and absolute voltage swing limits to produce sufficiently high $G_n\hat{V}$ to λ ratios. VCO voltage level output and the amplitude limiting values also equally

contribute to this ratio. These are device properties, however, and it is the concept that is developed here.

The most significant realization is that any uncertainty in m within those limits that render the amplitude ratio of adjacent sidebands to be acceptable does not result in any uncertainty in which frequency component is emphasized. The uncertainty in m due to quantization results only in the uncertainty of the amplitude of that frequency component. For example, by examination of Figure 3-15, for $0.9540 < m < 0.9615$ it is clear that the 84th lower sideband is emphasized. For any m in this range, the lowest amplitude associated with this frequency component is -2.2 voltage units. The greatest amplitude of the 83rd lower sideband will be about +1.2 voltage units while that of the 85th lower sideband is +1.0 voltage units. The worst case adjacent frequency to emphasized frequency amplitude ratio is about 6 dB. Best case separation is 15.6 dB. Recalling that both figures may be improved by increasing all $G_n\hat{V}/\lambda$, within the specified range of m, there is no uncertainty within 6 dB which frequency is emphasized. The nth (or 84th in this example) lower sideband is precisely expressed at $\omega = \omega_c - n\omega_m$ for any $m_\ell < m < m_u$, i.e. in this case $0.9540 < m < 0.9615$. The uncertainty is associated with the amplitude of the nth sideband component, but remains

uncertain only to within 6 dB. It becomes apparent that precise frequency may be expressed by means of a binary word of finite length actually used to express the amplitude variable, m. The probability density distributions of Figures 3-1 and 3-2 have been reversed. Equation (79) with (71) and (73) may be used to find that value of m in between the values required to peak the nth and (n-1)st components such that the amplitudes are within a specified tolerable proximity of each other. If the tolerable worst case amplitude separation is u dB then

$$\left| \frac{A_{n_1} + A_{n_2}}{A_{(n-1)_1} + A_{(n-1)_2}} \right| = 10^{u/20} \tag{81}$$

from which m may be found by solving the ratio formed by (70) and (73). The value of m_u becomes the tolerable upper bound on m. The lower bound is similarly found from (79), (71) and (73) by replacing (n-1) by (n+1) in (79) and considering the (n+1)st sideband. The tolerable worst case amplitude separation is ℓ dB according to

$$\left| \frac{A_{n_1} + A_{n_2}}{A_{(n+1)_1} + A_{(n+1)_2}} \right| = 10^{\ell/20} \tag{82}$$

from which m_ℓ may be found by solving the ratio formed by (70) and (73) for m.

The lower bound on m that will exhibit a defined tolerable amplitude separation between the nth or emphasized sideband and the (n+1)st by ℓ dB is termed m_ℓ. The corresponding upper bound on m that will exhibit a tolerable defined amplitude separation between the nth or emphasized sideband and the (n-1)st by u dB is termed m_u. Therefore, the range of m within which the emphasized sideband is known within ℓ dB on the low frequency side and u dB on the high frequency side is $m_\ell < m < m_u$. It must be stressed that within this range of m, "uncertainty" refers to the loss of precise amplitude information of a precise frequency component due to the quantization of m. The quantization gap is therefore $m_u - m_\ell$ and any value of m within the range $m_\ell < m < m_u$ will be quantized to $\frac{m_u + m_\ell}{2}$.

4-2 System Realization

Sideband amplitude peaks occur midway between $m = \frac{\beta}{k}$ and $\frac{\beta}{k \pm 1}$. The spread in m surrounding the enhancement value for a sideband is the absolute difference between these two quantities and is greatest for the smallest value of k that may be assigned. Since m cannot be greater than unity, k-1 is set equal to β and the worst case spread of m becomes $\left| \frac{\beta}{k-1} - \frac{\beta}{k} \right|$. The worst case difference quantity reduces to $\frac{1}{\beta - 1}$ for enhancement of the highest frequency (lowest sideband number beyond the βth, i.e. the (β+1)st). With this

realization there must be a minimum of $\frac{1}{(\beta-1)(m_u-m_\ell)}$ quantization gaps between peaks from n=β to n=β+1. Assuming that the same number is applied to all gaps from n=β to n=β+10, the number of quantization levels becomes $\frac{(\beta+10)-\beta-1}{(\beta-1)(m_u-m_\ell)}$. The number of binary bits necessary to express all quantization levels for the degree of amplitude uncertainty tolerated is r and may be found as

$$2^r = \frac{(\beta+10)-\beta-1}{(\beta-1)(m_u-m_\ell)} \tag{83}$$

or

$$r = \log_2 \frac{9}{(\beta-1)(m_u-m_\ell)} \tag{84}$$

Consistent with the example developed throughout and choosing $m_u-m_\ell = 0.0085$ from Figure 3-15 for 6 dB minimum amplitude uncertainty, it follows that $r = \log_2 (9/79(.0085))$ or that $r = \log_2 13.40 = 3.74$ or 4 bits. Although the determined value of r is the required number for the example, it seems to be a very small number of bits necessary to express frequency precisely.

A quantizer and binary encoder may be designed to express the emphasized frequency component in r bits by actually quantizing and encoding the amplitude variable, m. This would render the VCO as a local oscillator to be compatible with associated digital equipment. Also the rate

of change of emphasized frequency component, ω_s must be much less than the amplitude and angle modulation frequency, ω_m. This restriction was imposed so that integration time of the Fourier amplitude coefficients could be considered to be approximately from $-\infty$ to $+\infty$.

In the effort to use only those techniques that are individually realizable with known devices, a system block diagram that will produce the desired single frequency component of (71) as a function of m could be that of Figure 4-1. Figure 4-1 is derived from the modulation, filtering, amplifying, clipping, and time domain summing sequences just described. Each of these processes is individually well known and on this basis their realizations are not questioned. Therefore, it is concluded that the system of Figure 4-1 should also be realizable.

If amplitude modulation were applied in the form $(1-m \cos \omega_m t)$, all results would be the same except that sideband amplitude signs would not alternate with sideband number and component emphasis would be addressed to the upper sidebands rather than the lower sidebands. Either time domain subtractors would be necessary in place of the summers or time domain inverters with summers would be required in all odd or even numbered sideband legs of Figure 4-1.

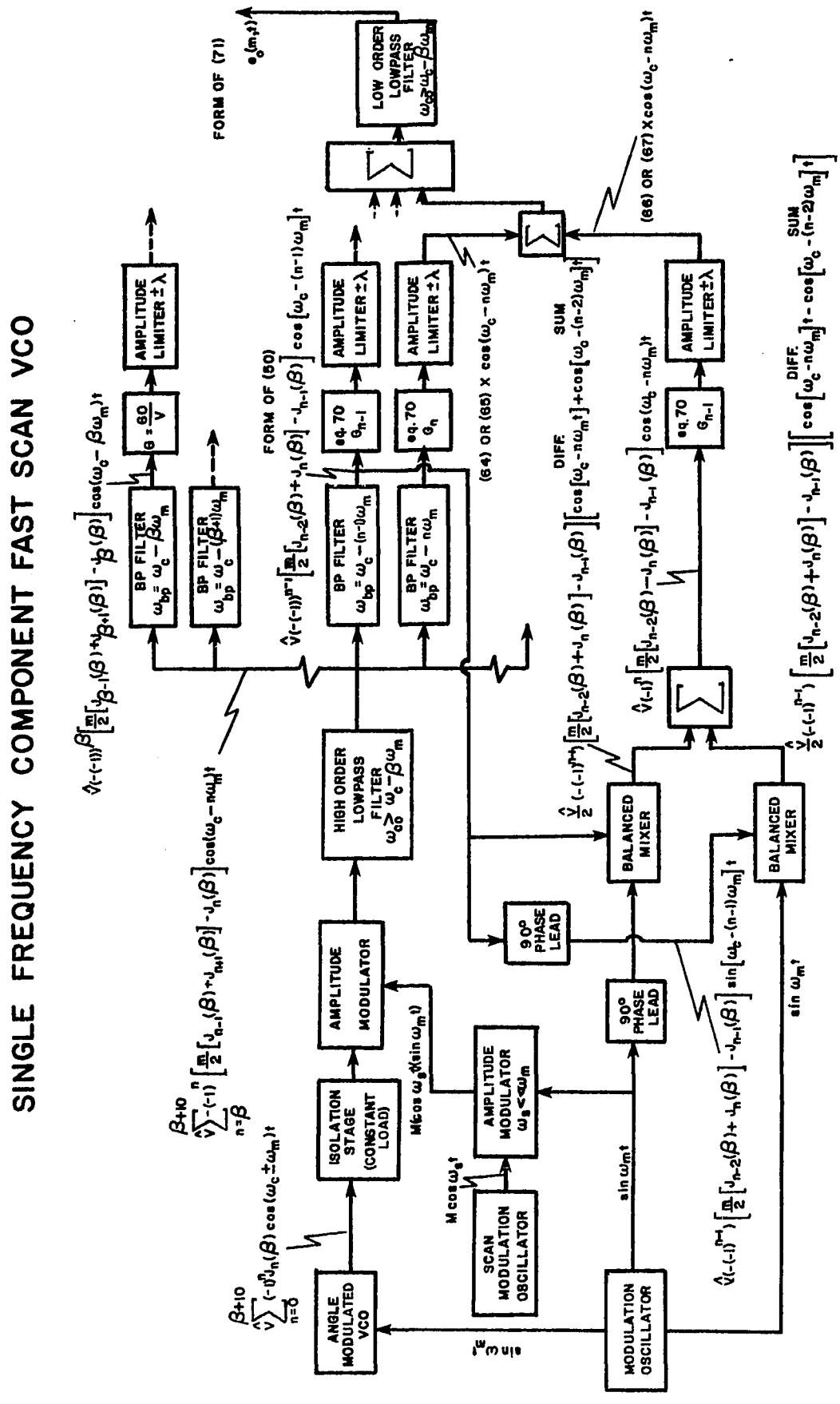

FIG. 4-1

CHAPTER V

AN EXAMPLE DESIGN

5-1 A Complete Example Design Problem - Problem Statement

As a complete example, suppose that it is desired to tune a superheterodyne receiver at a rate of 10^6 sweeps per second in a sinusoidal manner from 2.95 - 3.95 GHz and the first IF bandwidth of the receiver is 100 MHz centered around two GHz. The first mixer output of the receiver operates on the difference between the received frequency and the local oscillator frequency. The local oscillator signal injection level into the mixer must be 0.1 volt peak. The receiving frequency is to be digitized and binary encoded so that it is compatible with other digital processing equipment. The binary frequency words must be generated and transferred to the central processing unit to coincide with the dwell times for each frequency. Binary word length is to be eight bits.

5-2 Problem Solution

From the stated specifications

$$f_s = 1 \text{ MHz} \qquad \omega_s = 2\ (10)^6 \text{ rads/s}$$

$$f_m = 100 \text{ MHz} \qquad \omega_m = 2\ (10)^8 \text{ rads/s}$$

Choose amplitude modulation of the form $(1+m \cos \omega_m t)$ so that the lower sideband case may be used.

The range of the VCO sideband output must be the difference between 2.950 to 3.950 GHz and the IF frequency of two GHz so that the $(\beta+1)$st lower sideband will be at (3.950-2.000) GHz minus half the IF bandwidth or 1.900 GHz. The $(\beta+10)$th lower sideband must be at (2.950-2.000) GHz plus half the IF bandwidth or 1.000 GHz.

The remaining parameters to be specified do not have unique values since it is possible to produce the required sidebands with the information expressed this far. The two variables, f_c and β, while considering the specifications stated, may be chosen according to

$$f_c - (\beta+1) f_m = 1.900 \text{ GHz} \tag{85}$$

or

$$f_c - (\beta+10) f_m = 1.000 \text{ GHz} \tag{86}$$

Although no unique solution exists for either equation, the value assigned to β has strong implications regarding the practical limit of VCO's. For example, it is difficult to construct an RF sine wave oscillator with constant amplitude output over more than a relatively small frequency range. If $\beta = 80$ then by (85) or (86) it is seen that $f_c = 10$ GHz and $\Delta f = \beta f_m = 8$ GHz. The VCO would be required to sweep

from 2.0 to 18.0 GHz — a frequency span greater than three octaves. This requirement is considered to be beyond the state-of-the-art. Fortunately, it is not necessary.

A lower β will require a lower Δf, but is bounded by the proximity of the carrier and the stronger lower sideband components to the $(\beta+1)$st component. Higher Q filters would be required in Figure 4-1 to sufficiently suppress these components. A good design value of β is one which is not so great that the frequency deviation of the VCO is greater than an octave or so low that the carrier frequency is less than say 25% greater than the $(\beta+1)$st lower sideband.

If $\beta = 4$, from (85) or (86) $f_c = 2.4$ GHz and $\Delta f = \beta f_m = 4(0.1) = 0.4$ GHz. The VCO is required to sweep from 2.0 to 2.8 GHz and the frequency deviation is less than one octave. The $(\beta+1)$st lower sideband is $(2.4-1.9)/2.4 = 21\%$ removed from the carrier frequency. Therefore $\beta = 4$ is chosen.

For an eight bit word, $m_u - m_\ell$ may be determined from (84).

$$m_u - m_\ell = \frac{9}{(\beta-1)2^r} = \frac{9}{3(2)^8} = 1.172(10)^{-2}$$

The quantization signal to noise ratio may be calculated according to (12) remembering that this becomes an expression of amplitude uncertainty rather than frequency uncertainty.

Choosing $G_\beta = 1900$, the amplitude uncertainty due to quantization of m into 2^r or 256 levels is determined from (71), (73) and (79). If it is assumed that m_ℓ and m_u are symmetrically placed around the value of m at any peak amplitude (see Fig. 3-15 for $\beta = 80$), then

$$m_{n\ \text{peak}} - \frac{m_u - m_\ell}{2} < m_n < m_{n\ \text{peak}} + \frac{m_u - m_\ell}{2} \tag{87}$$

For $\beta = 4$, the corresponding values of m necessary to cause the nth sidebands of the basic VCO to cross through zero amplitude may be calculated from (39), the same condition necessary to generate the zero diagonal of Table 3-1 for $\beta = 80$. These values are contained in Table 5-1.

TABLE 5-1.--For $\beta = 4$, those values of m necessary to cause the nth sideband to have zero amplitude at the output of the basic VCO.

n	m_n
5	0.800
6	0.667
7	0.571
8	0.500
9	0.444
10	0.400
11	0.364
12	0.333
13	0.308
14	0.286

After processing the sideband output of the basic VCO according to Figure 4-1, the emphasized sideband contained in $e_0(m,t)$ (the output of the ultimate VCO) is peaked in relation to all other sidebands when $m_{n\ peak} = \frac{m_{n-1}+m_n}{2}$ ((78) interpreted) for $G\hat{V}/\lambda > 3000$. To continue the example, using the values of m_n in Table 5-1 for say n = 6

$$m_{6\ peak} = \frac{m_5+m_6}{2} = \frac{0.800+0.667}{2} = 0.734$$

therefore

$$m_{6\ peak} - \frac{m_u-m_\ell}{2} = 0.734 - \frac{1.172(10)^{-2}}{2} = 0.728$$

$$m_{6\ peak} + \frac{m_u-m_\ell}{2} = 0.734 + \frac{1.172(10)^{-2}}{2} = 0.740$$

so that for n = 6, (87) becomes

$$0.728 < m_6 < 0.740$$

It follows that u and ℓ in dB may be found from (71), (73) and (81) by substituting m_u and m_ℓ for m respectively. (It must be mentioned that since the lower sideband case is considered that u now refers to the next lower sideband rather than the next upper. Similarly, ℓ refers to the next upper sideband rather than the next lower).

It appears that construction of a rapid tune VCO using sidebands rather than instantaneous frequency is feasible with known components and devices. While this method offers precise frequency information at the cost of amplitude information, a significant disadvantage could be the requirement that the rate at which the emphasis of a particular sideband is changed must be much less than the rate at which the basic VCO is modulated to produce the sidebands. In the example, this quotient was 100. If the instantaneous frequency of the basic VCO were used as the oscillator injection rather than its sidebands, the receiver would be swept one hundred times faster. This realistically could be the requirement. If f_s were to be 100 MHz instead of one MHz, then f_m must be at least one GHz. Basic VCO sweep speeds at these rates are clearly beyond the current state-of-the-art for ten nanosecond settle-on times. On the other hand, sweeping a frequency band at a one MHz rate is a great improvement over present rates of 30 to 40 Hz.[3]

---

[3]The U.S. Navy AN/WLR-1 Search Receiver

CHAPTER VI

FREQUENCY MODEL OF THE VOLTAGE CONTROLLED OSCILLATOR

6-1 Modeling the Ultimate Voltage Controlled Oscillator

The example design problem presented in Chapter V represents a real requirement of a rapidly scanning superheterodyne receiver that must detect a single emitted pulse which may be as short as one μs. To demonstrate that the proposed solution to the local oscillator problem in a receiver of this type is possible to realize, a working frequency scaled model is designed and constructed. All frequency values presented in Chapter V are scaled by exchanging megahertz for hertz. Scaling to the audio frequency region allows extensive use of operational amplifiers in the rolls of active filters, limiters, amplifiers and summers. Restating the frequencies listed in section 5-2 in terms of the model ($\beta = 4$)

$f_s = 1$ Hz $\Delta f = 400$ Hz

$f_m = 100$ Hz $f_c - (\beta+1) f_m = 1900$ Hz

$f_c = 2400$ Hz $f_c - (\beta+10) f_m = 1000$ Hz

The zero amplitude values of m remain the same as those contained in Table 5-1.

6-2 Basic Components of the Frequency Scaled Fast Scan VCO

The building blocks of the frequency scaled fast scan VCO are limited to those types which have known microwave counterparts since a practical model must show feasibility in the frequency region from which it is modeled.

Before relating specific components to their roll in fulfilling the functional requirements of Figure 4-1, a brief description of component types is presented.

6-2-1 XR-205 Monolithic Waveform Generator

The XR-205 monolithic waveform generator is an analog integrated circuit capable of independent simultaneous amplitude and angle modulation over an instantaneous frequency range of 10:1 (ref.15). Angle and amplitude modulation are voltage controlled by the differential voltage present at two independent ports of the integrated circuit. Modulation voltage to frequency or amplitude is maintained linear to within 0.5% over the full frequency range and full amplitude range from zero to 100%.

The XR-205 is a low voltage device offering simultaneous square and triangle or sine output from a self contained buffer amplifier to a level of three volts peak-to-peak. Relatively low resistance loads may be driven.

The microwave counterpart to the XR-205 includes several discrete devices. The linear voltage to frequency conversion properties of the XR-205 are available in the

microwave VCO and linearizer.[4] The self contained buffer certainly has a counterpart in small signal solid-state field effect transistor (FET) linear amplifiers.[5] The amplitude modulator could be in the form of a solid-state FET mixer or class C drain modulated FET amplifier.

6-2-2 MC-1496G Balanced Modulator

The MC-1496G is an integrated circuit small signal balanced modulator. As such it is capable of double sideband suppressed carrier generation or general balanced mixing requirements to frequencies as high as 50 MHz (ref 16). When used in pairs, they may be configured for double balance mixing so that ideally, mixing results in a shift either up or down in frequency but not both. Also no input signal frequency appears in the output.

A microwave counterpart to the MC-1496G "balanced mixer" is simply called a microwave balanced mixer.[6]

6-2-3 Type 741 Operational Amplifier

The type 741 operational amplifier is a standard internally compensated operational amplifier with a gain-bandwidth product of 1 MHz.

---

[4]Watkins-Johnson Company, advertisement, Electronic Warfare (May/June 1976), 29.

[5]Narda Solid-State Amplifiers, advertisement, Electronic Warfare (May/June 1976), 111.

[6]Anaren Microwave Inc., advertisement, Microwave Systems News (April/May 1976), 74.

6-2-4 LM-3900 Quad Operational Amplifier

A single LM-3900 operational amplifier integrated circuit contains four independent compensated operational amplifiers on one substrate. They are conventional in the sense that their dynamic properties are similar to any other operational amplifier but unconventional in their bias requirements. They are single power source devices designed to quiesce at half the supply voltage when the inverting and non-inverting input currents are equal. The input differential amplifier makes use of a current mirror which forces the quiescent condition.

6-3 Description of Filters and Amplitude-Limiters

The active filters used throughout the frequency scaled fast scan VCO are made up of operational amplifiers of the types introduced in sections 6-2-3 and 6-2-4. All designs are conducted according to the simplified methods described by Hilburn and Johnson (ref.17). Filters, whether active or passive, certainly have their counterparts at microwave frequencies and are currently available as solid state packages.[7]

---

[7]Coleman Microwave Company, advertisement, Microwave Systems News (April/May 1976), 116.

6-3-1 Multiple Feedback Two-Pole Lowpass Active Filter[8]

Figure 6-1 illustrates the basic configuration of a multiple feedback two-pole lowpass active filter. To meet various lowpass requirements of the fast scan VCO; this configuration is used extensively throughout by cascading four stages to produce an eight pole filter. Figure 6-1 indicates the ac equivalent configuration of components and therefore is modified accordingly to reflect the type of bias necessary for a specific operational amplifier type. Transfer characteristics are summarized in Figure 6-1.

6-3-2 High-Q Biquad Bandpass Active Filter[9]

Figure 6-2 illustrates the basic high-Q biquad bandpass filter used throughout the model. Biquad refers to the ability of the basic configuration to produce a transfer function which is the ratio of two second order polynomials in "s" to produce lowpass, bandpass, highpass or allpass. This particular configuration of the active bandpass filter was chosen because it is very stable for a Q as high as 100. Adjustment is simple since center frequency is a function only of R6 while gain is adjusted by

---

[8]Hilburn, John L., David E. Johnson, Rapid Practical Designs of Active Filters, (New York 1975), pp.13-14.

[9]Hilburn, pp. 141-142.

MULTIPLE FEEDBACK TWO-POLE LOWPASS FILTER

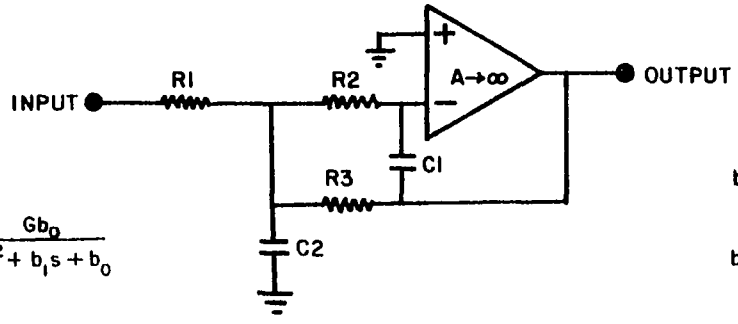

$$H(s) = \frac{Gb_0}{s^2 + b_1 s + b_0}$$

$$b_0 = \frac{1}{R_2 R_3 C_1 C_2}$$

$$b_1 = \frac{1}{C_2}\left(\frac{1}{R_1} + \frac{1}{R_2} + \frac{1}{R_3}\right)$$

$$G = -\frac{R_3}{R_1}$$

FIG. 6-1

HIGH-Q BIQUAD BANDPASS FILTER

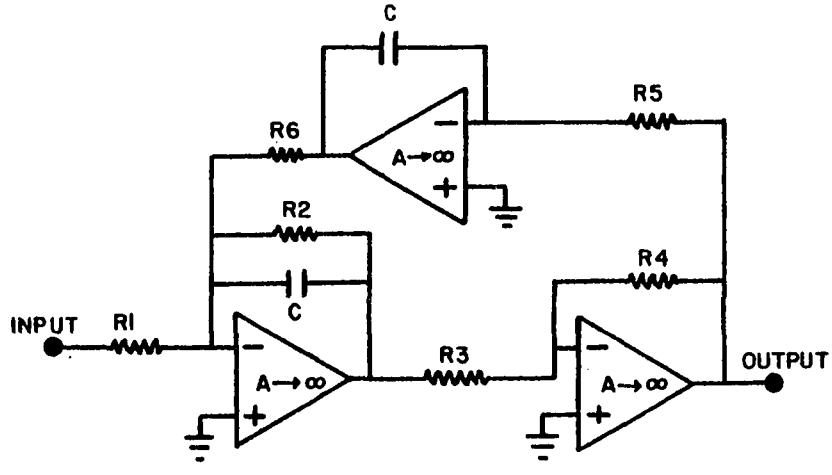

$$H(s) = \frac{GBs}{s^2 + Bs + \omega_0^2}$$

$$\omega_0^2 = \frac{1}{R_3 R_6 C^2}$$

$$R_3 = R_4 = R_5$$

$$B = \frac{1}{R_2 C}$$

$$G = \frac{R_2}{R_1}$$

FIG. 6-2

R1 and Q is independently controlled by R2. These relationships assume that all other component values are held constant. Bias arrangements for a particular type of device are ignored in Figure 6-2.

6-3-3 Single Operational Amplifier Phase Shift Network[10]

The basic single operational amplifier phase shift network or allpass filter is shown in Figure 6-3. This active configuration is used throughout the frequency model as a phase corrector after frequency shifting and as 90° phase shift networks for the balanced mixer input in the frequency shifting process. Only the dynamic configuration is shown with no regard to bias requirements of an actual device. Transfer characteristics appear in the figure.

6-3-4 Amplifier-Limiter

The amplifier-limiter consists of two cascaded stages each configured as an operational amplifier inverting amplifier which is alternately driven into saturation and cutoff. This is brought about by a combination of its high gain and low supply voltage. As a limiter, the operational amplifiers are operated from the lowest supply voltage which still maintains their operation. This allows for a high $G\hat{V}$ to λ ratio. G is made large because of the high ratio of feedback to input resistance of each stage.

---

[10]Hilburn, p.225.

SINGLE OPERATIONAL AMPLIFIER PHASE SHIFT NETWORK

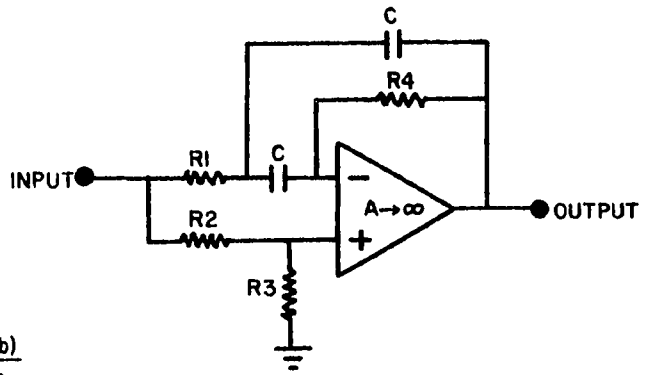

$$H(s) = \frac{G(s^2 - as + b)}{s^2 + as + b}$$

$$R_2 R_4 = 4 R_1 R_3$$

$$a = \frac{2}{R_4 C}$$

$$b = \frac{1}{R_1 R_4 C^2}$$

$$G = \frac{R_3}{R_2 + R_3}$$

FIG. 6-3

AMPLIFIER-LIMITER

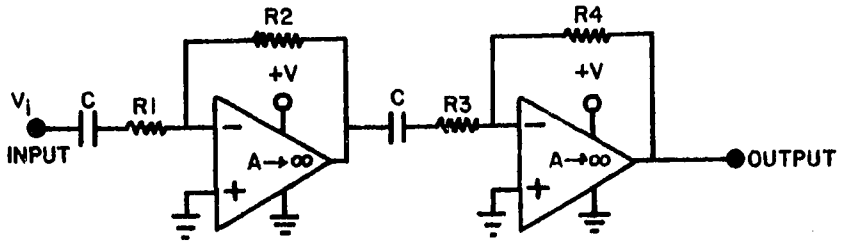

$$\frac{G\hat{V}}{\lambda} = \frac{V_i R_2 R_4}{(+V) R_1 R_3} \qquad \text{FOR} \quad X_C << R_1 \text{ or } R_3$$

FIG. 6-4

6-4 Circuit Description of the Model

6-4-1 Basic VCO and High Order Lowpass Filter

The components mentioned in section 6-2 make up all blocks of the functional fast scan VCO illustrated in Figure 4-1. All oscillators are XR-205 integrated circuits, all balanced mixers consist of MC-1496G integrated circuits while all filters consist of operational amplifiers. The amplitude limiters are made up of operational amplifiers driven into saturation.

In Figure 4-1, those blocks labeled ANGLE MODULATED VCO, ISOLATION STAGE and AMPLITUDE MODULATOR are contained in a single XR-205 integrated circuit. The angle modulation input port is biased so that the carrier frequency of the VCO is at 2400 Hz while the modulating signal (100 Hz) is adjusted in magnitude to cause 400 Hz frequency deviation. $\beta = 4$ is established in agreement with the solution to the example design problem in Chapter V.

Another XR-205 integrated circuit functions as the MODULATION OSCILLATOR which provides the signal for simultaneous amplitude and frequency modulation at 100 Hz. This signal is of the form $\sin \omega_m t$ and appears directly at the angle modulation input port of the VCO XR-205 just described. It appears indirectly at the amplitude modulation input port since it must first be modulated by the SCAN MODULATION OSCILLATOR signal of 1 Hz. The amplitude

modulation input port is biased at 0.5 so that the full swing of the SCAN MODULATION OSCILLATOR allows m to vary from 0 to 1.0. (The SCAN MODULATION OSCILLATOR is also an XR-205 integrated circuit). This process takes place in the AMPLITUDE MODULATOR $\omega_s < \omega_m$ block which consists of a single MC-1496G that is deliberately unbalanced to provide for true amplitude modulation and not a double sideband suppressed carrier output. The result of the interconnections of the three XR-205 and single MC-1496G integrated circuits is that the basic VCO is angle modulated by $\sin 2\pi(100)t$ and amplitude modulated by $M \cos 2\pi t \sin 2\pi(100)t$ where $m = M \cos 2\pi t$. The output of the AMPLITUDE MODULATOR block is at a carrier frequency of 2400 Hz while $\beta = 4$ and $f_m = 100$ Hz. This output is fed directly to a HIGH ORDER LOWPASS FILTER $\omega_{co} > \omega_c - \beta\omega_m$ with a cut-off frequency of 1950 Hz. This allows only those lower sidebands below the lowest instantaneous frequency of the basic VCO to be passed. Since the lowest instantaneous frequency is 2000 Hz, those sidebands at $f = 2000 - 100n$ Hz, $n = 1,2,3,\ldots$ are transmitted through the filter. It should be recalled that only these sidebands may have a zero amplitude for $0 < m < 1$. This filter is made up of four cascaded stages of, the type shown in Figure 6-1 using a single LM-3900 integrated circuit.

Since the sinusoidal output of the XR-205 is synthetically produced by rounding the corners of its triangular output, significant harmonic content is present. To ensure that modulation is applied to the basic VCO in the form of a single sinusoidal component at 100 Hz, the output of the 100 Hz oscillator is passed through a 100 Hz biquad bandpass filter ($Q \simeq 20$) before it is applied to the VCO. This filter is made up of three 741 operational amplifiers and follows the configuration of Fig. 6-2.

In summary, the schematic diagram presented in Fig. 6-5 performs those functions of the block diagram of Fig. 4-1 labeled: ANGLE MODULATED VCO, ISOLATION STAGE, AMPLITUDE MODULATOR, SCAN MODULATION OSCILLATOR, AMPLITUDE MODULATOR $\omega_s < \omega_m$, MODULATION OSCILLATOR and HIGH ORDER LOWPASS FILTER. Figures 6-1 and 6-2 aid in locating the individual components used in the filters. Each XR-205 is labeled according to frequency as an indicator of its specific function. The output labeled "X" corresponds to the output of the HIGH ORDER LOWPASS FILTER block of Figure 4-1. A detailed explanation of all components surrounding the XR-205 integrated circuits, bias and dc blocking capacitors of the operational amplifiers is considered to be unimportant and therefore not presented. Design values for those components having influence on the dynamic behavior of the active filters were determined

BASIC VCO, SIMULTANEOUS MODULATION, SCAN MODULATION AND LOW PASS FILTER

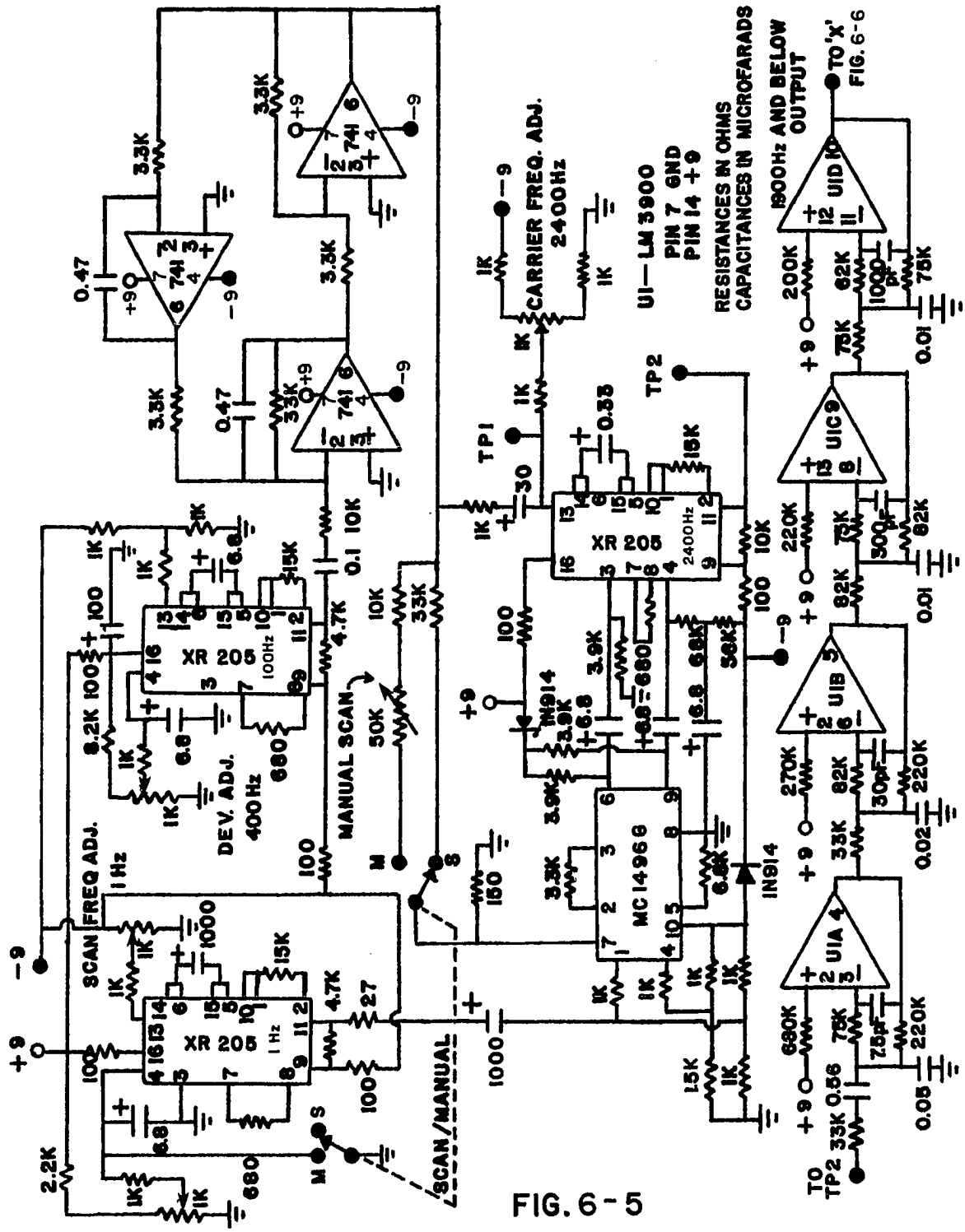

FIG. 6-5

according to the tabular methods described in reference 17.

6-4-2 Bandpass Filters

The function of the bandpass filters (labeled BP FILTER in Fig. 4-1) is to single out the individual frequency components appearing at point "X" in Fig. 6-5. Only those components from $\omega_c - (\beta+1)\omega_m$ to $\omega_c - (\beta+5)\omega_m$ are filtered since for the purpose of the model, they are sufficient to demonstrate the concept. Procedures and circuitry necessary to filter and process those frequency components at $\omega_c - (\beta+6)\omega_m$ to $\omega_c - (\beta+10)\omega_m$ are redundant in a model designed to demonstrate feasibility. The components at 1900 Hz, 1800 Hz, 1700 Hz, 1600 Hz and 1500 Hz are each filtered by two cascaded high-Q biquad bandpass filters of the type shown in Figure 6-2. Figure 6-6 illustrates the actual bandpass filters schematically for each frequency component. The gain of each is properly set to render the outputs at A, B, C, D, E approximately equal. The gain of each filter is consequently higher for the lower frequencies since Bessel function values monotonically decrease for increasing order and constant argument. This monotonic decrease in magnitude is a direct result of the observations made on general Bessel function behavior for $n > \beta$ in section 3-2. For example, the gain of the 1500 Hz filter is greater than that of the 1600 Hz filter. The gain of the 1600 Hz filter is correspondingly greater than that

HIGH Q BANDPASS FILTERS

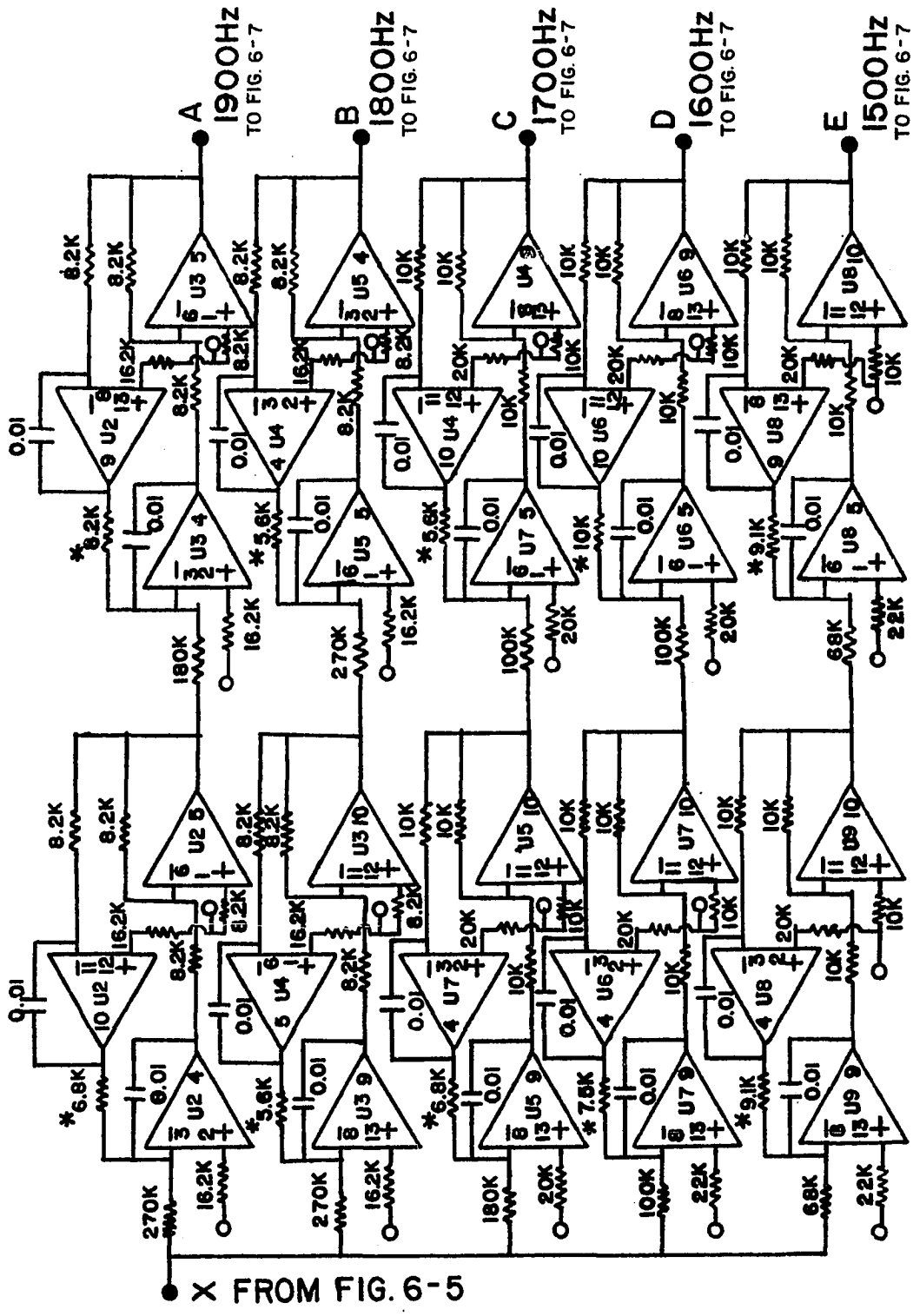

FIG. 6-6

of the 1700 Hz filter and so on. Table 6-1 indicates the absolute peak-to-peak voltage levels of the respective frequency components at the common input to the bandpass filters, i.e. point "X" in Figures 6-5 and 6-6. These values are for m = 1.

TABLE 6-1.--Absolute peak-to-peak voltage levels of the respective frequency components at the common input to the bandpass filters (m = 1)

$2\pi[\omega_c-(\beta+n)]\omega_m$ n = 1,2,3,4,5	P-P Volts at LP Filter Output (point "X")	Approximate BP Filter Gain Required
1900 Hz	360 mV	3
1800 Hz	270 mV	4
1700 Hz	126 mV	10
1600 Hz	43 mV	22
1500 Hz	10 mV	80

Peak-to-peak voltage of the various frequency components at the output of the high order lowpass filter is measured with a Telequipment D75 Dual Trace Oscilloscope and external active biquad bandpass filter with unity gain. Also shown is the nearest practical integer gain value of the follow-on bandpass filters for each component necessary to equalize signal levels to approximately 1 volt. All values are measured for m = 1.

Table 2-2 lists values of $J_n(\beta)$ for $\beta = 4$ for convenient reference.

TABLE 6-2.--Bessel function values

n	$J_n(\beta)$
0	-0.3971
1	-0.0660
2	+0.3641
3	+0.4301
4	+0.2811
5	+0.1320
6	+0.0490
7	+0.0151
8	+0.0040
9	+0.0009
10	+0.0002

6-4-3 Double Balanced Mixer Frequency Shifters

The double balanced mixers necessary to shift those frequencies corresponding to A through D in Figure 6-6 to b through e are shown in Figure 6-7. Each pair of MC-1496G balanced mixers constitutes a single double balanced mixer. Since any component from 1900 Hz through 1600 Hz is to be shifted down in frequency by an amount equal to the VCO modulation frequency, the 100 Hz output of the XR-205 oscillator is used as the mixing signal source. The functional relationship is shown in Figure 4-1. The frequency components A through D are connected directly to their respective balanced mixers while the 100 Hz signal is also connected directly to the corresponding second input of the same mixers. The second half of each double

PHASE SHIFTERS, DOUBLE BALANCED MIXERS, AND SUMMERS

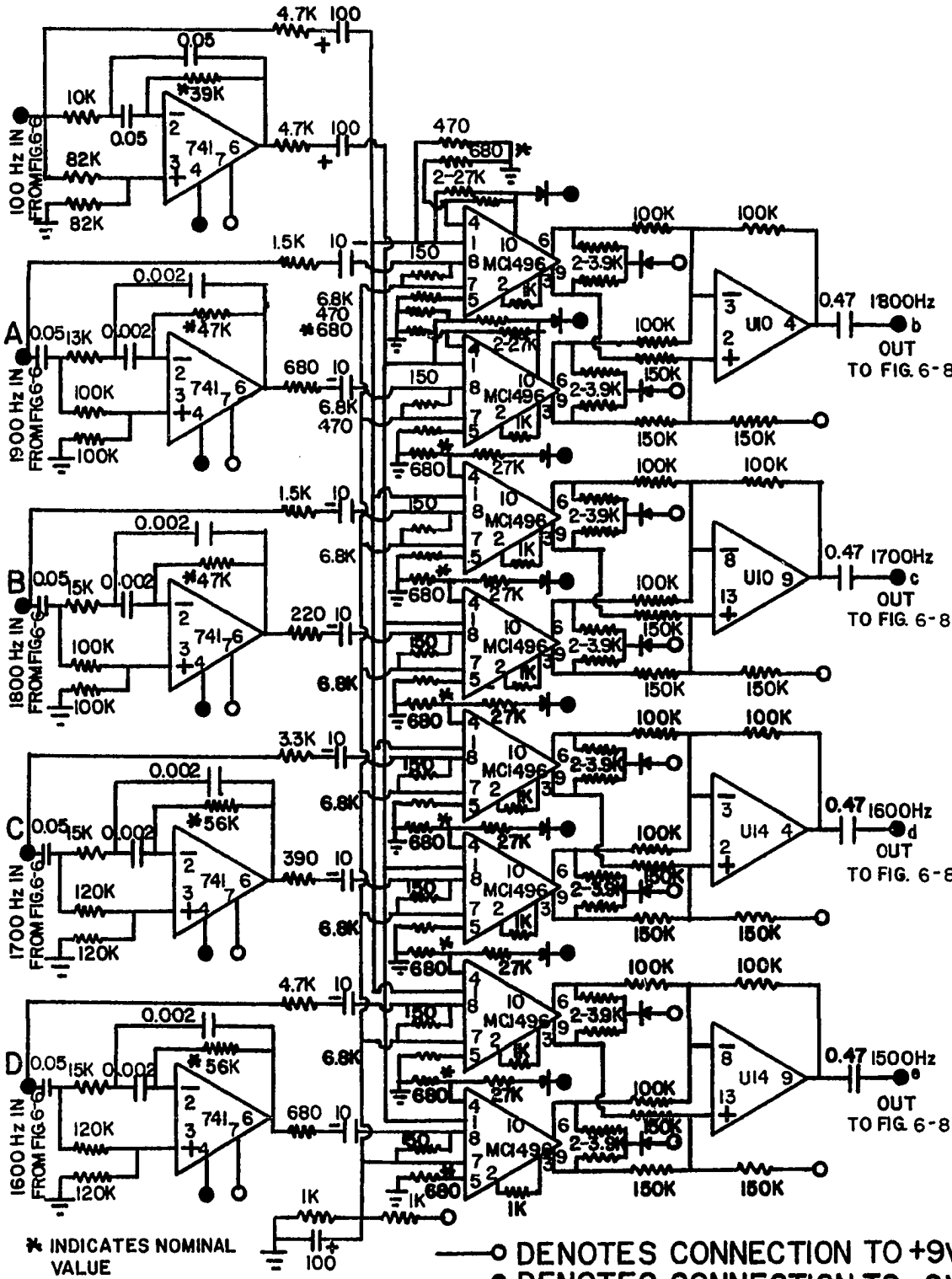

FIG. 6-7

balanced mixer is driven by the signals from A through D and the 100 Hz source after a 90° phase lead is applied to each. Performing time domain summation at the output of the double balanced mixer pairs results in a shift in frequency only in a downward direction since cancellation of the upward shift results. Phase shifting is brought about by the single operational amplifier type introduced in Figure 6-3 and designed according to reference 17.

The amplitudes of the signals at the output of the summers following the balanced mixers (b through e) will pass through zero for values of m corresponding to their parent frequencies (A through D).

It should be mentioned that although each balanced modulator is capable of operation using a single ended output, advantage is taken of using both outputs (pins 6 and 9 of the MC-1496G) so that the output voltage level is twice that for the single ended case. The pin 6 outputs are summed at the inverting input of each summer and the pin 9 outputs are summed at the non-inverting input. The summers are configured for an inverting input gain of unity while the non-inverting input gain is two. Balance is maintained by the bias resistor to each non-inverting input since its value is equal to the non-inverting input resistor. These two resistors which are connected in series divide the input voltage by two to the non-inverting input

rendering unity gain for both inputs.

6-4-4 Phase Correctors

Equation (50) and (51), the mathematics governing the product mixing of the ideal balanced mixer do not indicate the existence of any arbitrary phase angle in the sum and difference frequency components in the output. However, in reality a constant phase angle results which must be compensated for. Figure 6-8 illustrates pairs of amplitude-limiters of the type shown in Figure 6-4. The input signal to one-half of each pair is obtained from the bandpass filter outputs of Figure 6-6 corresponding to the frequencies indicated by upper case letters. The corresponding input of the opposite half of each amplitude-limiter pair is derived from the double balanced mixer summer circuit of Figure 6-7 after phase correction. These outputs are indicated by lower case letters.

For a value of m that should produce the cancellation of a particular frequency component, the phase difference between the upper case letter input and lower case letter input must be 180°. The single operational amplifier phase correctors of Figure 6-8 (shown in basic form in Figure 6-3) provide the additional phase shift that must be added to that resulting from the frequency shift process to equal 180°. The additional phase shift required was measured on a Telequipment D75 Dual Trace Oscilloscope with both

PHASE CORRECTORS, LIMITER-AMPLIFIERS, SUMMERS AND INDICATORS

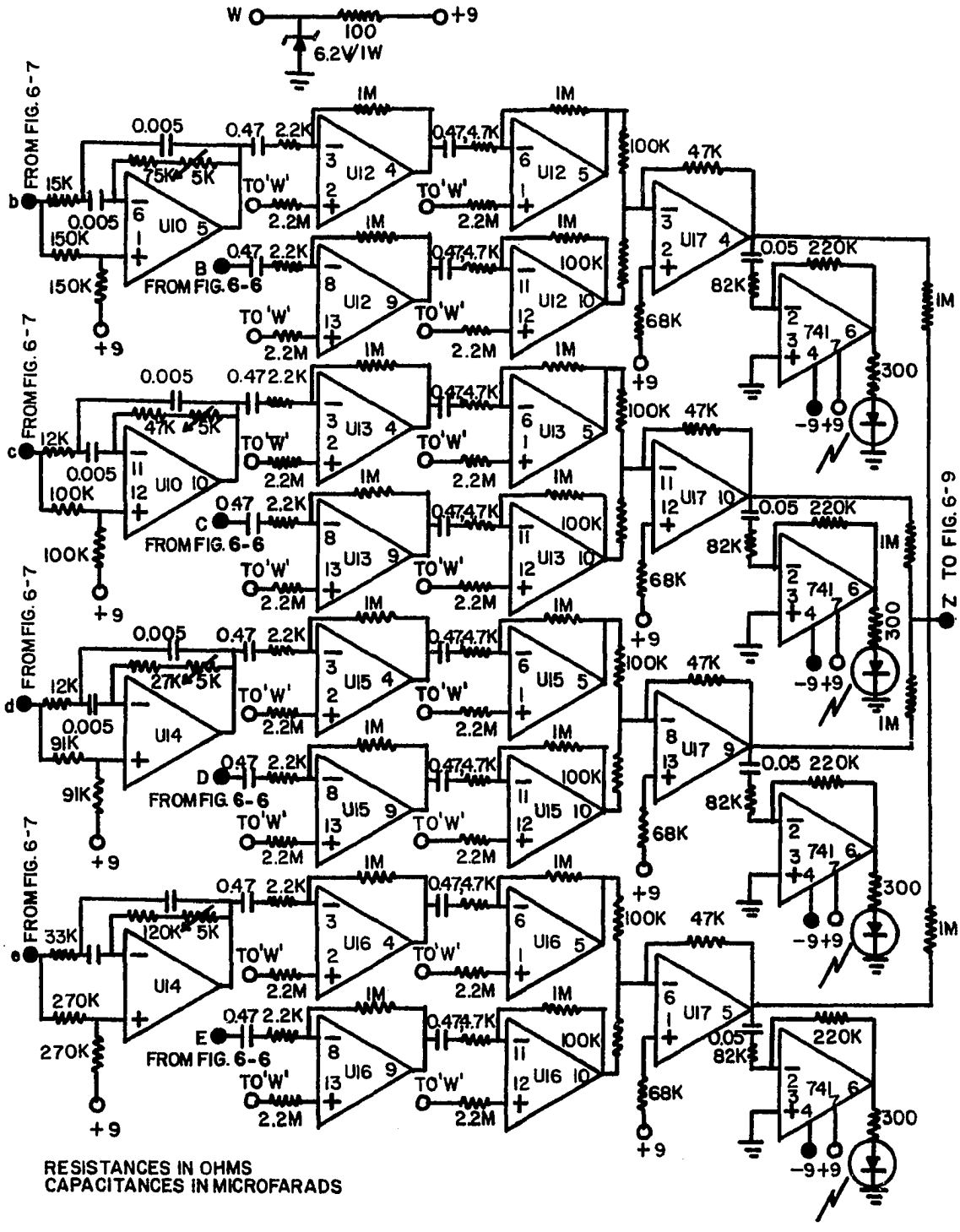

FIG. 6-8

traces synchronized to the same signal input. Phase corrector design is accomplished according to the procedure in reference 17. The amplitude-limiters are designed to produce a $G\hat{V}$ to λ ratio of at least 3000 in all cases.

The intensity of a frequency component is indicated by the intensity of a light emitting diode driven by a separate operational amplifier which senses the summation circuit output following each amplitude limiter pair.

The summer outputs are also summed at "Z" in Figure 6-8. At this point the signals exist in the form of rectangular waves bounded by the saturation and cut-off limits of the amplitude-limiter. Perfect sideband component cancellation for the regions of m that should not result in the enhancement of some component should be seen as a zero signal level at "Z". When m is in the region between the zero amplitude crossover of two adjacent frequency components of the basic VCO, one of the components is inverted in phase from that which causes component cancellation. Since they are both brought to the same frequency by the appropriate double balanced mixer, they no longer add to zero in the amplitude-limiter outputs but add to enhance.

To eliminate the harmonic content of the signal at the limiter outputs at "Z", it is further processed by a LOW ORDER LOWPASS FILTER so that only the 1800 Hz, 1700 Hz,

1600 Hz, and 1500 Hz signals may appear at the output of the ultimate VCO. This filter is shown schematically in Figure 6-9 and functionally in Figure 4-1. Relative to the lowpass filter associated with the basic VCO in Figure 6-5, it need only be of low order since the nearest harmonic frequency component is at 3000 Hz. Nevertheless an eight-pole filter was used since four operational amplifiers are available in a single LM-3900 package.

6-4-5 Dual Voltage Power Supply

The power supply for all circuit components of the fast scan VCO model is worthy of note since it also makes use of operational amplifiers. It delivers positive and negative nine volts regulated to within 0.1% for current drains up to 500 mA from each source. The schematic diagram of the power supply appears in Figure 6-10. Regulation and output voltage selection is made possible by means of a type 741 operational amplifier in each supply which senses the constant voltage drop across a heavily conducting silicon power diode connected between the inverting input resistor and ground. Current through the diode is limited by a series resistor to the unregulated supply. Heavy conduction ensures a constant voltage drop across the diode which is used as a reference for the inverting amplifier. The gain of the inverting amplifier configuration for each operational amplifier is adjusted according

OUTPUT LOWPASS FILTER

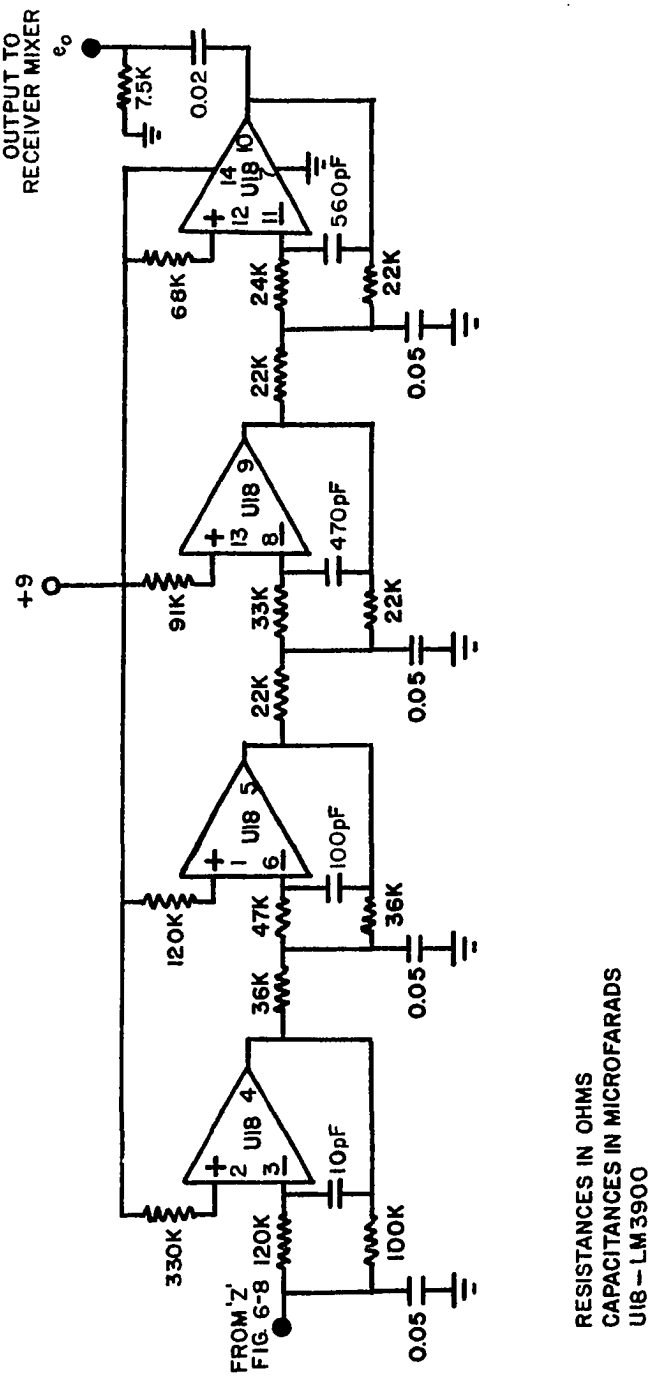

FIG. 6-9

POWER SUPPLY

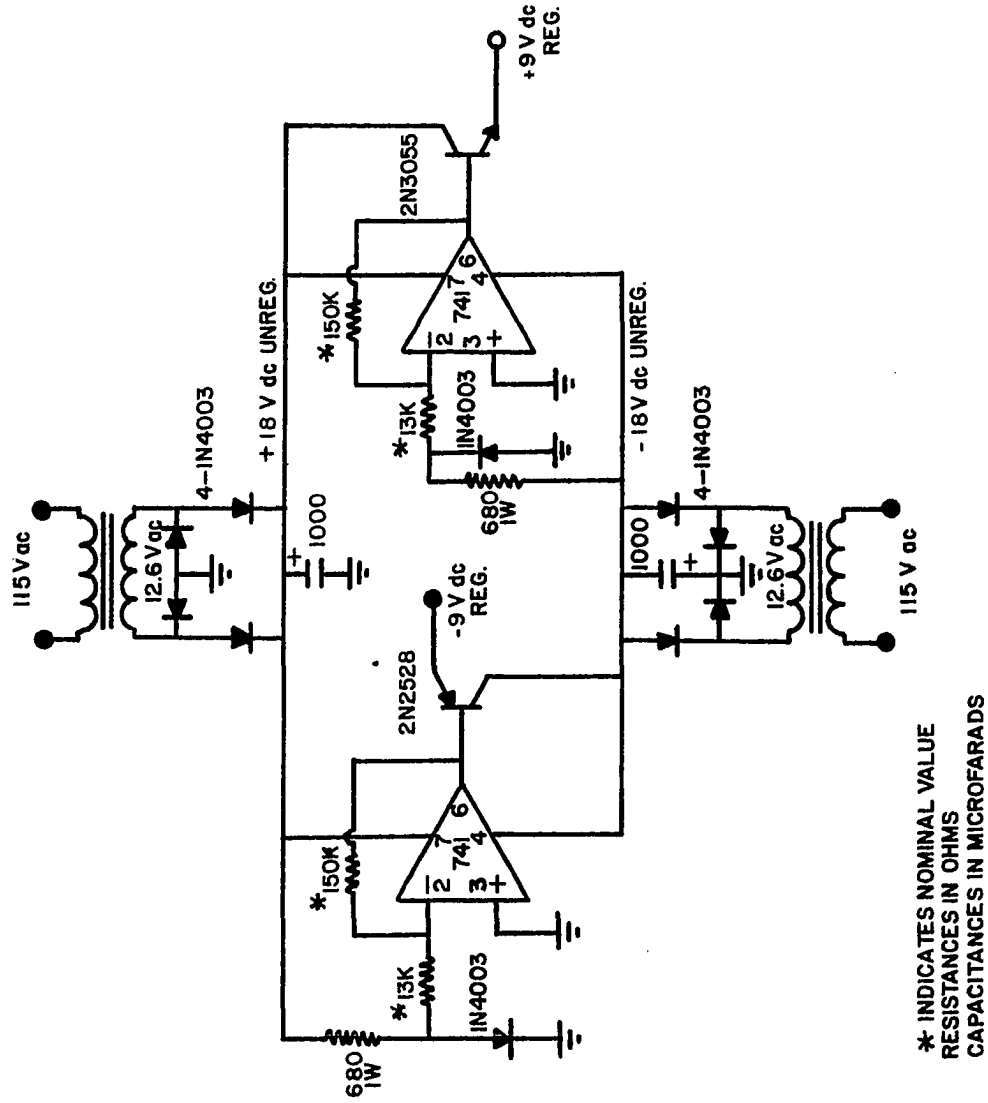

FIG. 6-10

to the feedback and input resistor ratio to cause the output to be approximately ten volts in magnitude. The amplifier outputs connect directly to the base of their respective pass transistors in a conventional series regulator circuit. All residual ac voltage in the unregulated portion of the supplies is forced to fall across the collector-emitter path of the pass transistors at the sacrifice of a one volt drop of regulated voltage across the base-emitter junction. This circuit proved far superior in regulation to other available complete voltage regulator integrated circuits since the output voltage of an operational amplifier in the inverting amplifier configuration is independent of its unregulated supply voltage. This remains true so long as the operational amplifier supply voltage does not fall below its output voltage level because of heavy load currents.

6-5 Practical Circuit Boards for the Fast Scan VCO Model

Figure 6-11 is a photographic reproduction of the circuit board containing all components for the model presented schematically in Figures 6-5 and 6-6. The circuitry of Figures 6-7, 6-8 and 6-9 is contained on the circuit board shown in Figure 6-12. Figure 6-13 shows all power supply circuitry illustrated schematically in Figure 6-10.

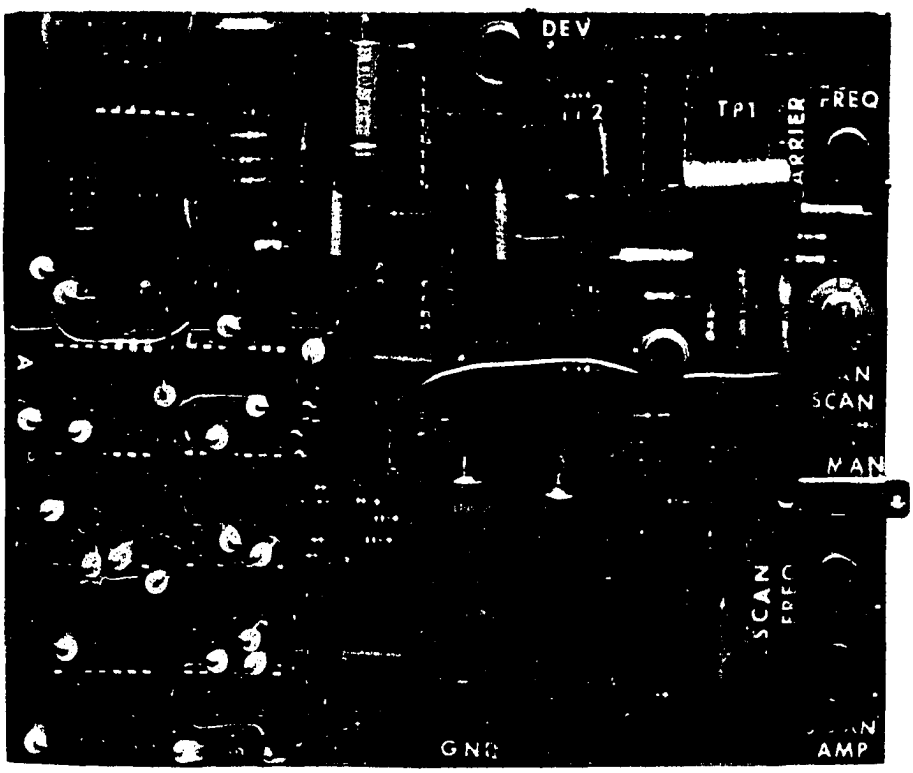

Fig. 6-11. This circuit board contains the BASIC VCO, SIMULTANEOUS MODULATORS, SCAN MODULATOR, HIGH ORDER LOWPASS FILTER and HIGH Q BANDPASS FILTERS of the frequency model. Circuitry for these functions is shown schematically in Fig. 6-5 and 6-6.

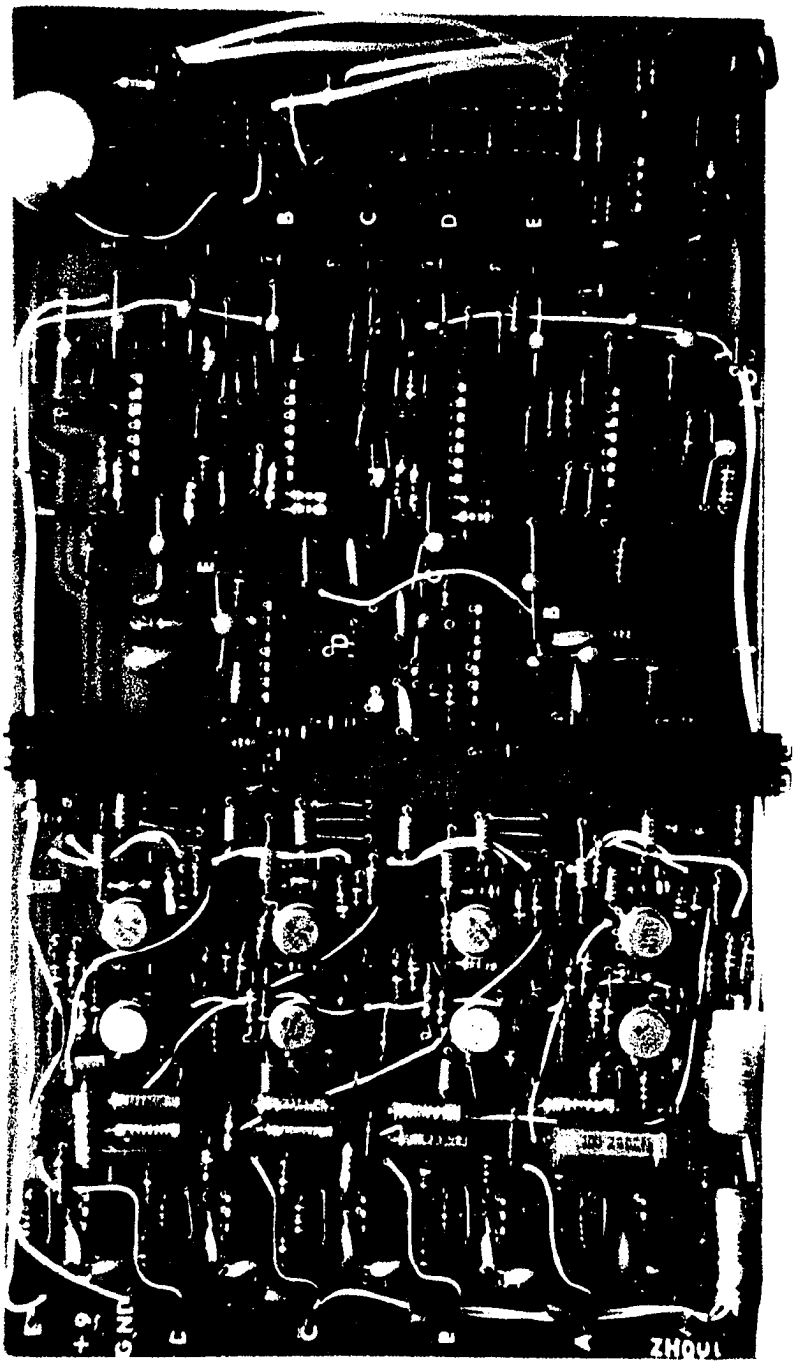

Fig. 6-12. This circuit board contains the PHASE SHIFTERS, DOUBLE BALANCED MIXERS, PHASE CORRECTORS, LIMITER-AMPLIFIERS, INDICATORS, and LOW ORDER LOW-PASS FILTER of the frequency model. Circuitry for these functions is shown schematically in Fig. 6-7, 6-8 and 6-9.

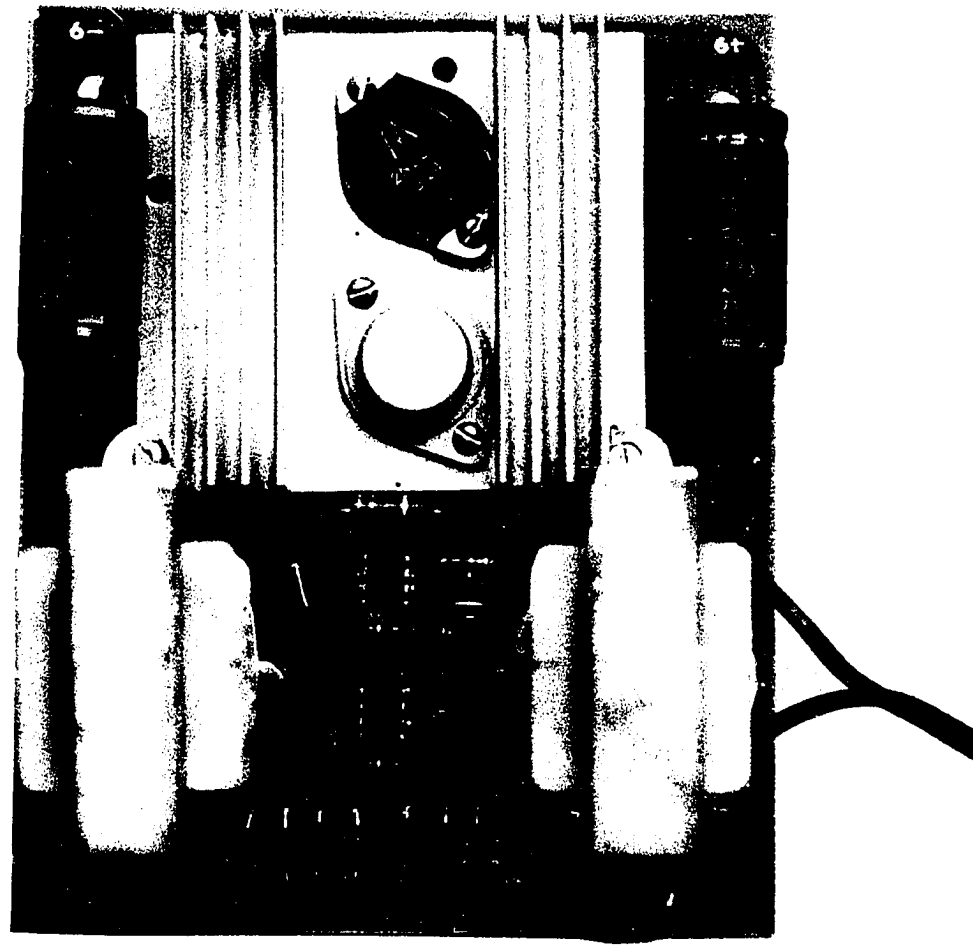

Fig. 6-13. This circuit board contains the dual voltage POWER SUPPLY with its associated voltage regulators. The power supply is shown schematically in Fig. 6-10.

CHAPTER VII

OBSERVED MODEL RESULTS

7-1 Results of Frequency Model Tests[11]

The schematic representation of the basic VCO and its modulation sources in Figure 6-5 shows a SCAN/MANUAL switch. This two position switch allows the 1 Hz scan oscillator to sweep m across its full range or allows m to be selected manually by the position of a potentiometer.

With the SCAN/MANUAL switch in the MANUAL position, Figure 7-1 is the time domain representation of the basic VCO output, i.e. point "X" in Figure 6-5, for m near 1.000. Angle and amplitude modulation of the proper phase relationship are apparent such that the maximum instantaneous frequency output (2800 Hz) at the amplitude maximum may be clearly distinguished from the minimum instantaneous frequency output (2000 Hz) at the amplitude minimum.

The corresponding frequency display appears in Figure 7-2 with the lower sidebands below the lowest instantaneous frequency (1900 Hz and below) clearly visible. Equation (39) predicts zero amplitude for the βth lower

[11]All photographs in this Chapter were produced by means of a Hewlett-Packard Model HP-197A Polaroid camera on a Hewlett-Packard Model 141T/8552B/8556A Spectrum Analyzer and an AN/USM-281-A Dual Trace Oscilloscope.

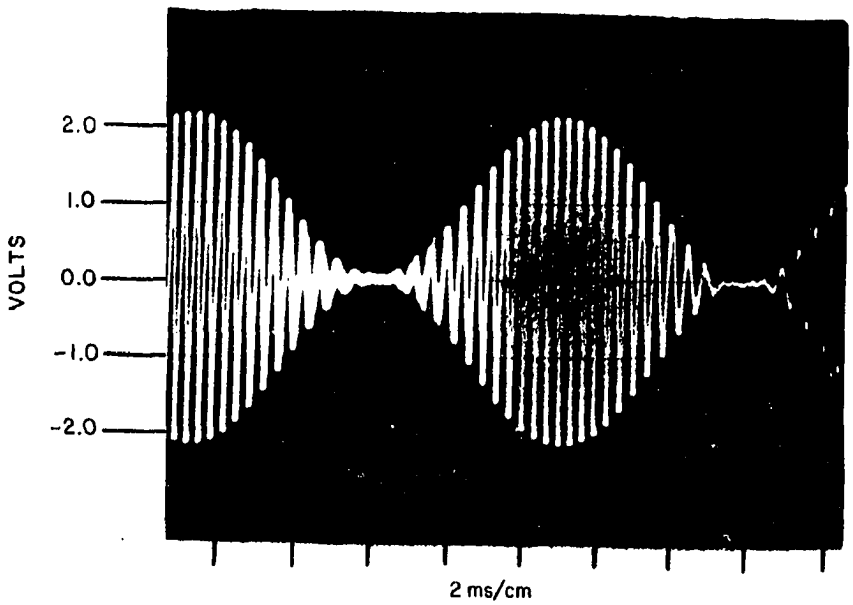

BASIC VCO OUTPUT FOR m=1.000
(PARTIAL SUPPRESSION OF 2000 Hz)

FIG. 7-1

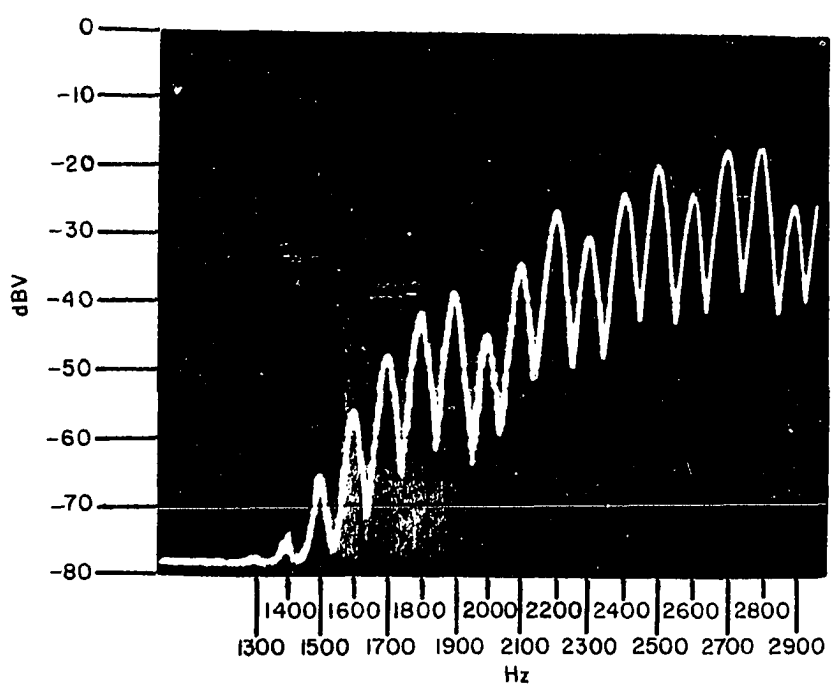

BASIC VCO OUTPUT FOR m=1.000

FIG. 7-2

sideband for m = 1.000. In the photographs m approximately equals one showing a depression of 12 dB rather than some greater number. Figures 7-3 and 7-4 are the time domain and frequency domain representations at point "X" for m ≈ 0.800, that value necessary to suppress the $(\beta+1)$st lower sideband. Likewise, Figure 7-5 through 7-10 show the same point for various values of m, each near that value necessary to suppress a sideband.

The frequency domain bandpass filter output for the highest lower sideband frequency component, point "A" in Figure 6-6 is shown in Figure 7-11 for m = 1.000. Successively lower frequency components are shown in Figures 7-12 and 7-13. (Outputs at 1700 Hz and 1600 Hz are not presented). Because of the relatively large magnitude of the 1900 Hz component compared with the lower frequency components, the 1500 Hz filter output shows significant output of unwanted sidebands even though the Q of all filters is generally the same (Q≈80). This contributes significantly to less than optimum signal cancellation in the ultimate VCO output.

At the B and b inputs to the amplitude-limiter pair for 1800 Hz in Figure 6-8, Figure 7-14 shows the phase and amplitude relationship of the original 1800 Hz sideband to the one derived from 1900 Hz. At this point the frequency shifted signal has been phase corrected so that they are

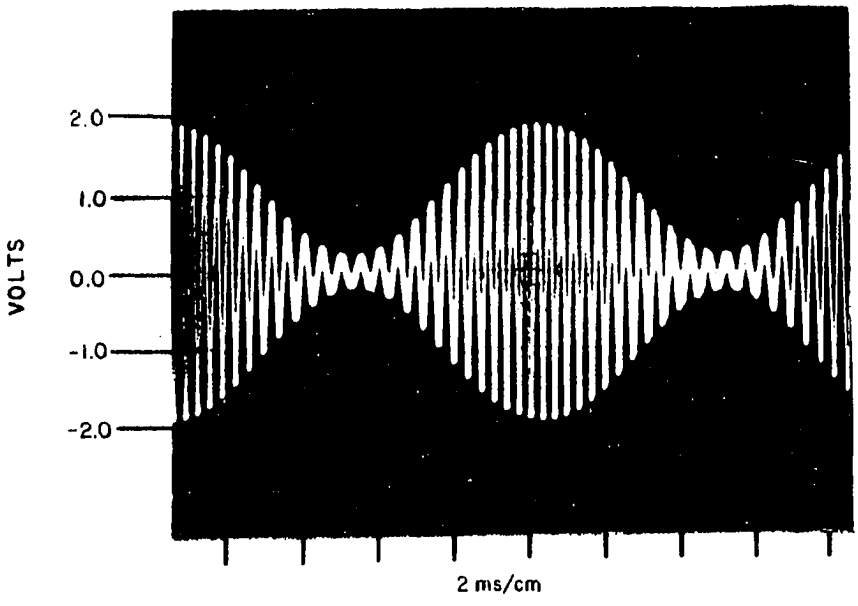

BASIC VCO OUTPUT FOR m = 0.800
(PARTIAL SUPPRESSION OF 1900 Hz)

FIG. 7-3

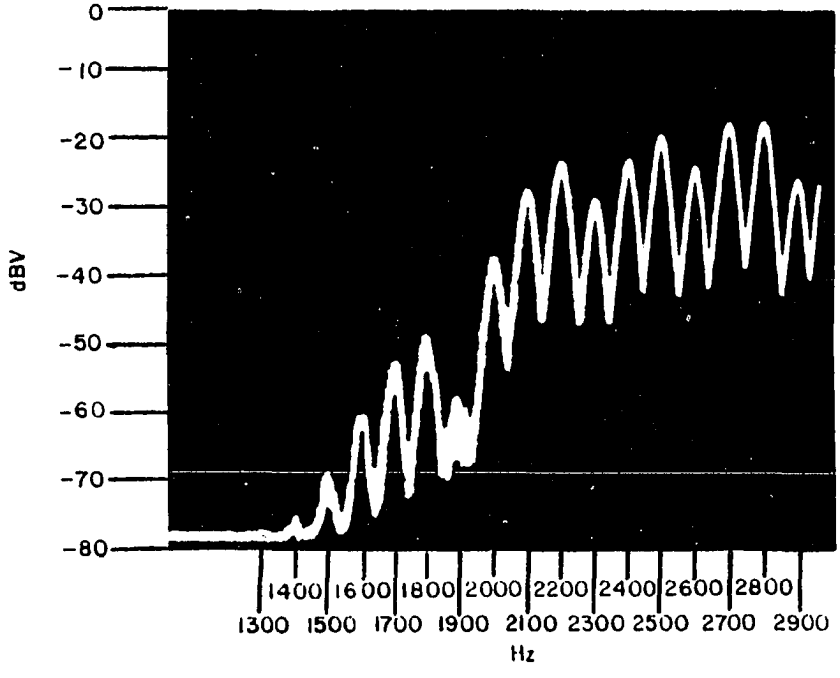

BASIC VCO OUTPUT FOR m = 0.800

FIG. 7-4

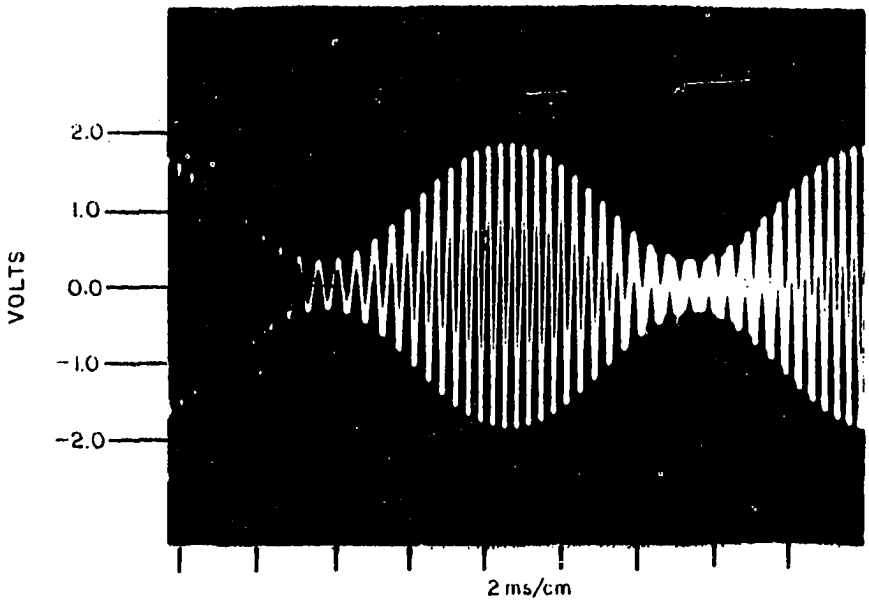

BASIC VCO OUTPUT FOR m = 0.666
(PARTIAL SUPPRESSION OF 1800 Hz)

FIG. 7-5

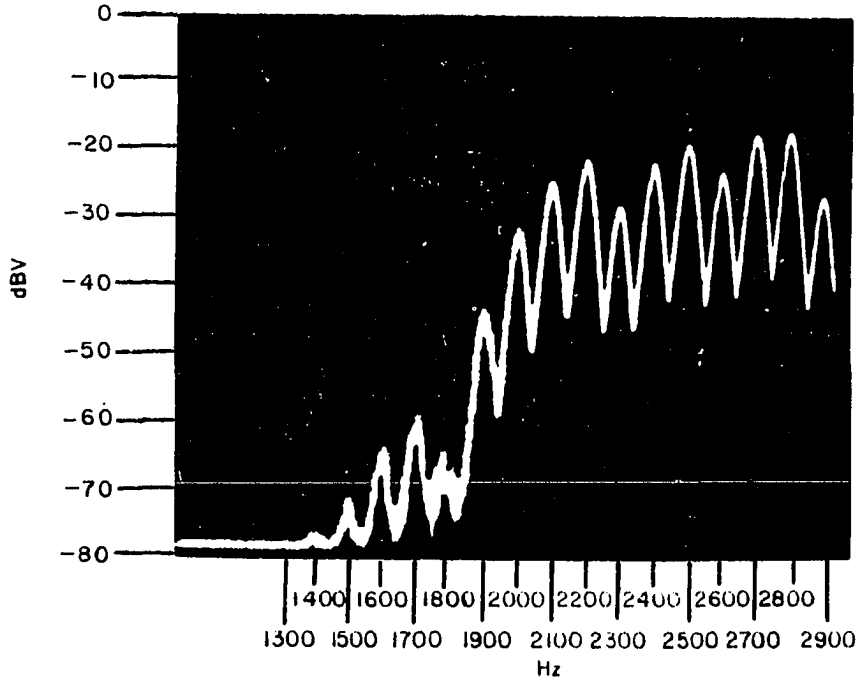

BASIC VCO OUTPUT FOR m = 0.666

FIG. 7-6

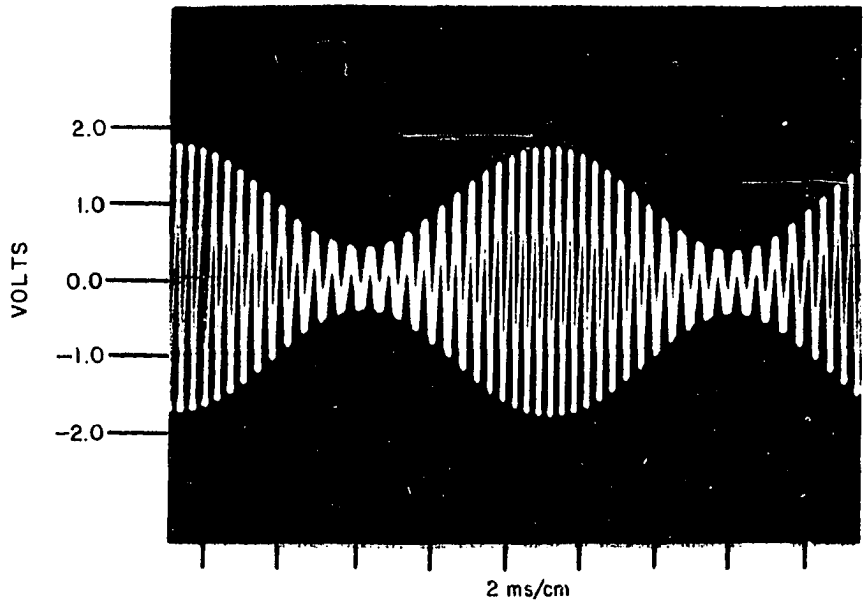

BASIC VCO OUTPUT FOR m = 0.570
(PARTIAL SUPPRESSION OF 1700 Hz)

FIG. 7-7

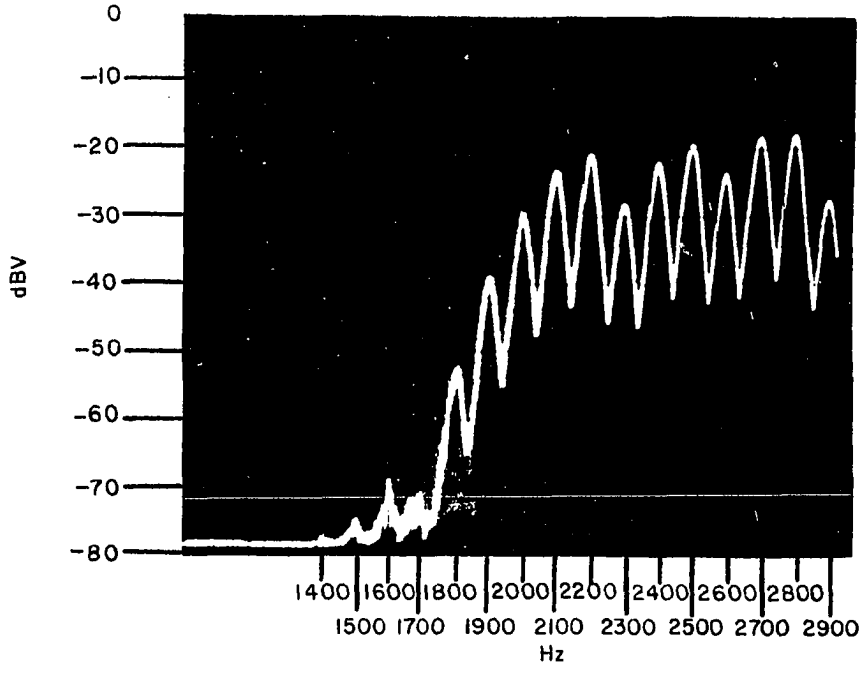

BASIC VCO OUTPUT FOR m = 0.570

FIG. 7-8

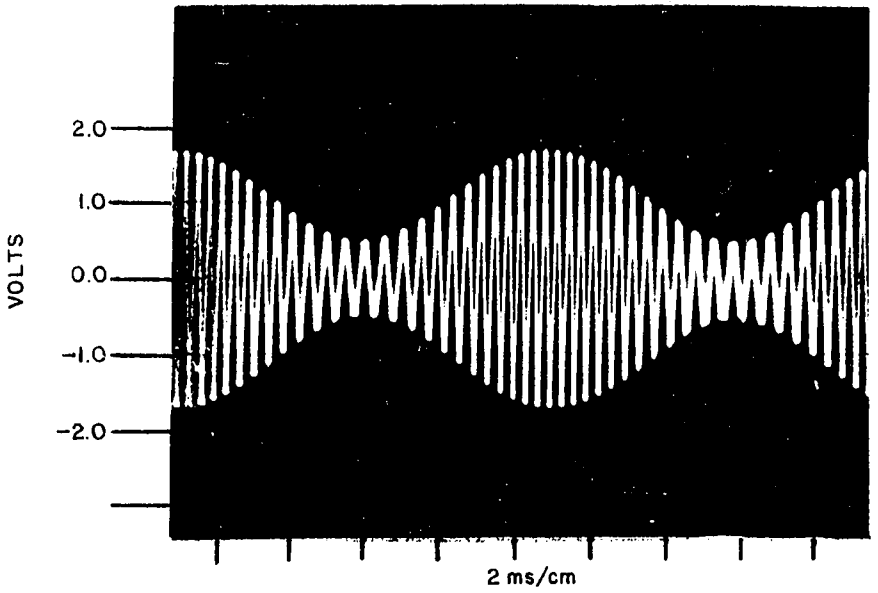

BASIC VCO OUTPUT FOR m = 0.499
(PARTIAL SUPPRESSION OF 1600 Hz)

FIG. 7-9

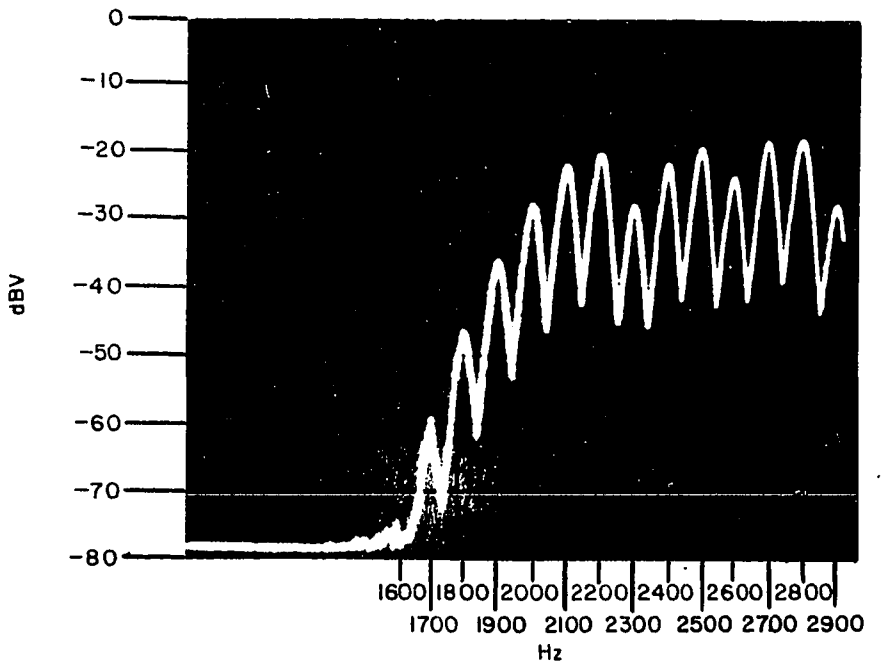

BASIC VCO OUTPUT FOR m = 0.499

FIG. 7-10

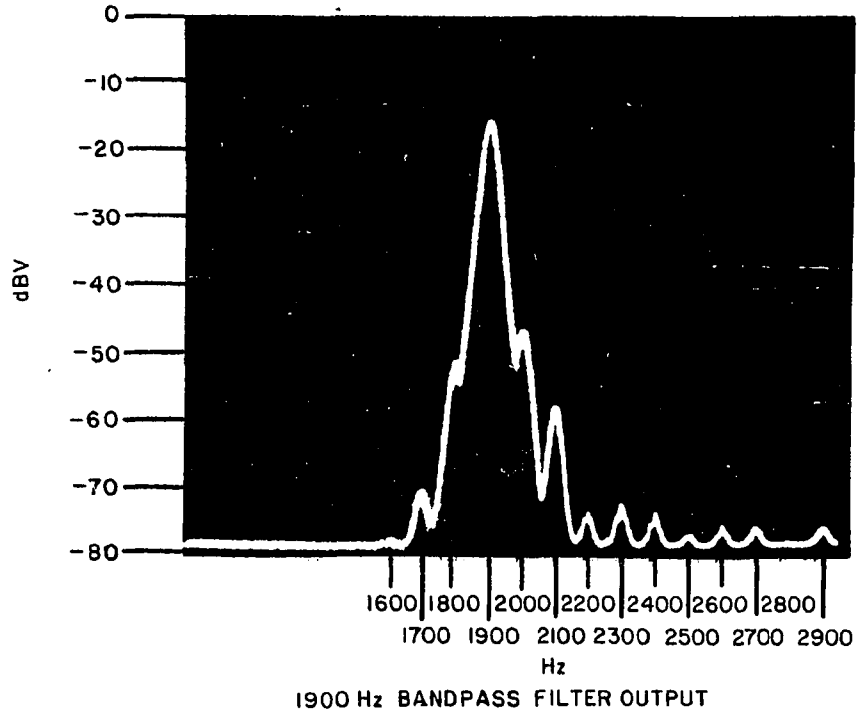

FIG. 7-11

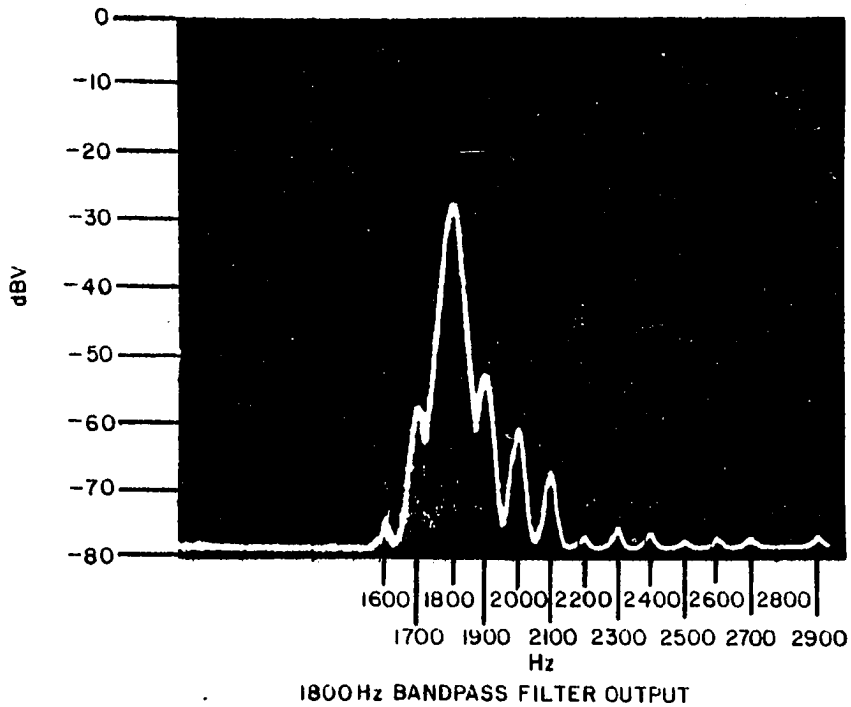

FIG. 7-12

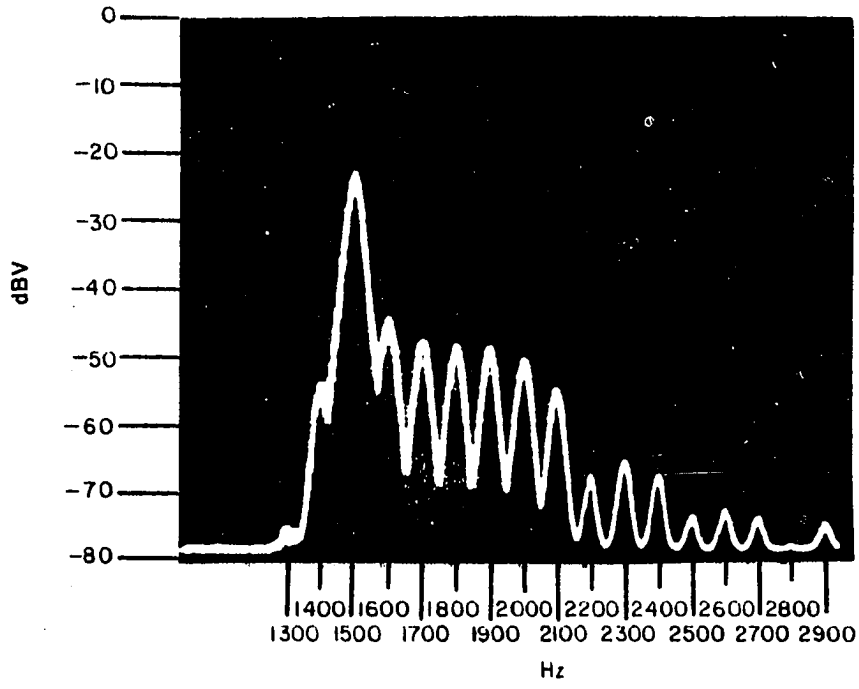

1500Hz BANDPASS FILTER OUTPUT

FIG. 7-13

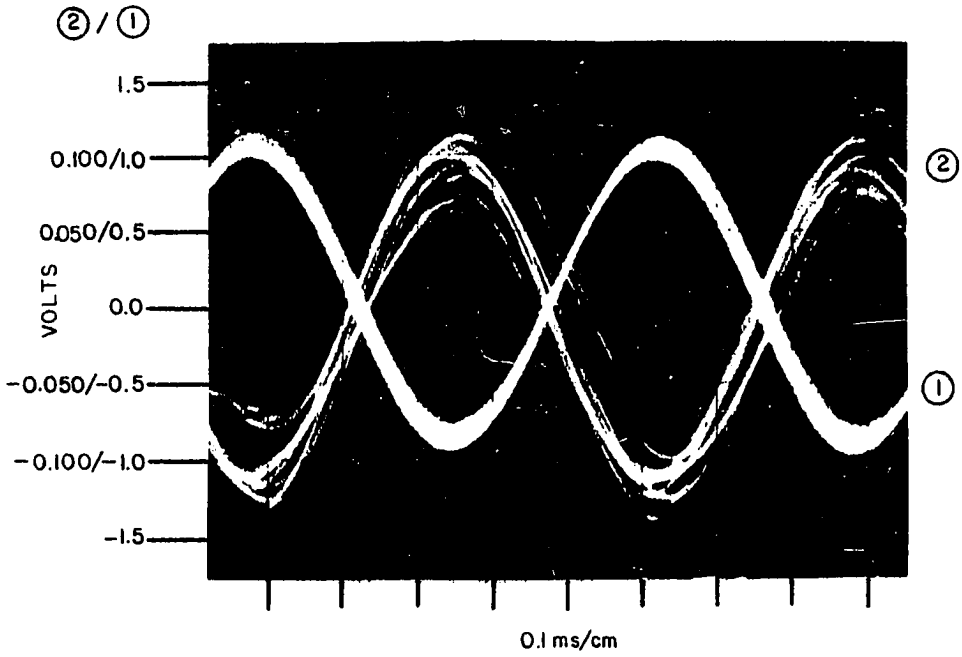

① 1800 Hz BANDPASS FILTER OUTPUT

② 1800 Hz DOUBLE BALANCED MIXER OUTPUT (PHASE CORRECTED, $m < 0.666$)

FIG. 7-14

180° out of phase with each other for m not in the range for 1800 Hz enhancement. It is apparent that if both signals are greatly amplified and equally amplitude limited before summing that the net output ideally is zero. (Addition of equations of the forms of (64) or (65) and (66) or (67). As m is changed to a value between that which inverts one of the amplitude-limiter inputs and not the other, the two signals become in phase and will have a net addition not equal to zero at the summed output of the amplitude-limiter pair. This phenomenum is shown in the photograph of Figure 7-15.

Figure 7-16 illustrates the relative phase and amplitude of the unclipped waveforms for the range of m resulting in cancellation on the opposite side of the enhancement region from that shown in Figure 7-14. Both signals have been inverted and once again are out of phase adding to zero.

Figure 7-17 is a dual trace time domain representation of the two outputs of the associated amplitude-limiter pair for 1800 Hz. The supply voltage to the limiter is deliberately reduced to six volts so that saturation occurs early in the rise of a sine input. These are high gain stages designed with the intent to obtain a high $G\hat{V}$ to λ ratio. The effects of input offset voltage in the first of a cascaded pair of limiters is prevented from upsetting the

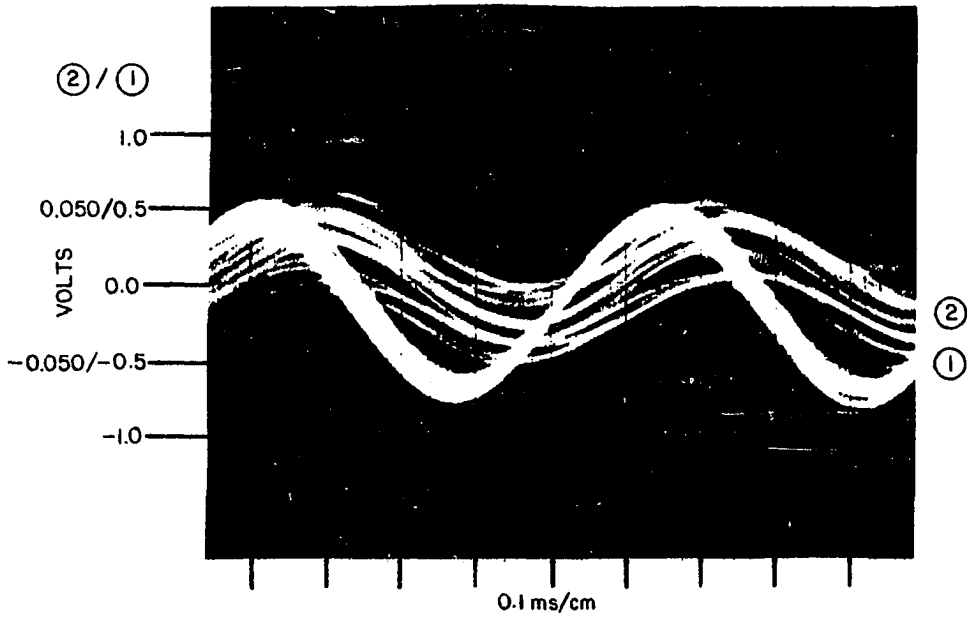

① 1800 Hz BANDPASS FILTER OUTPUT

② 1800 Hz DOUBLE BALANCED MIXER OUTPUT (PHASE CORRECTED, $0.666 < m < 0.800$)

FIG. 7-15

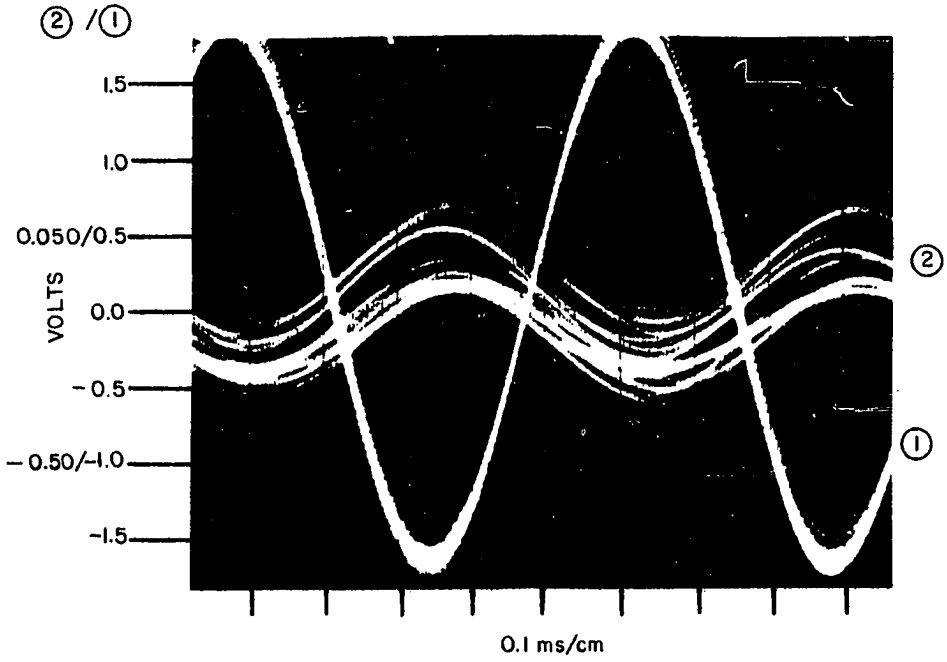

① 1800 Hz BANDPASS FILTER OUTPUT

② 1800 Hz DOUBLE BALANCED MIXER OUTPUT (PHASE CORRECTED, m>0.800)

FIG. 7-16

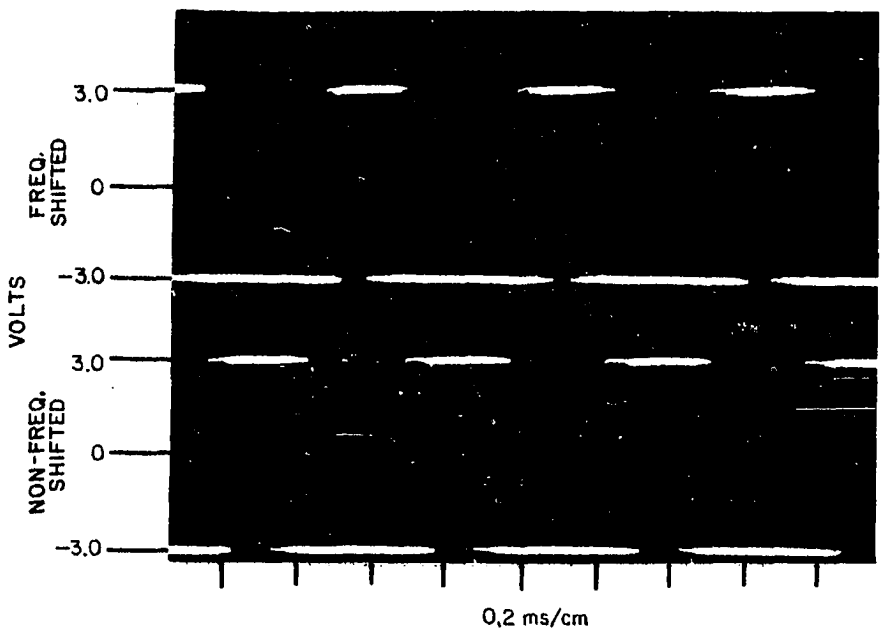

OUTPUT OF THE 1800 Hz AMPLITUDE-LIMITERS
FOR $m < 0.666$

FIG. 7-17

proper quiescent point of the second amplifier by a dc blocking capacitor between the output of the first and the input of the second. It should be noticed that the waveforms of Figure 7-17 indicate asymmetrical clipping and phase jitter. The causes and effects are discussed in Chapter VIII.

Figures 7-18 through 7-21 illustrate the enhancement of each sideband frequency component corresponding to their respective range of m. The point of measurement is at the output of the ultimate VCO, e_0 in Figure 4-1 or 6-9. Enhancement is clearly present in each case but is less than optimum. Best case enhancement occurs in Figure 7-21 for 1500 Hz. The 1500 Hz component is 16 dB greater than the component of the next highest amplitude and 25 dB greater than the component with the least magnitude. Worst case enhancement occurs in Figure 7-19 where the enhanced 1700 Hz signal is only 6 dB greater than that of the 1600 Hz component.

The concept of discrete frequency component enhancement by establishing a corresponding range on a continuous amplitude variable is demonstrated. The degree of enhancement in the fast scan VCO frequency model is certainly less than optimum, however, further separation of desired to undesired signal levels may be improved by consideration

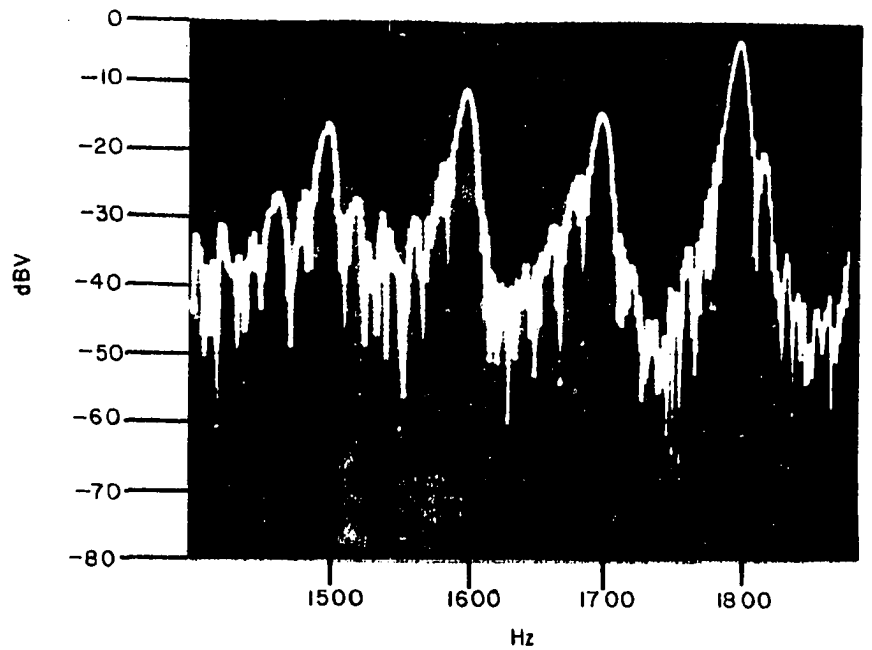

ULTIMATE VCO OUTPUT WITH 1800 Hz ENHANCEMENT,
$e_o(m)$ FOR $0.666 < m < 0.800$

FIG. 7-18

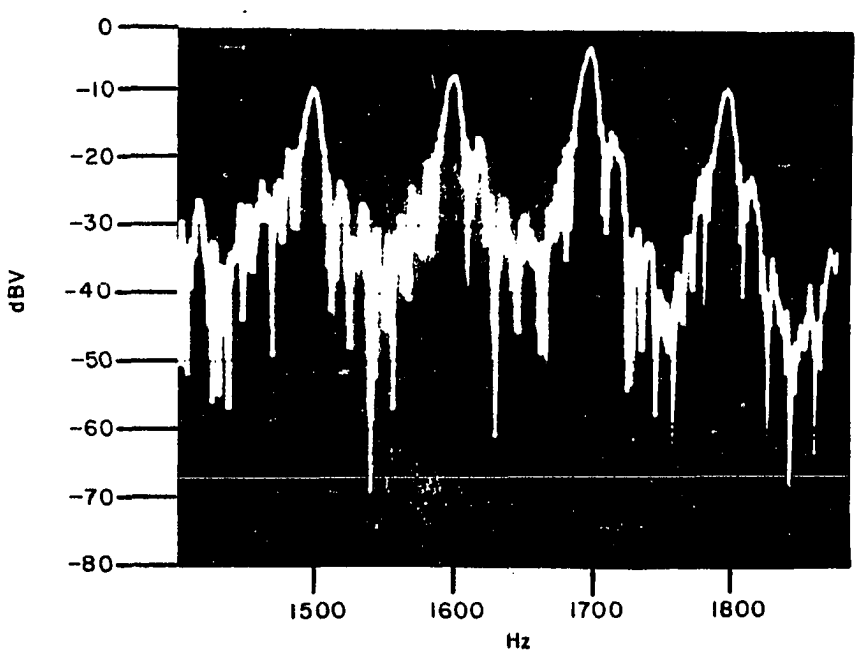

ULTIMATE VCO OUTPUT WITH 1700 Hz ENHANCEMENT,
$e_o(m)$ FOR $0.570 < m < 0.666$

FIG. 7-19

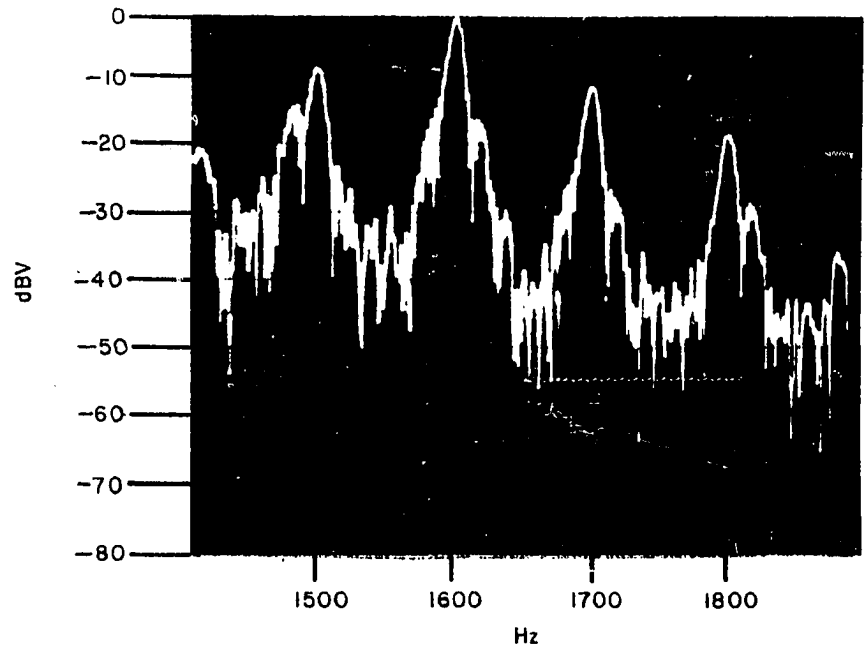

ULTIMATE VCO OUTPUT WITH 1600 Hz ENHANCEMENT,
$e_o(m)$ FOR $0.499 < m < 0.570$

FIG. 7-20

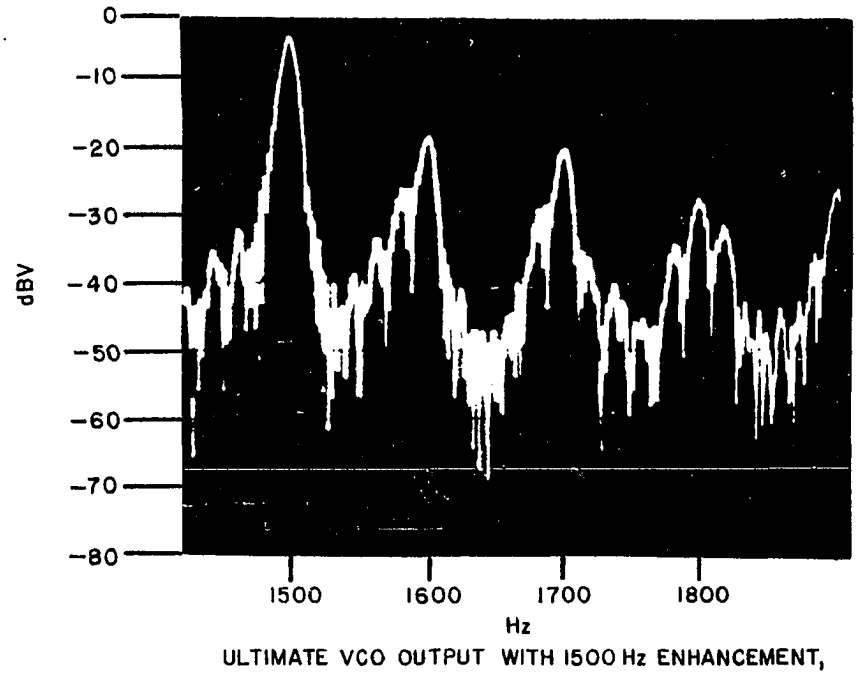

ULTIMATE VCO OUTPUT WITH 1500 Hz ENHANCEMENT,
$e_o(m)$ FOR $0.447 < m < 0.499$

FIG. 7-21

given to properties of the devices chosen for use in the model. Chapter VIII deals with these problems.

CHAPTER VIII

CONCLUSIONS

8-1 Frequency Model Observations and Conclusions[12]

Unwanted sideband suppression at the output of the ultimate VCO should be much greater than that demonstrated by the frequency model. The minimum required is a function of superheterodyne receiver specifications, however, it is thought that at least 60 dB must be achieved in any case. Factors contributing to less than optimum separation in the model are believed to be unique to the devices used. Each source of "noise" accumulatively contributing to insufficient separation is discussed.

8-1-1 Bandpass Filter and Balanced Mixer Properties

Figure 8-1 shows the relative uncleanliness of the output of the 1800 Hz bandpass filter. Modulation at 100 Hz is seen to exist indicating the presence of components at 1900 Hz, 1700 Hz and perhaps others. This modulation is also indicated by Figures 7-11 through 7-13.

Filters with sharper skirts are necessary to prevent unwanted frequency components from traveling the wrong path to the ultimate VCO output with any significant magnitude.

---

[12]All photographs in this chapter were produced by means of a Hewlett-Packard Model HP-197A Polaroid Camera on a Hewlett-Packard Model HP-141T/8552B/8556A Spectrum Analyzer.

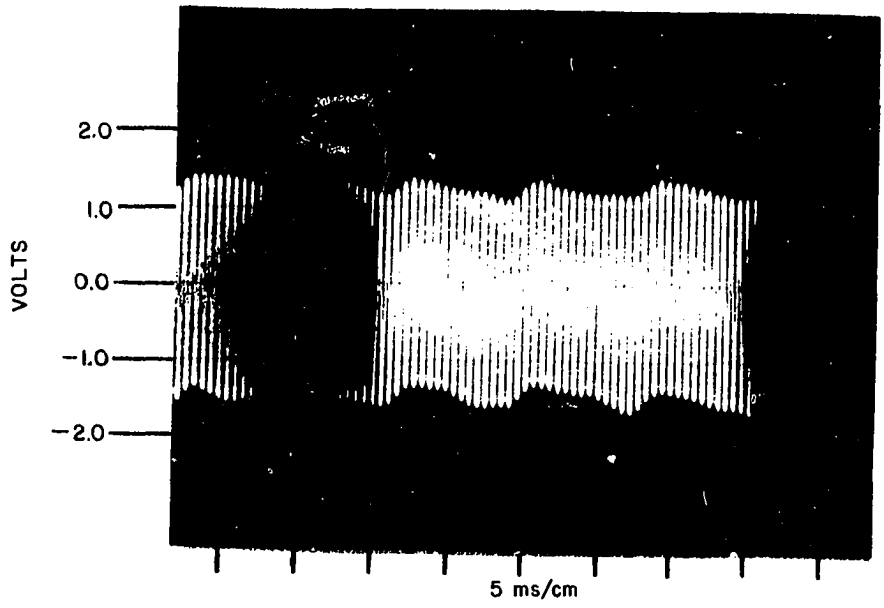

ENVELOPE OF 1800 Hz BANDPASS FILTER OUTPUT
$m < 0.666$

FIG. 8-1

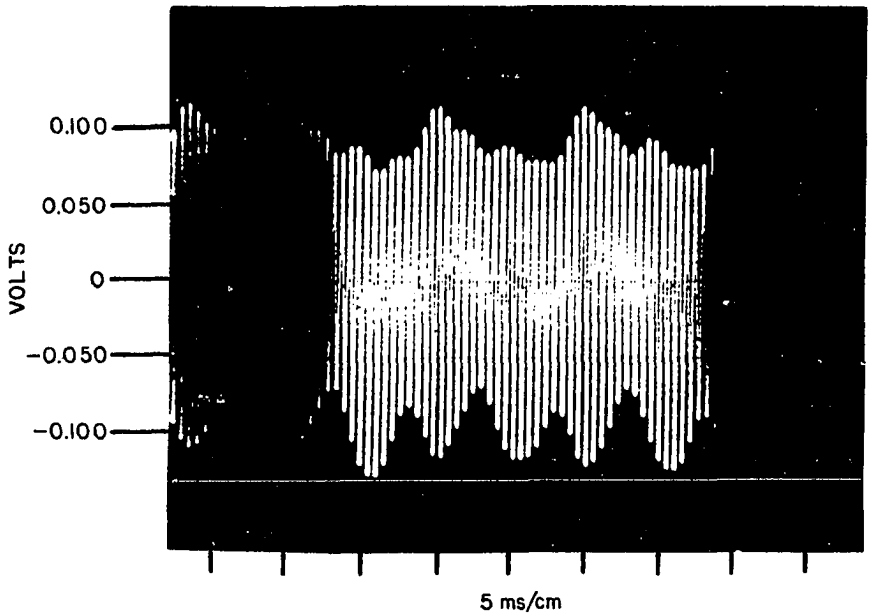

ENVELOPE OF DOUBLE BALANCED MIXER 1800 Hz OUTPUT
$m < 0.666$

FIG. 8-2

Figure 8-2 shows the presence of unwanted components at the output of the 1900 Hz to 1800 Hz frequency shifter or double balanced mixer. A combination of insufficient balance and unwanted sideband content from the bandpass filter from which the signal is derived is cause for the high level of modulation. The cascading effect of the unwanted components at the bandpass filter output and double balanced mixer output serve only to degrade cancellation in follow-on circuitry.

8-1-2 Amplitude-Limiter Pairs and Noise Sources

Referring to Figure 7-17, asymmetrical clipping combined with phase and amplitude jitter contribute even further to less than optimum component cancellation. These waveforms must add to zero for all time of each period for perfect cancellation.

The constant asymmetrical condition is caused by a difference in the saturation to supply voltage and the cut-off to zero voltage of the LM-3900 operational amplifier. The asymmetry may be minimized by properly placing the input sinusoidal waveform symmetrically about the true average value between saturation and cut-off by adjusting the bias current to the current mirror (inverting input) of the operational amplifier. The severe case of asymmetry of Figure 7-17 is deliberately introduced to illustrate one of the causes of less than optimum cancellation.

The amplitude jitter on the signals shown in Figure 7-17 is cause for an asymmetrical clipping condition that is not so easily corrected since the $G\hat{V}$ to λ ratio cannot be made constant. The amplitude of the input signal is always changing. This effect could be minimized by using much higher $G\hat{V}$ to λ ratios. This would cause the flat tops of the clipped waveforms to be more nearly equal in duration in spite of amplitude jitter. Another way of expressing this effect is to say that the rise and fall times of the clipped waveform (derived from the input sinusoid) are more nearly constant in slope. Calling for higher $G\hat{V}$ to λ ratios is in agreement with the prediction made in Chapter IV where a value of 3000 was arbitrarily judged to be sufficient. The amplitude jitter does not originate in the amplitude-limiters but the severity of the effects may be partially compensated in this stage. Figure 7-14 shows considerable amplitude jitter at the output of the phase corrector following the double balanced mixer. The ultimate source is found to be the double balanced mixer. Jitter not present on the balanced mixer inputs lead to the conclusion that it is a strong function of devices used.

Phase jitter is also present on one of the amplitude-limiter inputs. This condition is also evident in Figure 7-14. Its source is traced back to the double balanced mixer where it is suspected that it is generated

along with the amplitude jitter. Exact cause remains unknown.

8-1-3 The Addition of Class-C Amplifiers

Even though phase and amplitude jitter and other noise sources contribute to less than optimum enhancement, it should be possible to compensate for these imperfections by some means. Referring to Figures 7-18 through 7-21 the insertion of a Class-C amplifier at each input to the final summer in Figure 4-1 will prevent a component from feeding through to the ultimate VCO output until its level reaches that which allows the amplifier to pass a signal. The amplifiers could be biased to a point above the worst case suppression level shown in the figures so that no signal is passed until it is driven into conduction by a small amount of sideband enhancement. Of course, an additional bandpass filter is required following each Class-C amplifier since the nonlinearity introduced by less than full wave conduction breeds significant harmonic content in each sideband.

Although this technique to improve the enhanced to suppressed amplitude levels has not been tried, it should succeed with little difficulty.

8-1-4 Measurement of Amplitude Modulation Index

No attempt is made to measure and quantize m since this is largely an exercise in envelope peak and valley

detection of the output waveform of the basic VCO. After quantization (similar to that which takes place in a digital voltmeter), a small amount of digital processing is necessary to form the ratio of the difference to the sum of the voltages to find m. These techniques and processes are well explored in communication signals detection methods and digital signal processing (ref. 18).

8-1-5 General Comments

The content of this chapter is purposely qualitative since a quantitative critique of results is largely prevented by such things as jitter and insufficient suppression of unwanted sidebands at the output of the bandpass filters and balanced mixers. For example, calculating m_u and m_ℓ for the enhancement of each sideband is impossible since u and ℓ are masked by phase and amplitude noise. This is to no avail, however, because the technique of discrete sideband enhancement as a function of continuous variable m is conclusively demonstrated to be possible. It is a matter of "refinement" in rendering the concept useful as a fast scan VCO superheterodyne receiver local oscillator.

LIST OF REFERENCES

1. Ghirardi, Alfred A., Radio Physics Course., 2nd ed. New York: Murray Hill Books, Inc., 1932.

2. Viterbi, Andrew J., Principles of Coherent Communications. New York: McGraw Hill Book Co., 1966.

3. Houts, Ronald C., Richard S. Simpson. Fundamentals of Analog and Digital Communications Systems. Boston: Allyn and Bacon, Inc., 1971.

4. Lindsey, William C., Marvin K. Simon. Telecommunication Systems Engineering. Englewood Cliffs, N.J.: Prentice-Hall, Inc., 1973.

5. Robbins, Kenneth W. "Transistors and ICs in a Phase Locked Local Oscillator." QST (January 1972), 43-47.

6. Penfield, P., R. Rafuse, "Varactor Applications." Cambridge, Massachusetts: MIT Technology Press, 1962.

7. Abramowitz, H.M., F.A. Marki, M.G. Walker. "MESFET Amplifiers Go to 18 GHz." Microwave Systems News, VI (April/May 1976), 39-48.

8. RCA Electronic Components. A Development Program for Fast Tuning Speed VCO's with Accurate Settability. Unpublished Engineering Notes. Harrison, N.J.: RCA Electronic Components Microwave Devices Operations Department, October 1973.

9. Buswell, Ronald N. "Voltage Controlled Oscillators In Modern ECM Systems." Watkins-Johnson Tech-Notes, I No. 6 (November/December 1974), 1-11.

10. Lathi, B.P., Communication Systems. New York: John Wiley and Sons, 1968.

11. Westman, H.P., ed. Reference Data for Radio Engineers., 5th ed. New York: Howard W. Sams and Co., Inc., 1969.

12. Klaassen, Clarence F. "ECM Waveform Analysis System." Electronic Warfare, VII No. 5 (September/October 1975), 133-137.

13. Westman, H.P., ed. Reference Data for Radio Engineers., 5th ed. New York: Howard W. Sams and Co., Inc., 1969.

14. Hildebrand, F.B., Advanced Calculus for Engineers. New York: Prentice-Hall, Inc., 1950.

15. EXAR Integrated Systems, Inc., "Application Notes for the XR-205 Monolithic Waveform Generator," March 1972.

16. Motorola Semiconductor Products, Inc., The Microelectronics Data Book. Phoenix: Motorola Technical Information Center, 1969.

17. Hilburn, John L., David E. Johnson. Rapid Practical Designs of Active Filters. New York: John Wiley and Sons, 1975.

18. Westman, H.P., ed. Reference Data for Radio Engineers., 5th ed. New York: Howard W. Sams and Co., Inc., 1969.

BIOGRAPHY

Timothy P. Hulick was born to Peter V. Hulick, MD and Helen Barno Hulick on 2 April 1942 in Phillipsburg, Pennsylvania. At the age of three his family permanently relocated to La Crosse, Wisconsin. His deep interest in electronic communication originated when his father presented him with a "crystal radio set" at the age of seven years. This interest grew so quickly that he pursued and received the general class radio amateur license at the age of twelve years.

Throughout junior and senior high school he was very active in the Wisconsin Junior Academy of Science sponsored by the University of Wisconsin. He actively participated in state science meets and those sponsored by the National Science Foundation - Future Scientists of America receiving First Place awards in five of six years.

In 1960 Mr. Hulick was appointed to the United States Naval Academy. He was graduated in 1964 with the Bachelor of Science Degree and was first in his class for all the courses in electrical engineering. While a naval officer he responded to military orders to the Massachusetts Institute of Technology as a full-time student from 1966 to 1969 where he earned the Master of Science (Nuclear Engineering) and the Naval Engineer degrees.

After serving as the Navy's Project SHORTSTOP Shore Based Test Site Coordinator, he voluntarily resigned his commission to pursue a higher degree and a career in electrical engineering. He is currently employed as the Technical Director of Systems Consultants, Inc. Virginia Beach, Virginia. He is a member of Eta Kappa Nu, life member of the American Radio Relay League, and a senior member of the Institute of Electrical and Electronics Engineers. His publications that earned him the "Cover Plaque" award for the best technical article for the month in QST include:

"Handi-Talkie for 7 Mc." QST (November 1963), 45-49, 162, 164.

"A Medium Power HF SSB/CW Transmitter." QST
(May 1973), 11-16, 41.
(June 1973), 37-44.
(September 1973), 32-40.

Other publications include:

"The Companion, a Matching Receiver for the Heath SB-400 Transmitter." CQ (April 1967), 12-21.

"A Two KW PEP Linear Amplifier." CQ (November 1968), 89-95.

"Add Variable Bandwidth to Your Fixed Bandwidth Receiver." QST (March 1977).